The Quest for Better Cancer Therapies: Identification of Transcription Factor Involvement in ATP7B Regulation via dCas9-Apex2 (Caspex), TOX4 as a Potential Regulator of Cisplatin Resistance

by

Batuhan Altay

A Dissertation Submitted to the
Graduate School of Health Sciences
in Partial Fulfillment of the Requirements for
the Degree of

Master of Science

in

Cellular and Molecular Medicine

25th July 2023

To my supporting family.

ABSTRACT

The Quest for Better Cancer Therapies: Identification of Transcription Factor Involvement in ATP7B Regulation via dCas9-Apex2 (Caspex), TOX4 as a Novel Regulator of Cisplatin Resistance

Batuhan Altay

Master of Science in Cellular and Molecular Medicine

25th July 2023

Abstract

The identification of specific transcription factors and epigenetic modifications that regulate the ATP7B gene could provide new insights into the development of therapeutic strategies targeting cancer drug resistance mechanisms. Here, we used genomic locus proteomics dCas9-Apex2 (CASPEX) to identify proteins that interact with the promoter of ATP7B which can provide a deeper understanding of the role of transcription factors and chromatin modifiers in the regulation of the ATP7B, and ultimately, contribute to the development of new therapies for diseases associated with ATP7B dysfunction and cancer drug resistance.

To explore the transcriptional regulators responsible for controlling the expression of the ATP7B gene, we dissected the -3000 bp to +1 bp region at the ATP7B promoter into seven distinct regions, which was carried out to comprehensively cover the proteins that bind to the promoter, using the CASPEX labeling system. The targeting efficiency of the gRNAs on ATP7B promoter was confirmed via chromatin immunoprecipitation (ChIP). Following mass spectrometry, we identified over 150 transcription factors that were enriched at the ATP7B promoter. We selected specific candidates to examine their impact on ATP7B expression through overexpression or knock-out experiments. Additionally, we investigated their ability to bind to the ATP7B promoter using ChIP-qPCR analysis. Our screening suggested that TOX4 acts as a novel regulator of ATP7B in HEK293T and HUH7 cell lines. The activity of TOX4 at the ATP7B promoter was confirmed via both luciferase reporter assays and ChIP-qPCR experiments. Furthermore,

while TOX4 Ox conferred cisplatin resistance, its downregulation lead to sensitization by out hypothesis.

In conclusion, our discoveries offer new perspectives on the regulatory mechanisms governing the ATP7B gene, which could have significant implications for comprehending and addressing cancer drug resistance involving TOX4. The recognition of these transcription factors, particularly TOX4, as crucial regulators of the ATP7B gene, opens up possibilities for potential targeting in future cancer therapeutic approaches.

Keywords: ATP7B, Cisplatin Resistance, TOX4, Proteomics, Molecular Biology

Cisplatin Direncini Aşma Arayışı: ATP7B Düzenlemesinde Transkripsiyon Faktörlerinin dCas9-Apex2 (Caspex) Aracılığıyla Belirlenmesi ve Cisplatin Direncinde Bir Düzenleyici Olarak TOX4'ün Tanımlanması

Batuhan Altay

Hücresel Ve Moleküler Tıp, Yüksek Lisans

24 Temmuz 2023

ATP7B geninin düzenlenmesinde belirli transkripsiyon faktörlerinin ve epigenetik modifikasyonların tanımlanması, kanser ilaç direnci mekanizmalarına yönelik terapötik stratejilerin geliştirilmesinde yeni perspektifler sunabilir. Bu çalışmada, ATP7B'nin promoteriyle etkileşime giren proteinleri belirlemek için genomik lokus proteomik dCas9-Apex2 (CASPEX) kullanılmıştır. Bu, transkripsiyon faktörlerinin ve epigenetiklerin ATP7B'nin düzenlenmesindeki rolünün daha iyi anlaşılmasını sağlayabilir ve sonuç olarak ATP7B işlev bozukluğu ve kanser ilaç direnci ile ilişkili hastalıkların tedavisine katkıda bulunabilir. CASPEX aracılığıyla transkripsiyon faktörlerini incelemek için ATP7B'ye hedeflenen etkili gRNA'larla +1 transkripsiyon başlangıç noktasından -3000 baz çiftine kadar olan 7 bölge seçilmiştir. Ayrıca, ATP7B promotöründe gRNA'ların hedefleme verimliliği, kromatin immünopresipitasyonu (ChIP) ile doğrulanmıştır. Ayrıca, ATP7B CASPEX'in kitle spektrometrisi sonuçlarından, ATP7B ve kanserle ilişkili çeşitli parametrelere sahip 150'den fazla zenginleştirilmiş transkripsiyon faktörü adayı belirlenmiştir. Doğrulamalarımız sonucunda, TOX4'ün ATP7B ve Cisplatin direncinin HEK293T ve HUH7 hücre hattında yeni bir düzenleyici olduğunu tespit ettik. TOX4 Knockout, ATP7B seviyesini azaltırken, TOX4'ün aşırı ifadesi transkripsiyonel olarak ATP7B seviyelerini arttırmaktadır. Ardından, TOX4'ün ATP7B promoterine bağlanmasını eksogen luciferaz deneyleri ve ChIP-qPCR ile doğruladık. Ek olarak, TOX4'ün ekpresyonuna bağlı olarak hücrelerin cisplatine karşı hassaslaştırılması ve direnç geliştirilmesi doğrulandı.

Özet olarak, bu bulgular, ATP7B geninin düzenlenme mekanizmaları hakkında yeni perspektifler sunmakta ve ATP7B işlev bozukluğu ile ilişkili hastalıkların anlaşılması ve tedavisi için önemli olabilir, bunlar arasında kanser ilaç direnci de bulunmaktadır. Bu transkripsiyon faktörlerinin ve TOX4'ün ATP7B geninin ana düzenleyicileri olarak tanımlanması, gelecekteki kanser terapötik stratejilerde hedef alınabilecek potansiyeli taşımaktadır.
Anahtar Kelimeler: ATP7B, Cisplatin Direnci, TOX4, Proteomiks, Moleküler Biyoloji

ACKNOWLEDGEMENTS

I am deeply grateful to acknowledge my advisor, Prof. Ceyda Acilan Ayhan, for her unwavering support and guidance in the field of cancer research. Her dedication and attentive listening throughout my academic journey have been invaluable. Furthermore, I extend my utmost gratitude to Dr. Can Ozcan, my postdoctoral mentor, whose unwavering passion for genuine and cutting-edge scientific inquiry has inspired me greatly. His constant encouragement to expand my knowledge and apply the latest advancements in science to my master's studies has been instrumental in my growth.

I am filled with immeasurable gratitude for my project mate, Ayca Acar MSc, who embarked on this master's journey alongside me and provided unwavering support both on an emotional and intellectual level. Her constant presence and steadfast friendship have been instrumental in my academic progress. The genuine camaraderie we share, and her unwavering optimism have consistently motivated me to push the boundaries of scientific exploration within our laboratory. I am truly indebted to her for being an indispensable source of inspiration as a friend and for the CASPEX project, and encouragement throughout this remarkable journey. I would like to wholeheartedly express my gratitude to Baris Sergi, a Ph.D. student who has brought immense joy, served as a valuable scientific consultant, and provided a safe space for open discussions.

I extend my gratitude to my esteemed committee members, Dr. Nathan Lack and Dr. Umamaheswar Duvvuri, whose profound expertise and invaluable insights in the field of molecular biology have been instrumental in shaping my research. Their profound knowledge and guidance have served as a constant source of inspiration. I am grateful to my fellow lab members, whose understanding and willingness to engage in discussions extended beyond the boundaries of our work. Their support has been invaluable throughout my journey. I am thankful for the enriching conversations we have had, where they generously shared their insights, not only regarding our research but also on various aspects of life.

I am delighted to acknowledge that this thesis is the culmination of the TUBITAK-1001 research project titled "Characterization of the Transcriptional Regulation of

ATP7B Gene by Genomic Locus Proteomics and the Role of ATP7B Regulators on Cisplatin Resistance in Cancer." I am grateful for the financial support provided through this bursary, which enabled me to conduct the extensive experiments and investigations outlined in this study. Engaging in this project has significantly enhanced my understanding of the complex mechanisms involved in transcription factors and transcriptional regulation.

I am filled with boundless gratitude towards Fulya Mina Kucuktas, MSc, for her unwavering support and genuine care. Throughout our journey together, she has been an exceptional listener, always attentive to my goals and dreams, and shares my inspirations. I am truly fortunate to have her in my life, as she consistently provides endless encouragement and support, making her one of the most remarkable individuals I have had the pleasure to know. Words cannot fully convey the depth of my admiration and affection for her, as she holds a special place in my heart, and I am truly grateful for her presence in my life.

Finally, I would like to express my heartfelt appreciation to my family, who have consistently supported and believed in my pursuit of a career in science. Their unwavering encouragement and unwavering support have played a crucial role in shaping my journey. I am deeply grateful for their selflessness and willingness to assist without any hesitation or expectation of return. Their love, guidance, and endless faith in my abilities have been a constant source of strength and motivation. I will forever cherish their invaluable contributions and remain indebted to them for their support.

Thank you all,

Batuhan Altay

TABLE OF CONTENTS

LIST OF TABLES

LIST OF FIGURES

ABBREVIATIONS

APEX2	Ascorbic Acid Peroxidase
ATF3	Activating Transcription Factor-3
BioID	BioID Proximity Labeling
Cas9	CRISPR-associated protein 9
CASPEX	dCas9-APEX2
cDNA	Complementary DNA
ChIP	Chromatin Immunoprecipitation
CRISPR	Clustered Regularly Interspaced Short Palindromic Repeats
DMEM	Dulbecco's Modified Eagle Medium
DNA	Deoxyribonucleic Acid
DOX	Doxycyline
DSB	Double-Strand Break
EDTA	Ethylenediaminetetraacetic Acid
FBS	Fetal Bovine Serum
HDAC	Histone Deacteylase
HDR	Homology-Directed Repair
IP	Immunoprecipitation
LC-MS	Liquid Chromatography-Mass Spectrometry
LEF1	Lymphoid Enhancer Binding Factor-1
mRNA	Messenger RNA
MS	Mass Spectrometry
NHEJ	Non-Homologous End joinig
NT	Non-targeting
NT	Non-Treated
PAGE	Polyacrylamide Gel Electrophoresis
PBS	Phosphate-Buffered Saline
PCR	Polymerase Chain Reaction
qPCR	Quantitative Polymerase Chain Reaction
RNA	Ribonucleic Acid
RNA Pol	RNA Polymerase
rRNA	Ribosomal RNA

RT-PCR	Reverse Transcription Polymerase Chain Reaction
RT-qPCR	Reverse Transcription Quantitative Polymerase Chain Reaction
SDS-PAGE	Sodium Dodecyl Sulfate Polyacrylamide Gel Electrophoresis
sgRNA	Single Guide RNA
SRB Assay	SulfoRhodamine B Assay
TF	Transcription Factor

Chapter 1:
INTRODUCTION

1.1 ATP7B

ATP7B is a protein that belongs to the P type ATPases which mainly regulates copper transportation throughout the cell. Due to essentiality of copper in the cellular metabolism, ATP7B is crucial to regulate copper hemoastasis in the human body (Bartee & Lutsenko, 2007). ATP7B, plays a critical role in the cellular excretion of copper, primarily in hepatocytes, to promote cellular detoxification and maintain copper homeostasis. The ATP7B protein encompasses multiple functional domains, including the N-terminal domain, A and P domains, membrane transport domain, cytoplasmic domains, and six distinct metal binding domains (MBDs) (Bitter et al., 2022). These domains collectively contribute to the efficient regulation of copper transport within the cell. The nomenclature of the MBDs is based on their sequential arrangement, beginning with the MBD1, which is situated closest to the N-terminal domain, and progressing through MBD6. The interactions and stability of these domains are of paramount importance for the proper maintenance of copper homeostasis in cellular systems (Ariöz et al., 2017). The ATP7B protein mediates the transport of copper from the cytoplasm to various extracellular compartments, including the bile canaliculi found in hepatocytes. This process relies on the coordinated functioning of its distinctive domains. The N-terminal domain regulates protein trafficking and localization, ensuring the precise targeting of ATP7B to specific cellular compartments involved in copper transport. The A and P domains, which are characteristic features of P-type ATPases, play essential roles in ATP hydrolysis and copper binding, respectively. Through their interplay, these domains form a dynamic complex that facilitates the ATP-dependent translocation of copper ions across the cellular membrane. Additionally, the membrane transport domain provides the necessary structural framework for the interaction between ATP7B and the lipid bilayer, enabling efficient and controlled transmembrane movement of copper. Mutations in the ATP7B gene have been identified as the underlying cause of various dysregulations within the body. Particularly, these mutations result in the accumulation of copper, leading to pathological consequences. Excessive copper levels in the body can

induce toxicity, as copper is a heavy metal with potential adverse effects. This condition is commonly known as Wilson's disease, referring to ATP7B as the Wilson's disease protein (Roy et al., 2020).

In addition to its role in copper metabolism and Wilson's disease, ATP7B has emerged as a significant contributor to cisplatin resistance in cancer cells. Cisplatin, a platinum-based chemotherapeutic agent, is widely used in the treatment of various malignancies. However, the effectiveness of cisplatin treatment can be compromised by the development of resistance, leading to treatment failure and disease progression. ATP7B plays a crucial role in this resistance mechanism by facilitating the efflux of platinum-based drugs from cancer cells, thereby conferring resistance against chemotherapy (Lukanović et al., 2020).

1.1.1 Copper

Copper is one the trace elements that is classified as a heavy metal along with essential for progression and proliferation of the cells and vital for the metabolism. Copper takes important roles in the energy metabolism, such as uptake of iron into cells, cellular signalling as well as working as an antioxidant. It plays an essential role for the energy metabolism as gathering of cuproenzymes, a group of proteins that uses copper as a cofactor, in the respiratory complex to cytochrome c oxidase. Additionally, copper maintains the transportation of oxygen, and cytochrome c oxidase uses copper and iron as a cofactor to electron transport chain (Ruiz et al., 2021). Copper cannot be produced in the cells; therefore, it should be maintained from the diatery resources and environment. Due to its essentiality, deficiency of copper leads to metabolic disorders since its essential for every cell’s energy, signalling and transcriptional mechanisms. However, excessive accumulation of copper leads to the induction of reactive oxygen species to damage cells (Kardos et al., 2018). Copper which is a cofactor-metal should be regulated in the cell, and it is neither insufficient nor excessive. ATP7B is essential to maintaining adequate copper levels.

1.1.2 Transcriptional Regulation of ATP7B

Mutations in the ATP7B gene can result in the pathological consequences, and one of the important one is a rare genetic disorder, Wilson’s disease (Wu et al., 2015) ATP7B

also known as Wilson's Disease Protein because of these pathological consequences. In Wilson's disease patients, ATP7B is mutated, and mutation can occur in several places on the genome such as copper binding domains of ATP7B through to promoter of ATP7B, in addition to untranslated regions (Bartee & Lutsenko, 2007; Höflich et al., 2021). Up to now, more than 500 variants of ATP7B mutations are established from the sequenced genomes of Wilson's disease patients. One of the patients include a mutation placed on the 400 bp upstream of transcription start site of ATP7B, and this mutation effects the binding of transcription factors such as a crucial regulator of metal regulatory proteins, metal regulatory transcription factor 1 (MTF1) (H. I. Chen et al., 2018). MTF1 is a highly conserved protein found across various organisms, spanning from insects to humans. Its primary function is to mitigate the cellular and organismal burden imposed by heavy metals through the activation of metallotheonins and other genes associated with copper, zinc, and silver metabolism, including ATP7B. MTF1 exerts regulatory control over genes involved in heavy metal homeostasis by binding to the promoter regions of these genes, specifically targeting the metal regulatory elements (MRE) (Stalke et al., 2020). In addition, MTF1 is a nuclear shuttling protein that is mostly activated by accumulation of heavy metals in the cytoplasm. Accumulation of the heavy metals as copper or zinc leads MTF1 into nucleus and DNA binding domains of the MTF1 leads the protein to the MRE regions of heavy metal responsible genes (Günther et al., 2012). MTF1 binds to the metal regulatory elements which are located on the ATP7B promoter region, in four different places up to -1000 bp transcription start site of the ATP7B gene and increases its expression when heavy metal levels are elevated (Stalke et al., 2020).

The regulation of gene expression by transcription factors is integral to the modulation of cellular processes, including drug resistance in cancer. In the context of ovarian cancer, TFEB have been implicated in the regulation of ATP7B, a key gene involved in the platinum pathway. Understanding the mechanisms underlying platinum-based chemotherapy drugs is crucial for investigating their efficacy and developing strategies to overcome resistance (Petruzzelli et al., 2022). ATP7B is a crucial gene in the copper homeostasis, and it requires a tight and rapid regulation to maintain level of copper in the body.

1.1.3 ATP7B in Cisplatin Resistance

Cisplatin, a platinum-based chemotherapy drug, was approved by the U.S. Food and Drug Administration (FDA) in the early 1980s for the treatment of tumors. Since its introduction, the anti-cancer potential of cisplatin has been observed and applied in the treatment of numerous patients. Cisplatin exerts its mode of action by entering the cell and undergoing aquation, resulting in the formation of a highly active form that exerts its effects on both the cytoplasm and DNA (Galluzzi et al., 2011).

Within the cytoplasm, cisplatin interacts with various proteins, including metallothioneins, glutathione, and several other proteins through their cysteine residues. This interaction leads to an increase in the levels of reactive oxygen species (ROS) within the cytoplasm. Simultaneously, the aquated form of cisplatin rapidly binds to DNA, exerting its effects through two mechanisms. Firstly, it forms protein-DNA complexes, and secondly, it generates adducts within the DNA strands, leading to the formation of DNA lesions.

Consequently, when cisplatin enters the cell, it triggers the activation of various proteins, initiating a cascade of events aimed at reducing the detrimental effects of cisplatin and promoting cell survival by evading apoptosis. The disturbance caused by cisplatin adducts within the DNA strands activates nucleotide excision repair proteins (NER), which facilitate the repair of damaged DNA strands. This repair mechanism is vital for preventing the accumulation of cisplatin within the cell (D. W. Shen et al., 2012).

However, cancer cells have the capacity to develop adaptive mechanisms to counteract the accumulation of cisplatin. One crucial factor in this adaptation process is the copper transporter-1 (CTR1), which plays a role in the uptake of cisplatin into the cells. In resistant cancer cells, CTR1 tends to be downregulated, thereby reducing the cellular uptake of cisplatin. Another set of key regulators involved in modulating the cellular levels of cisplatin are ATP7A and ATP7B (L. Wang et al., 2021). These copper transporting ATPases work cooperatively, but ATP7B is particularly associated with cisplatin resistance. Its upregulation is commonly observed in various cancer types, including ovarian, head and neck, and liver carcinomas.

Understanding the molecular mechanisms underlying cisplatin resistance and the role of proteins such as CTR1, ATP7A, and ATP7B is crucial for developing strategies to

overcome resistance and improve the efficacy of cisplatin-based chemotherapy in cancer treatment (Leonhardt et al., 2009).

In addition to its role in cisplatin resistance, ATP7B is a key player in the molecular pathways that contribute to chemotherapy resistance in cancer cells. Understanding the transcriptional regulators of ATP7B is of paramount significance in unraveling the inter mechanisms underlying cisplatin resistance. Identifying the transcription factors and signaling pathways that govern ATP7B expression can provide critical insights into the regulatory networks involved in modulating cisplatin sensitivity. By elucidating the transcriptional control of ATP7B, we can uncover novel therapeutic targets that can be manipulated to sensitize cancer cells to cisplatin treatment, thereby enhancing its effectiveness.

ATP7B has been shown to be upregulated on various cancer types, and lysosomal sequestration mechanisms of ATP7B has an influence on developing drug resistance on cancer patients's treatments (Lukanović et al., 2020). ATP7B plays a crucial role in cellular detoxification when exposed to platinum-based drugs, leading to the development of resistance mechanisms in cancer cells and enhancing their survival. Aside from its potential as a therapeutic target in cancer treatment, ATP7B has also been studied as a biomarker for predicting how patients will respond to chemotherapy (Miyashita et al., 2003). In addition to its potential as a therapeutic target for cancer treatment, ATP7B has also been investigated as a biomarker for predicting patient responses to chemotherapy. Studies focusing on ovarian, lung, and oral cancers have provided compelling evidence indicating a positive correlation between elevated levels of ATP7B and resistance to cisplatin therapy. This observation suggests that ATP7B plays a significant role in mediating resistance to cisplatin, a commonly used chemotherapy drug for the treatment of various cancer types. Therefore, ATP7B is suggested as a valuable predictor of the appropriate therapy type and also holds prognostic significance (Nakayama et al., 2004). The regulation of ATP7B is crucial for the cancer because it plays a critical role in the copper homeostasis and in addition to that since ATP7B directly controls in copper metabolism, relative levels of ATP7B also control the cellular energy metabolism (Petruzzelli & Polishchuk, 2019). The expression levels of ATP7B do not consistently correlate with the levels of MTF1, indicating that there are additional factors involved in regulating copper metabolism. It is imperative to gain a deeper understanding of the copper metabolism protein to enhance chemotherapeutic strategies (Safaei et al., 2004).

Furthermore, the identification of transcriptional regulators of ATP7B can have clinical implications (Petruzzelli et al., 2022). It may enable the development of biomarkers that can predict cisplatin resistance based on the expression levels or activity of these regulators. Such biomarkers could help guide treatment decisions, allowing for more personalized therapeutic approaches and potentially avoiding the use of cisplatin in patients who are likely to be resistant.

The regulation of the ATP7B gene is significant, not only due to its involvement in maintaining copper homeostasis and its association with conditions like Wilson's disease, but also due to its potential influence on the development of drug resistance in cancer. The regulation of this gene is mediated through various mechanisms, including transcription factors and epigenetics. Here we report that identification of transcriptional regulators of ATP7B and their relationship with the cisplatin resistance overcome chemotheurapetic complications and offer additional tumor treatment options.

1.2 Transcription Factors

Transcription factors are pivotal proteins involved in the fundamental control mechanisms governing gene expression, thus playing a crucial role at the onset of the central dogma. These sequence-specific binding factors are responsible for recognizing distinct DNA sequences and exerting regulatory control over gene expression through the formation of complexes on chromatin DNA. By precisely orchestrating gene expression, transcription factors ensure the timely and context-dependent regulation of genetic information, particularly during developmental processes and in response to various stimuli (S. A. Lambert et al., 2018). Transcription factors function as essential modulators of gene expression, acting as molecular switches that govern whether a particular gene is turned "on" or "off" in each cellular context. They accomplish this regulatory role by binding to specific DNA sequences known as transcription factor binding sites (TFBSs), which are in the promoter or enhancer regions of target genes. TFBSs are mostly conserved regions between eukaryotes (Katzman et al., 2007). The binding of transcription factors to these regulatory regions can either promote or inhibit the recruitment of RNA polymerase and associated transcriptional machinery, ultimately dictating the expression levels of downstream genes.

The ability of transcription factors to recognize these specific DNA sequences is mediated by structural domains that are integral components of these proteins. Notably, transcription factors possess various structural domains, including Helix-loop-helix, Basic leucine zipper, GCC box, Helix-turn-helix, Zinc fingers, Paired boxes, and Homeobox domains (Wingender et al., 2013, 2015). These structural motifs enable sequence-specific interactions between transcription factors and their target DNA, leading to the formation of transcription factor-DNA complexes(Brayer & Segal, 2008). By facilitating the recruitment of additional regulatory proteins, these complexes enable the subsequent establishment of transcriptional initiation or repression complexes. As a result, they exert precise control over gene expression programs, ensuring proper regulation (Ma, 2011). Understanding the functional significance of these structural domains and their contribution to the formation of transcription factor-DNA complexes is crucial for unraveling the intricate mechanisms underlying gene regulation and its implications in various biological processes and diseases (Lee & Young, 2013).

1.2.1 Transcription Factors and Cancer Drug Resistance

Transcription factors play a pivotal role in cancer drug therapy, as they can contribute to the development of drug resistance through various mechanisms. The ability of transcription factors to regulate the expression of a diverse range of genes, activating some and repressing others, makes them potent modulators of cellular processes. In the context of chemotherapy, cancer cells exploit transcription factors to evade cell death and acquire resistance to anticancer drugs (Islam et al., 2021). This manipulation of transcription factors can occur through several mechanisms, including mutation of transcription factor domains, alterations in the expression levels of specific transcription factors, and the subsequent impact on their target genes(Vishnoi et al., 2020).

The genes affected by the modulation of transcription factors in cancer cells encompass a wide array of functional categories. These include glycoproteins, ATPases, drug pumps, DNA damage response proteins, hypoxia-inducing factors, factors involved in cell proliferation, invasive capability, metastasis, and the modulation of cancer stem cell differentiation. By exerting control over these genes, transcription factors can confer adaptive advantages to cancer cells, allowing them to overcome the cytotoxic effects of chemotherapy drugs and develop resistance (A. Chen & Koehler, 2020; Spitz & Furlong,

2012). One mechanism by which cancer cells acquire resistance involves mutations in the domains of transcription factors. These mutations can alter the structure or function of transcription factors, leading to changes in their DNA-binding specificity or affinity. Consequently, the affected transcription factors may no longer effectively regulate the expression of target genes involved in drug sensitivity or apoptosis, resulting in diminished response to cancer therapies (Belluti et al., 2020).

Furthermore, alterations in the expression levels of specific transcription factors can also contribute to the development of drug resistance. Cancer cells can upregulate the expression of certain transcription factors that promote the transcription of genes associated with drug efflux pumps, DNA repair mechanisms, or cell survival pathways. Conversely, downregulation of transcription factors involved in the regulation of pro-apoptotic or drug-sensitivity-related genes can confer a survival advantage to cancer cells in the presence of chemotherapeutic agents (Ma, 2011; Redell & Tweardy, 2006).

Transcription factors play a critical role in modulating various chemotherapeutic approaches in different cell lines. Among these factors, NF-kB and STAT3 have been identified as key contributors to drug resistance and cancer progression. NF-kB, a pro-inflammatory transcription factor, promotes increased proliferation of cancer cells while inhibiting apoptosis (Bentires-Alj et al., 2003; Vishnoi et al., 2020). It serves as a known regulator of the multidrug resistance-1 (MDR1) gene, leading to the development of drug resistance, particularly in colon cancer.

NF-kB-mediated regulation of MDR1 gene expression has been implicated in conferring resistance to multiple chemotherapeutic agents. The upregulation of NF-kB activity promotes the Ox of MDR1, which encodes a drug efflux pump responsible for reducing intracellular drug concentrations (Godwin et al., 2013). This mechanism enables cancer cells to evade the cytotoxic effects of chemotherapy and contributes to treatment failure in colon cancer (Bentires-Alj et al., 2003).

Similarly, STAT3, another transcription factor, exhibits a comparable but distinct regulatory role in drug resistance and oncogenesis. Enhanced expression and phosphorylation of STAT3 have been associated with increased oncogenic potential, drug resistance, and enhanced proliferative capabilities in cancer cells. The activation of STAT3 signaling pathways can promote cellular survival, immune evasion, and the acquisition of drug resistance mechanisms.

By deciphering the underlying molecular mechanisms and identifying key transcription factor-mediated pathways, it may be possible to devise more effective therapeutic approaches that can circumvent or overcome drug resistance and improve patient outcomes in cancer treatment (Cohen-Solal et al., 2018; Martinez-Balibrea & Ciribilli, 2021; Mitra, 2020; Redell & Tweardy, 2006).

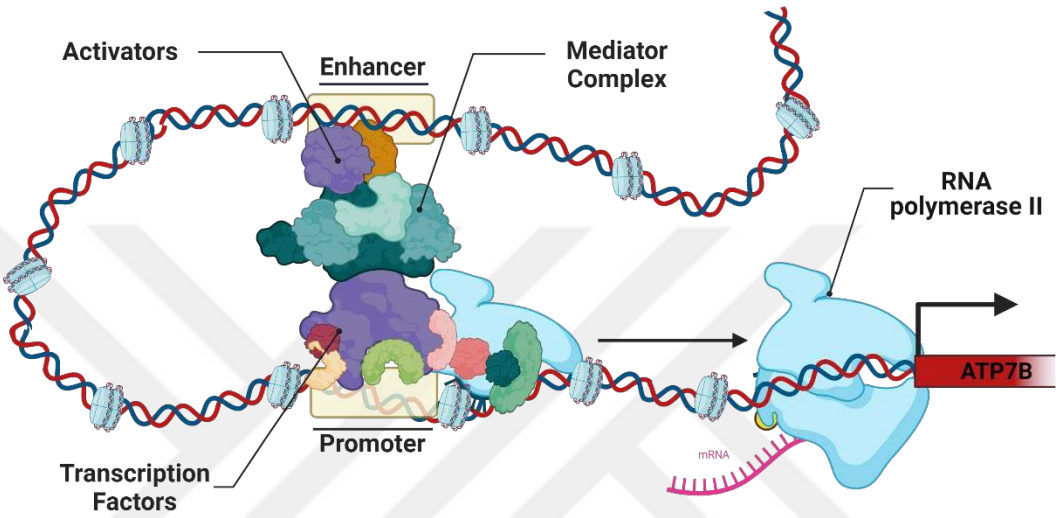

Figure 1.1 Transcriptional Regulation of ATP7B.

1.3 dCas9-Apex2 (Caspex) Proximity Labelling

Proximity labelling is a valuable technique for investigating protein-protein interactions that occur near a target protein. There are several methods for carrying out proximity labelling, including BioID, TurboID, and APEX2. These methods differ in terms of the biotinylating protein used, the duration of biotinylation, and the substrates employed. By using proximity labelling, researchers can enlighten a better understanding of the protein complexes and signaling pathways involved in various biological processes. This knowledge can help to inform the development of new therapeutic strategies for a wide range of diseases (Qin et al., 2021) Proximity labelling approaches are particularly useful for detecting weak or transient protein-protein interactions that may be difficult to identify using other techniques. By enabling the identification of proteins that are near the target protein, even those with low affinity or short-lived interactions can be captured. These fusion proteins (BioID, TurboID, APEX2 etc.) which are evolved to become more

efficient, expands our understanding of the dynamic nature of protein interactions and can provide important insights into cellular processes, disease mechanisms on proteomics level (Cho et al., 2020; Shkel et al., 2022). Various methods have been developed to study DNA-protein interactions, including approaches that use BioID with BirA protein and ascorbate peroxidase, APEX2 (B. R. Kim et al., 2017; Qiu et al., 2019; Ummethum & Hamperl, 2020). APEX2 provides faster results with higher resolution compared to other methods. In addition, the ability of Cas9 to target specific DNA regions has been enhanced, and a mutated form known as dcas9 can bind to DNA without endonuclease activity. Recent studies have combined dcas9-BirA to generate cell lines and biotinylate locus-specific proteins to identify chromatin regulators. Furthermore, a more advanced version known as CASPEX, which fuses dCAS9 with APEX2, has been developed to biotinylate transcription factors and epigenetic regulators in a shorter period, allowing for their identification using mass spectrometry. Another study has used a similar approach to restricted spatial tagging (C-Berst) (Gao et al., 2018; Lam et al., 2014; Myers et al., 2018; Qiu et al., 2019).

In our study, we aim to identify the transcriptional regulators of ATP7B and investigate their effects on cisplatin resistance in cancer. The differences in the expression of the ATP7B gene are directly related to copper metabolism disorders such as drug resistance in cancer, poor patient prognosis, and Wilson's disease, and little is known about its transcriptional regulation. Our aim is to identify the proteins present in the promoter region of ATP7B through genomic locus proteomics (Myers et al., 2018; Nguyen et al., 2020). In addition, the effects of the identified transcription factors on ATP7B expression and cisplatin resistance in cancer cells will be examined. In the long term, treatment alternatives may be proposed for some Wilson mutations that reduce protein stabilization or localize to the promoter region, but this project does not plan to investigate copper metabolism.

Inhibition of ATP7B is a promising approach to help treat drug-resistant cancer cells, according to studies. Rather than screening for small molecule inhibitors that inhibit ATP7B, the proposed approach aims to identify the proteins that regulate ATP7B (Inoue et al., 2010; Janardhanan et al., 2022; Leonhardt et al., 2009). Small molecule inhibitors can be discovered through "drug repurposing" by screening available inhibitor libraries on the market. However, inhibitor discovery alone cannot answer fundamental scientific questions about the regulation of ATP7B in cancer and why its expression increases.

Furthermore, discovering the regulation of ATP7B will provide important information for the literature not only in the field of cancer but also in the development and pathology of Wilson's disease. Identifying the reasons for increased expression can provide better inhibitor options in the future. Additionally, if ATP7B and other transporter proteins are regulated by similar factors, inhibition of a single regulator target may reduce different proteins with similar functions.

The goal of this study is to identify specific transcription factors and epigenetic modifications that regulate the ATP7B gene and to understand their role in diseases associated with ATP7B dysfunction, including cancer drug resistance. The study uses genomic locus proteomics, CASPEX, to identify proteins that interact with the ATP7B gene and efficient gRNAs to investigate transcription factors. The study then confirms the targeting efficiency of the gRNAs via ChIP and selects positively enriched transcription factor candidates to regulate ATP7B expression via mass spectrometry. Furthermore, the study uses CRISPR-mediated knockout (Ko) and overexpression (Ox) of these transcription factors to test their role in ATP7B regulation and cancer drug resistance. The findings of this study provide new insights into the mechanisms of ATP7B gene regulation and may have implications for the understanding and treatment of diseases associated with ATP7B dysfunction. The identification of these transcription factors as key regulators of the ATP7B gene could potentially be targeted in future therapeutic strategies. As a result, from this study, identification of specific transcription factors and epigenetic modifications that regulate the ATP7B gene will provide new insights into the development of therapeutic strategies targeting these regulatory mechanisms for diseases associated with ATP7B dysfunction, including cancer drug resistance.

Chapter 2:**MATERIALS AND METHODS**

2.1 Cell line maintenance and HEK-CASPEX Construction

HEK293T (ATCC) and HUH7 cells maintained at DMEM high glucose medium (Sigma Aldrich, D5796), containing 10% heat inactivated FBS and 1% Penicillin-Streptomycin. Inducible CASPEX (Addgene; 97421) plasmid co-transfected with Piggy-bacTransposase (System Biosciences; PB210PA-1) with Lipofectamine 3000 (Thermo; L300015) on $10x10^4$ seeded HEK293Ts on 6 wells. 24 hours from transfection medium changed and at 48 hours after transfection, 2 µg/ml puromycin added to the medium to allow cells to be selected for 4 days.

2.2 Flow Cytometry and Single Cell Sorting

After the selection with puromycin, HEK-CASPEX Cells treated with 2 µg/ml doxycycline to express CASPEX construct with +GFP. In the end of the 48^{th} hours with doxycline, cells collected, and cells contained in PBS containing 1% FBS. Then, single +GFP cells sorted with channel Sony Cell Sorter (SH800S) on a 96 well plate with one cell on one well. Single cells allowed to grow on puromycin containing medium for 14 days, then visible single colonies delivered on 12 well plates. HEK-CASPEX single colonies treated with 2µg/ml doxycyline for 48 hours. Then, colonies collected for flow cytometry to validate +GFP efficiency expression of HEK-CASPEX colonies. The best colony selected for further validations and frozen.

2.3 Immunoflourescence Staining (IF)

HEK-CASPEX single colony expressing 99% +GFP on its population, growed, and seeded on coverslips covered with Poly-L-Lysine (Sigma, P1274). Then, allowed to grow with doxycyline for 48 hours to prepare for fixation step. Cells were washed with PBS and fixed with both on -20°C with methanol and with 4% Paraformaldehyde in room temperature. Next, cells were permabilized with 0.3%Triton X for 15 minutes and blocked with 1% Bovine Serum Albumin (BSA) (Sigma; 9048) containing PBS for 15 minutes. Coverslips treated with primary antibody of 1:100 diluted anti-V5 (Invitrogen, R960) for overnight at +4°C. Coverslips washed with PBS 3 times and incubated with anti-mouse IgG - Alexa Fluor 594 (Abcam, ab150116) secondary antibody for 1 hour at

room temperature. Next, coverslips washed for 3 times and mounted with DAPI (Abcam, ab228549). Coverslips analyzed under a fluorescence microscope (Axiocam 506 mono Imager M1 from Zeiss).

2.4 Immunoprecipitation

HEK-CASPEX Cells and HEK293T cells seeded on 2.5 x 10^6 and treated for 48 hours with doxycline. Then, cells were trypsinized and washed with PBS. Pellets were lysed with RIPA buffer (EcoTech Biotechnology, RIPA-100) on ice for 30 minutes with vortexing. Mixture was centrifuged at 16.000 x g at +4°C for 15 minutes and supernatant collected as proteins and stored at -80°C. Proteins were quantified with BCA kit (Pierce; 23225). 500 µg of proteins used for immunoprecipitation protocol and samples incubated with anti-FLAG (Sigma, F1804) and mouse IgG (Abcam; ab37355) for 4 hours at +4°C. Next, antibody-lysate complexes incubated with protein g Dynabeads (Invitrogen; 10003D) for overnight. Then, Laemli buffer containing beta-mercaptoethanol added to the samples and incubated at 95°C. for 10 minutes to elute the samples. Eluted samples loaded on SDS-PAGE gel, then transferred on the PVDF membrane for overnight with wet-transfer. Next day, membranes blocked with 5% NFDM (BioRad, 1706404) for 1 hour and incubated with 1:7500 anti-FLAG in 5%NFDM for overnight. The membrane washed with 1% TBST and incubated with 1:5000 secondary antibody anti-mouse HRP (Abcam; ab6789). LICOR Oddysey Imaging system used for imaging of membranes.

2.5 Western Blotting

Cells trypsinized and washed with PBS. Pellets were lysed with RIPA buffer (EcoTech Biotechnology, RIPA-100) on ice for 30 minutes with vortexing. Mixture was centrifuged at 16.000 x g at +4°C for 15 minutes and supernatant collected as proteins and stored at -80 °C. Proteins were quantified with BCA kit (Pierce; 23225). 30 to 100 µg of proteins per SDS-PAGE well prepared and incubated with Laemli buffer containing beta-mercaptoethanol or DTT to induce bonds at 95°C. SDS page transferred with wet-transfer overnight on a PVDF Membrane (Bio-Rad #1620177). Next day membranes blocked with 5% NFDM (BioRad, 1706404) for 1 hour and incubated with different antibodies in 5%NFDM for overnight. Membranes washed with 1% TBST for 3 times

and incubated with appropriate to primary antibody, secondary antibody-HRP linked for 1 hour. Then, membranes visualized and analyzed on LICOR system.

Following antibodies used in this study: anti-GAPDH rabbit (Cell Signalling Technologies, 14C10), anti-ATP7B Rabbit (ABclonal, A5676), anti-ATP7B Rabbit (Santa Cruz, sc-373964), anti-ATP7B rabbit (Novus NB100-360), anti-FLAG mouse (Sigma, F1804), anti-V5 mouse (Invitrogen, R960), anti-TP53 rabbit (Abclonal, A3185).

2.6 Cloning of ATP7B promoter targeting gRNAs

gRNAs designed in Benchling software (www.benchling.com) with highest efficiencies possible with 7 different regions and 2 gRNA for each region (*Table 2.1*). Lentiguide hygro plasmid (Addgene; 139462) digested and its sticky ends dephosphorylated with antactric phosphatase (NEB; M0289). gRNAs annealed and ligated into cut Lentiguide hygro plasmid with T4 PNK enzyme (NEB, M0201) and T4 Ligase (NEB, M0202). Then, annealed plasmids transformed into competent bacteria to isolate and confirm that insertion of gRNA with a Polymerase Chain Reaction (PCR) reaction. With hU6 forward and reverse of each gRNA PCR performed and reaction run on gel to confirm 250 bp. Selected colonies isolated and prepared for lentiviral production.

Table 2.1 ATP7B Promoter Targeting gRNAs Primer List

gRNA for Promoter regions	Forward Primer	Reverse Primer
NT	CACCGTATTACTGATATTGGTGGG	aaacCCCACCAATATCAGTAATAC
g1.1	CACCGTGAGATCCCAGTACAGTGT	aaacACACTGTACTGGGATCTCAC
g1.2	CACCGGGCTCACCCACCGCCTGCG	aaacCGCAGGCGGTGGGTGAGCCC
g2.1	CACCGCGTAGACTAGTGTTCGGCG	aaacCGCCGAACACTAGTCTACGC
g2.2	CACCGCACTGCTGTCCCGCCCACGG	aaacCCGTGGGCGGGACAGCAGTGC
g3.1	CACCGATTACCTTAGATTCATGACA	aaacTGTCATGAATCTAAGGTAATC
g3.2	CACCGAAAATTTAGCTACACTGGAC	aaacGTCCAGTGTAGCTAAATTTTC

g3.3	CACCGCAGTGAAGCAGAAGAAAACG	aaacCGTTTTCTTCTGCTTCACTGC
g3.4	CACCGAAGTTGTTGAGGTGAGCAGC	aaacGCTGCTCACCTCAACAACTTC
g4.1	CACCGTTTAAGTGACGTGTTAACAA	aaacTTGTTAACACGTCACTTAAAC
g4.2	CACCGCGTGTTAACAATGGCAGTTT	aaacAAACTGCCATTGTTAACACGC
g5.1	CACCGTACTGCTATTCAGGAAGCTA	aaacTAGCTTCCTGAATAGCAGTAC
g5.2	CACCGCCTGAACAAAAATATGTAGG	aaacCCTACATATTTTTGTTCAGGC
g6.1	CACCGTCATAAAAGCAACACTACAG	aaacCTGTAGTGTTGCTTTTATGAC
g6.2	CACCGTTGTGCTCCATGGACCATGC	aaacGCATGGTCCATGGAGCACAAC
g7.1	CACCGGCTAACTTAGACATGTAGT	aaacACTACATGTCTAAGTTAGCC
g7.2	CACCGTTAGACATGTAGTAGGAAAA	aaacTTTTCCTACTACATGTCTAAC

2.7 Lentiviral Production

Early passage HEK293T cells seeded on 3.5 x 10^6 on 100mm plates and next day antibiotic free medium changed. Then, transfection mixed prepared with 2.25 µg psPAX2 (Addgene, 12260), 250 ng VSVG (Addgene, 8454) and finally 2.5 µg of plasmid, and up to 200 µl Optimem (31985062) added. On another tube, 200 µl Optimem and 15 µl PEI (Sigma; 408727) prepared and 2 tubes mixed, incubated for 25 minutes in room temperature. Then, transfection mixture added gently on the HEK293Ts incubated for 18-24 hours and medium changed. Furthermore, after 48^{th} and 72^{th} hours of transfection medium collected 2 times. To concentrate viral particles medium filtered and mixed PEG8000 (Sigma; 25322). 24 hours of later, mixture centrifuged at 3000 x g for 30 minutes and pellet dissolved with PBS, then aliquoted on viral transduction, stored at -80°C.

Viral transductions complete by seeding of 5×10^4 cells on a 6 well plate and 30 µl of viral particle delivered after 24 hours of seeding with 8µg/ml protamine sulfate. Then, next day medium changed and let them grow for 1 day. At 48^{th} hour of transduction, medium

changed with 300 μg/ml hygromycin for selection procedure. Between 2 days, medium changed and antibiotic added until control cells die completely.

2.8 T7E Assay

Stable gRNA containing HEK293T cells seeded 5 x 10^4 on 6 well plate, 1 day later pspCas9-GFP (Addgene; pX458) plasmid which contains active Cas9 under the promoter of CMV, transfected with PEI protocol. Cells collected 72 hours later and from the pellets genomic DNA isolation performed with Macherey-Nagel NucleoSpin Tissue kit according to the manufacturers protocol (MN, 740952.50). T7E primers specially designed for our gRNAs to specifically span around 1000 bp as gRNA placement from 400 to 600 bp from T7E Forward-Reverse primer (*Table 2.2*). With T7E primers Phusion PCR (NEB, M0530) performed according to the manufacturers protocol. 1000 bp products set with a reaction on thermal cycle with T7E enzyme (T7E reaction contains denaturation, annealing, digestion) (NEB; M0302). T7E recognizes the mismatches that Cas9+gRNA created on targeted area. Reaction ran on a 1% gel and quantified with ImageJ software. Then, percentage of gene editing calculated with % gene modification = 100 x (1 – (1- fraction cleaved)$^{1/2}$).

Table 2.2 T7E Primers to Amplify Region

T7E	Forward Primer	Reverse Primer
Region-1	GAGAAAACGTCTGTGAGCCCA	CCCTTCATTTGGGACCGG
Region-2	GACGTGTTAACAATGGCAGT	GGTCCCAAAGGAAGCAACC
Region-3	TTATTAGTGGAGGGCAAGGC	CACGCCGAACACTAGTCTAC
Region-4	GCAACACTACAGAGGACAGT	CTTCTGTAGGGGTACTTGCC
Region-5	CTTCTCTGATGCTAGACCACA	CTGCCATTGTTAACACGTCAC
Region-6	CCTCCAGATATTGCCAAATGC	GGTTCTTCCCTGTCATACGT
Region-7	GGTTGAGAACCAGTGGTTTAC	GGTTCTTCCCTGTCATACGT

2.9 Chromatin Immunoprecipitation (ChIP)

Stable gRNA containing HEK-CASPEX cell lines growed on 100 mm with inducing doxycyline for 48 hours. Then, 9 million cells collected and fixed with 1% of PFA in PBS for 10 min in room temperature. Then, mixture divided into 3 tube and added 125 mm glycine to quench the reaction. Pellets washed 3 times and centrifuged at 1000 x g. ChIP Lysis buffer with SDS (10 mM Tris; 1 mM EDTA; 140 mM NaCl; 1% Triton X-100; 0.1% Na-deoxycholate; 1% SDS; 1 mM PMSF; Protease Inhibitor Cocktail) and incubated on ice for 15 minutes. Next, samples sonicated to shear the DNA-protein complexes with Diagenode-Bioruptor Sonication Machine with 45 sec on 15 sec on, 40 cycles. Then centrifuged at 10000 x g for 10 min and supernatant is sheared chromatin which stored at -80°C for further steps.

Protein A/G dynabeads washed twice with Tris Edta and PBST buffer to prepare for pulldown reaction. 1nput separated as 1 tube for further reactions. For FLAG and IgG tubes, lysates occupied with only beads for 30 minutes in room temperature as a pre-clearence step. While its preclearing, on another tube, FLAG-Bead complexes prepared by adding 10 µg of antibody from FLAG and IgG tubes. 20 µl of Protein A/G beads used for each reaction. 1 hour later, Antibody-Bead complex mixed with cleared lysates and rotated on +4°C for overnight. Furthermore, ChIP tubes washed with following buffers to reduce the background activity: ChIP lysis buffer, low-salt buffer (0.1% SDS, 1% Triton-X 100, 2 mM EDTA, 20 mM Tris-HCl, 140 mM NaCl), high salt buffer (low-salt buffer, 500 mM NaCl), LiCl buffer (0.25 M LiCl, 1% IGEPAL-CA 630, 1% deoxychalate, 1 mM EDTA, 10 mM Tris) and Tris-EDTA. Elution step requires Elution buffer which is freshly prepared everytime (1% SDS and 0.1 M $NaHCO_3$), to rip-off DNA-protein complex from the beads. Elution repeated 2 time with 15 minutes of rotation. Then, samples are treated with RNAase A (Thermo Fisher Scientific, 12091021) and 5M of NaCl for 30 minutes in 37°C. Proteinase K treatment applied for 1 hour at 65°C. Finally, ChIP DNA clean-up kit used to prepare DNA for qPCR reaction (Zymo Research, D5205).

qPCR primers designed specifically for gRNAs as in spanning around gRNAs with 80-180 bp ordered from Macrogen. qPCR reaction ran on RocheLight Cycler 480 device.

Table 2.3 ATP7B Promoter gRNAs ChIP-qPCR Primers.

ATP7B Promoter ChIP Region	Forward Primer	Reverse Primer
g1.2	CTTCCTTTGGGACCCACGG	CGCAGACTCAGCTCCCAG
g2.2	GTAGACTAGTGTTCGGCGTGG	CTGTCAATCACAGGCCACG
g3.4	GACGGGCAAGTACCCCTACA	GAAAGGAGCTGGTGCCTGTG
g4.2	AGCAGAGGATTCAACATAAGCT	GAAACCGGATCTTCCTTCTCATC
g5.1	GCCTGAACTTTTGAAAGAATTAGG	CACCTACATATTTTTGTTCAGGCTG
g6.1	CAGAGTCTGACAAAAGTGGTAAG	GTCCTGAGAAAGCAAACTGTC
g7.1	CTGTTTCTGCATTCAATCTAGTG	GTGGTCTAGCATCAGAGAAG

2.10 qRT-PCR

RNA extraction was performed using the Zymo RNA Isolation Kit (Zymo, R1051). A total of 500 ng of RNA from each sample was reverse transcribed into cDNA using M-MLV Reverse Transcriptase (Thermo Fisher Scientific, 28025013). Subsequently, 10 ng of the synthesized cDNA was loaded onto qPCR plates and combined with LightCycler 480 SYBR Green I Master mix (Roche Diagnostics, 04707516001) and 0.15 µM of qPCR primers. Primers designed from NCBI Primer Blast tool (*Table 2.4*). Roche Light Cycler 480 device used to run samples with an annealing temperature of 55 °C. qPCR results calculated with $2^{(-\Delta\Delta CT)}$ method normalizing with GAPDH and Controls.

Table 2.4 Expression qPCR Primers

Gene	Forward Primer	Reverse Primer
GAPDH	AGCCACATCGCTCAGACAC	GCCCAATACGACCAAATCC
ATP7B	GTGGGCAATGACACCACTTT	TGGGTGCCTTTGACATCTGA
TP53	GCAGTCAGATCCTAGCGTCG	CGTTGTTTTCAGGAAGTAGTTTCCA
ATF3	CGCTGGAATCAGTCACTGTCAG	CTTGTTTCGGCACTTTGCAGCTG
LEF1	TACAGGAATCTGCATCAGGTACAGG	CACGTTGGGAATGAGCTTCGT
TOX4	GATTTCCGGAGGCAACTTCC	GGCAGCCTGTGTATCACGAA
ATP7A		

	TTT GGA ACT TGT TGT GAG GGG	AGG GCC ACG GAG CAG TAT AG
ABCC 2	CCT GGT TGA TGA AGG CTC TGT	ACG GTC ACT TGC AAA GGA GA
CTR1	TGC GTA AGT CAC AAG TCA GCA	AGG TGA GGA AAG CTC AGC ATC
ERCC1	GCTGGCTAAGATGTGTATCCTG G	ATCAGGAGGTCCGCTGGTTTCT
RAD52	CACGCAGCAGAATGTGGATTTT	AGCTGGACCCTCACAAATGC

2.11 CASPEX Biotinylation and Streptavidin Pulldown

HEK-CASPEX + Stable gRNA cell lines seeded on 10 x 150 mm plates coated PLL with 60% confluency. Then, 2 µg/ml doxycyline induction applied to the cell lines for 48 hours. 500 µM final concentration of Biotin-tyramide phenol (Iris Biotech-LS 3500) and incubated for 30 minutes at incubator. Next, H_2O_2 added with a final concentration of 1mM to the plates and shaked gently for 1 minute to start biotinylation. 1 minute later medium removed and quickly added dexotification buffers (Cold PBS Containing 10 mM Sodium Azide (Thermo; 26628-22-8), 10mM Sodium Ascorbate (Thermo; 134-03-2), 5mM TROLOX (Thermo; 53188). Then, washed 3 times with PBS and trypsinized and pellets washed 2 times with PBS.

CASPEX biotinylated pellets first exploded with Hypotonic buffer (20 mM Tris-HCl, pH 7.4, 10 mM NaCl, 3 mM $MgCl_2$) and incubated on ice for 30 minutes with vortexing 3 times in total. In the end of the incubation, 10% of NP40 added and vortexed for 30 seconds. Samples centrifuged for 30 min on 3000 x g and supernatant contains cytosolic proteins while pellet contains nuclear proteins. Pellet and supernatant separated and stored. Pellet resuspended with RIPA Buffer and incubated on ice for 30 min. Next, samples were sonicated on Bioruptor for 30 min with 30 cycle. Finally, samples are centrifuged at 14000 x g for 30 min and supernatant contains nuclear proteins. Protein concentrations quantified by Pierce BCA Assay kit. 4~5 mg of protein incubated with 400 µl of Streptavidin Magnetic beads overnight. Then, bead protein complexes washed

2 times with RIPA, 1M KCI, 0.1 M Na_2CO_3 buffers which will be prepared for mass spectrometry analysis.

2.12 Mass Spectrometry

For the mass spectrometry analysis, protein mixtures were prepared and subjected to on-bead trypsin digestion using Streptavidin beads. This involved washing the beads with an 8M urea solution and treating the proteins with DTT and iodoacetamide for reduction and alkylation, respectively. Following alkylation, the beads were washed with ammonium bicarbonate solution and incubated overnight with trypsin at 37 °C. The resulting peptide mixtures were collected and desalted using C18 STAGE to remove salts. Subsequently, the peptides were analyzed using C18 nanoflow reversed-phase liquid chromatography (nLC) coupled with a Q Exactive Orbitrap mass spectrometer. The samples were resolved on a C18 column using a gradient of acetonitrile and formic acid, and the eluted peptides were monitored by MS1 scanning.

2.13 LFQ Analysis

The raw files obtained from mass spectrometry experiments were processed using MaxQuant software. The analysis was performed with specific parameters, including classical LFQ (Label-Free Quantification) analysis and an identification number set to 2. Trypsin digestion was used for protein fragmentation, and the human proteome FASTA file from Uniprot with the accession number UP000005640_9606 was utilized for protein identification. The IBAQ (Intensity-Based Absolute Quantification) method was activated during quantification. For peptide matching between different runs, the "Match between runs" feature was enabled. Additionally, the quantification method used was Razor, and unique peptides were considered for analysis.

Furthermore, analysis of protein group files from MaxQuant was performed using the Cassiopeia LFQ analysis tool obtained from GitHub. Cassiopeia utilizes the Limma package and various statistical tools to identify proteins and assess the enrichments in LFQ (Label-Free Quantification) data (Varnavides et al., 2022). By applying these analytical methods in R software, Cassiopeia enables a comprehensive exploration of the proteomic data, allowing for the identification and characterization of proteins of interest and the evaluation of their quantitative changes in the LFQ analysis.

Lastly, the analyzed data was further examined by comparing it to the human transcription factor database and the MORF (Multiplexed Ox of Regulatory Factors) library to identify specific transcription factors associated with the observed changes. Volcano plots were generated using R software, with p-value cutoffs and LogFC (fold change) thresholds set at both 0.5 and 1. These plots allowed for the visualization and highlighting of transcription factors that exhibited significant changes in expression and were potentially involved in the regulatory processes underlying the observed biological phenomena.

2.14 Generation of Knockout and Overexpression Cell lines

Ko cell lines generated by annealing of gRNAs into LentiCRISPR-V2 plasmid (Addgene; 52961) by annealing and digestion of plasmid with Bsmb1-V2 (NEB; R0739). Additionally, we generated Ox of selected transcription factors. In shortly, coding sequence of each transcription factor determined on NCBI (*Table 2.5*). Primers ordered according to the desired Ox vector (Addgene; 163447). pLJC2-GPT2-3XFLAG plasmid digested with PacI (NEB; R0547), Not1 (NEB; R0189) to generate sticky ends and remove the gene inserted (GPT2). Next, using HEK293T cDNA with Phusion PCR and primers of selected transcription factor of interest, we amplified desired region. Again, desired insertable fragment double digested and run on a 1% gel. By using, MN Gel/PCR cleanup Kit, selected fragment isolated. Cloning performed with T4 ligase and its conditions. Transformed plasmids isolated and prepared for viral particle production. Then, viral particles produced as previously transfected and transduced on cells.

Table 2.5 Knockout and Overexpression Primers.

TOX4-Pac1-F	ATATATTTAATTAAATGGAGTTTCCCGGAGG
TOX4-NotI-R	ATATATGCGGCCGCTTTCACAAACACCACTGTGTTTG
ATF3-PacI-F	ATATATTTAATTAAATGATGCTTCAACACCCAGG
ATF3-NotI-R	ATATATGCGGCCGCGCTCTGCAATGTTCCTTCTTTTATC
LEFI-PacI-F	ATATATTTAATTAAATGCCCCAACTCTCCGGAGG

LEF1-NotI-R	ATATATGCGGCCGCGATGTAGGCAGCTGTCATTCTTGG
TOX4 KO g1-F	CACCGATGGTGTTGAGGATTTCCGG
TOX4 KO g1-R	aaacCCGGAAATCCTCAACACCATC
TOX4 KO g2-F	CACCGTCCTAATGCCACTTTTGGTG
TOX4 KO g2-R	aaacCACCAAAAGTGGCATTAGGAC
ATF3 KO g1-F	CACCGTGTCAGCGACAGACCCCTCG
ATF3 KO g1-R	aaacCGAGGGGTCTGTCGCTGACAC
ATF3 KO g2-F	CACCGAAAGTGCCGAAACAAGAAGA
ATF3 KO g2-R	aaacTCTTCTTGTTTCGGCACTTTC
LEF1 KO g1-F	CACCGAACATCAAATAAAGTGCCCG
LEF1 KO g1-R	aaacCGGGCACTTTATTTGATGTTC
LEF1 KO g2-F	CACCGTCAGGAGCCCTACCACGACA
LEF1 KO g2-R	aaacTGTCGTGGTAGGGCTCCTGAC
ATP7B KO-F	CACCGCTCATTAAAGCTACCCACG
ATP7B KO-R	AAACCGTGGGTAGCTTTAATGAGC

2.15 Luciferase Assays

ATP7B promoter cloned with following primers into pMDR1-1202 plasmid (Addgene; 37627) with Sma1 and BglII enzymes (NEB; R0141, R0144) to remove MDR1 gene, remaining is empty luciferase vector. Amplifications comleted with Phusion PCR from genomic DNA of HEK293T, and desired lengths of promoter digested with same enzymes and cloned into the luciferase vector with T4 ligase enzyme. Finally, DNA sequences of putative ATP7B promoter (200, 500, 1000, 2000, 3000 bp) from transcription start site cloned and ready for transfection.

HEK293T cells seeded on PLL coated 96 well plate 1.5 x 10^4 and 1 day later, transfection completed with Lipofectamine 3000 manufacturer's protocol. 18 to 24 hours later medium changed and at 48 hours later 30 µg of Luciferin delivered on medium and allowing 1 min to penetrate cells, next, luminescence read completed on microplate reader (Synergy H1 Hybrid reader, BioTek). After that medium removed and cells lysed on plate with 25 µl of 0.2% of SDS solution for 10 min in RT. Then, Pierce BCA kit used for

quantification of the protein amount from a well. Total Relative Luminescence Unit divided by Total protein from a well to determine Relative Luminescence Unit per Protein (µg).

Additionally, For the HDAC inhibitor experiments, cells were transfected with exactly the same protocol, 24 hours of later medium changed and 5µM of (MS275, Chidamide, KD5170, PAOA, Pyroxamide) added and on 72th hour of transfection luminescence read taken with total protein concentration.

Table 2.6 Cloning Primers of ATP7B Promoter

ATP7Bp-3kb-SMA1-F	ATATCCCGGGAATGTCTTGCGAAGGGCAAAAAT
ATP7Bp-2kb-SMA1-F	ATATCCCGGGCCTGTCCTTTAAGTCTGGTTAGTG
ATP7Bp-1kb-SMA1-F	ATATATCCCGGGAAAACGTCTGTGAGC
ATP7Bprom-0.5kb-SmaI-F	ATATATCCCGGGGGTGCGGAGTTCACTCTT
Sma1-ATP7Bp-200bp-F	ATATATCCCGGGAGAACACTGTGGCACC
ATP7Bprom-BglII_R	ATATATAGATCTAACCGCCCCTTCATTTGGGA

2.16 Transcription Factors ChIP-qPCR

For the ChIP-qPCR of selected transcription factors (ATF3, TOX4). Same protocol from 2.9 followed and CASPEX regions gRNA targeting ChIP-qPCR primers used to span the area. ChIP-qPCR calculated by Input% method and fold change method.

%Input = 100*2^ (CtInput-Log (% of Input Saved)) – CTAntibody)

Fold Change = $2^{(-\Delta\Delta CT)}$

2.17 Cisplatin and Copper Treatment

Desired cells (HEK-HUH7) and generated cell lines seeded on 96 well, 4 x 10^4. Following day cells treated with cisplatin and copper treatments (Cisplatin: 100 to 0 µM, Copper: 2 to 0 mM). Allowing cells to incubate for 72 hours.

2.18 Sulforhodamine B Assay

72 hours of incubation with drugs 96 well plates fixed with 50% of TCA (Sigma, T6399) for 1 hour at 4°C. Plates are washed with water 5 times and allowing them to dry for 1 day. Then, 0.4% and 50 µl of SRB (Santa Cruz, sc-253615) solution used for dying viable cells for 30 min at RT. Next, plates were washed 5 times with 1% of Acetic Acid and allowed to dry. After plates dried, 10 mM of Tris-Base solution (Sigma, T1503) used for solving the dye and measurements completed on microplate reader at 564 nm (Hybrid reader, BioTek).

2.19 Colony Formation Assay

A total of 500 cells were plated on 12-well plates. After one day, the cells were treated with varying concentrations of Cisplatin (0.5 µM, 1 µM, and 2 µM). The cells were then allowed to incubate for three days. Then, fresh medium replaced and cells growed 11 more days when colonies become visible. Finally, plates fixed with ice cold methanol for 20 minutes. Then, plates dyed with 0.5% of crystal violet and washed with distilled water. Scanner used to record results.

Chapter 3:**RESULTS**

3.1 In-Silico Analysis of ATP7B

3.1.1 Conservation of ATP7B Promoter

Transcription factors possess conserved sequences that allow them to recognize distinct motifs in DNA, enabling them to regulate gene expression levels. Our study aimed to investigate the extent of conservation within the ATP7B promoter region by conducting a comparative analysis across eight different animal species (He et al., 2011; Martínez Corrales & Alic, 2020; Nitta et al., 2015). Specifically, we analyzed the DNA sequence from the transcription start site (+1) to -3000 base pairs (bp) upstream of the ATP7B transcription start site. The primary objective was to identify conserved regions within this promoter region that play a critical role in the functioning of the copper ATPase (Figure 3.1).

Through the comparison of DNA sequences across these diverse animal species, we successfully identified specific areas within the ATP7B promoter that demonstrated a notable degree of conservation. Notably, regions such as -600 bp and between -900 to -1000 exhibited a high level of conservation. These conserved regions signify the functional significance of DNA motifs in regulating ATP7B expression. It suggests that specific transcriptional modulators may have the ability to influence ATP7B expression by acting as activators or repressors in these conserved areas.

Furthermore, this analysis also reveals that conservation within the ATP7B promoter extends up to -3000 base pairs, even among hominids. This finding suggests the presence of additional regulatory regions within this extended region of the promoter. The conservation of these regulatory elements across closely related species underscores their functional importance and raises intriguing possibilities regarding their role in the precise control of ATP7B expression. Further investigation of these conserved regions could provide valuable insights into the transcriptional regulation of ATP7B and offer potential avenues for therapeutic intervention in conditions associated with ATP7B dysregulation.

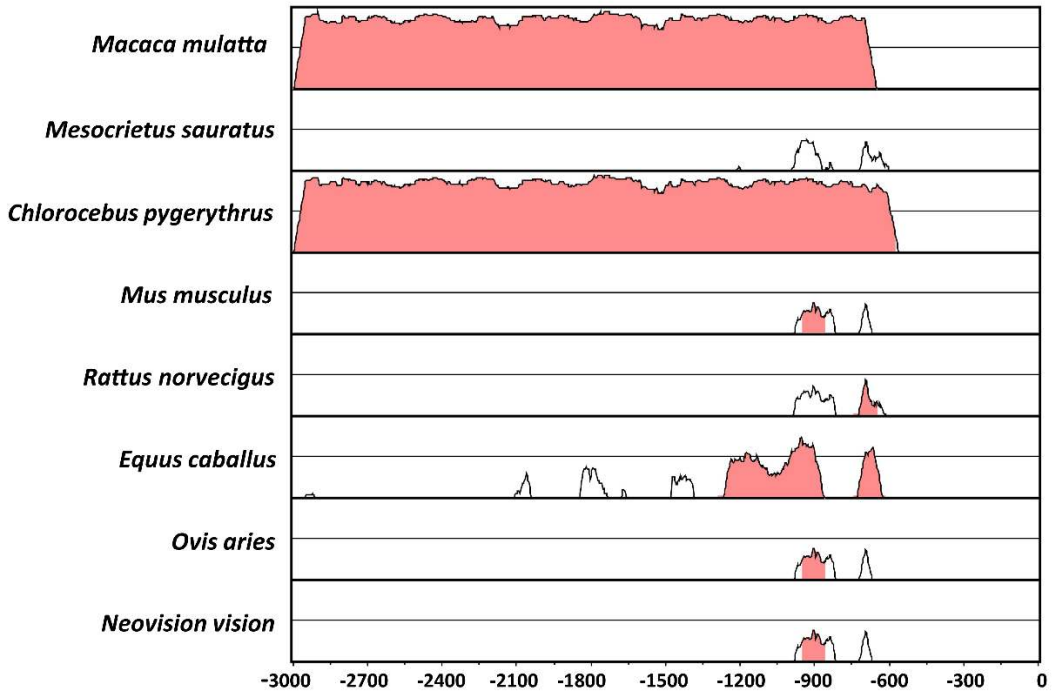

Figure 3.1: Conservation Analysis of ATP7B Promoter Across Eight Species from +1 Transcription Start Site to -3000 bp.

This figure illustrates the conservation of the ATP7B promoter region across eight different species. The analysis spans from the +1 Transcription Start Site to -3000 bp upstream of the ATP7B gene. By comparing the sequences from various organisms, we can identify regions that are evolutionarily conserved, indicating potential functional significance in regulating ATP7B gene expression. The conservation analysis provides valuable insights into the critical regulatory elements governing the expression of ATP7B across different species.

3.1.2 Potential Transcriptional Regulators of ATP7B

Through our analysis of the conserved ATP7B promoter region, spanning from the transcription start site to -3000 base pairs, we discovered numerous transcription factor motifs. These motifs provide binding sites for transcriptional and epigenetic regulators, enabling them to modulate the regulation of ATP7B.

To identify potential transcriptional regulators within this region, we utilized two databases: TRANSFAC and PROMO. The TRANSFAC database revealed the presence of 122 distinct transcription factors, while the PROMO database identified 80 potential transcription regulators associated with ATP7B (Farré et al., 2003; Matys et al., 2006).

Notably, there were 22 transcription factors that were common to both databases within the analyzed region. Among these regulators, some are well-known for their transcription factor binding sites (TFBSs), including P53, LEF1, POU2F1, and MAZ (Figure 3.2).

Importantly, among the identified transcription factors as potential regulators of ATP7B, there were factors (MAZ, STAT1, LEF1, P53) associated with tumor proliferation and carcinogenesis. This suggests a potential link between ATP7B regulation and processes related to tumor development and progression (X. Li et al., 2021; Olivier et al., 2010; Santiago et al., 2017a; Yang et al., 2019).

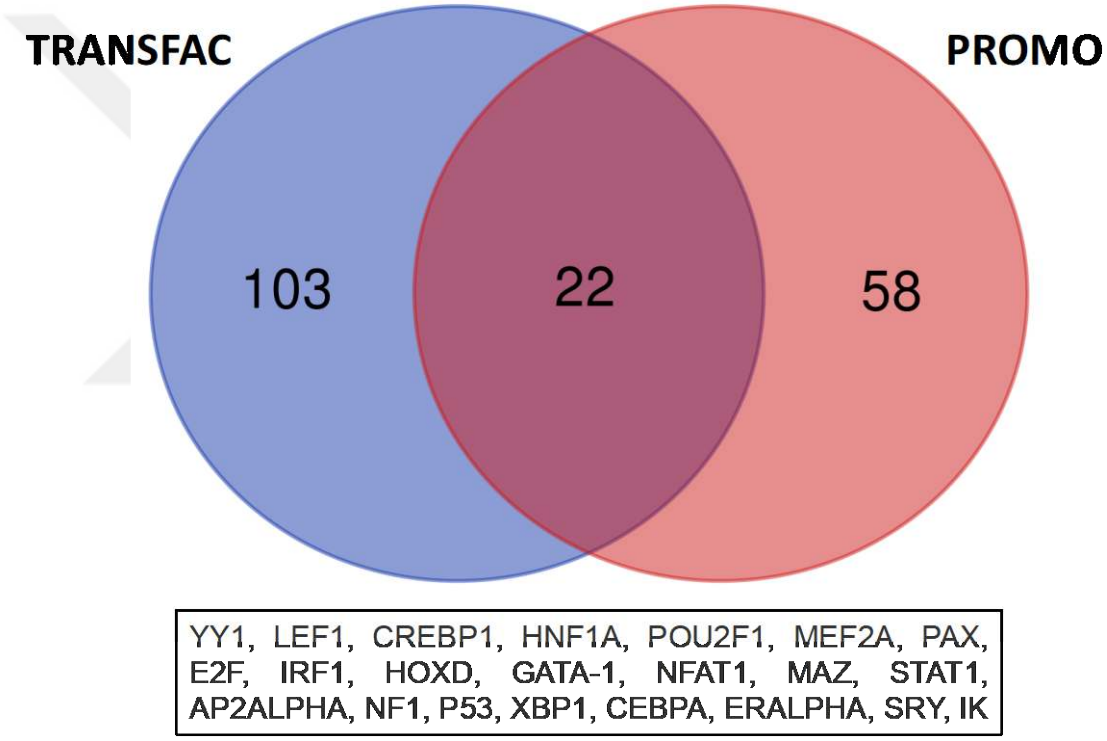

Figure 3.2 Identification of Potential Transcriptional Regulators of ATP7B Promoter from -3000 bp to +1 Transcription Start Site Using TRANSFAC and PROMO Databases.

Figure generated with Dr. Selahattin Can Ozcan and Baris Sergi, PhD Candidate.

3.2 HEK-CASPEX Cell Line Generation and Targeting ATP7B Promoter

3.2.1 Generation of HEK-CASPEX Cell line

To determine the precise location of proteins on the DNA, we employed the CASPEX system, which utilizes the APEX2 protein for proximity labeling. This engineered protein enables the detection of proteins in close-proximity, thereby facilitating their identification (Gao et al., 2018; Myers et al., 2018). APEX2 is an ideal biotinylation protein for the detection of transcriptional regulators due to its rapid biotinylation capability. With a short exposure time of only 1 minute to hydrogen peroxide (H_2O_2), APEX2 efficiently biotinylates proteins in proximity (Lam et al., 2014; Nguyen et al., 2020; Qiu et al., 2019). This quick labeling process allows for the accurate identification and characterization of transcriptional regulators associated with the ATP7B promoter. By harnessing the targeting capability of dCas9 towards DNA and utilizing efficient guide RNAs (gRNAs), CASPEX can specifically target a desired locus on the DNA. Subsequently, through the biotinylation ability of APEX2, proteins associated with the DNA, including epigenetic, chromatin, and transcriptional regulators, can be labeled and identified using mass spectrometry (Figure 3.3B).

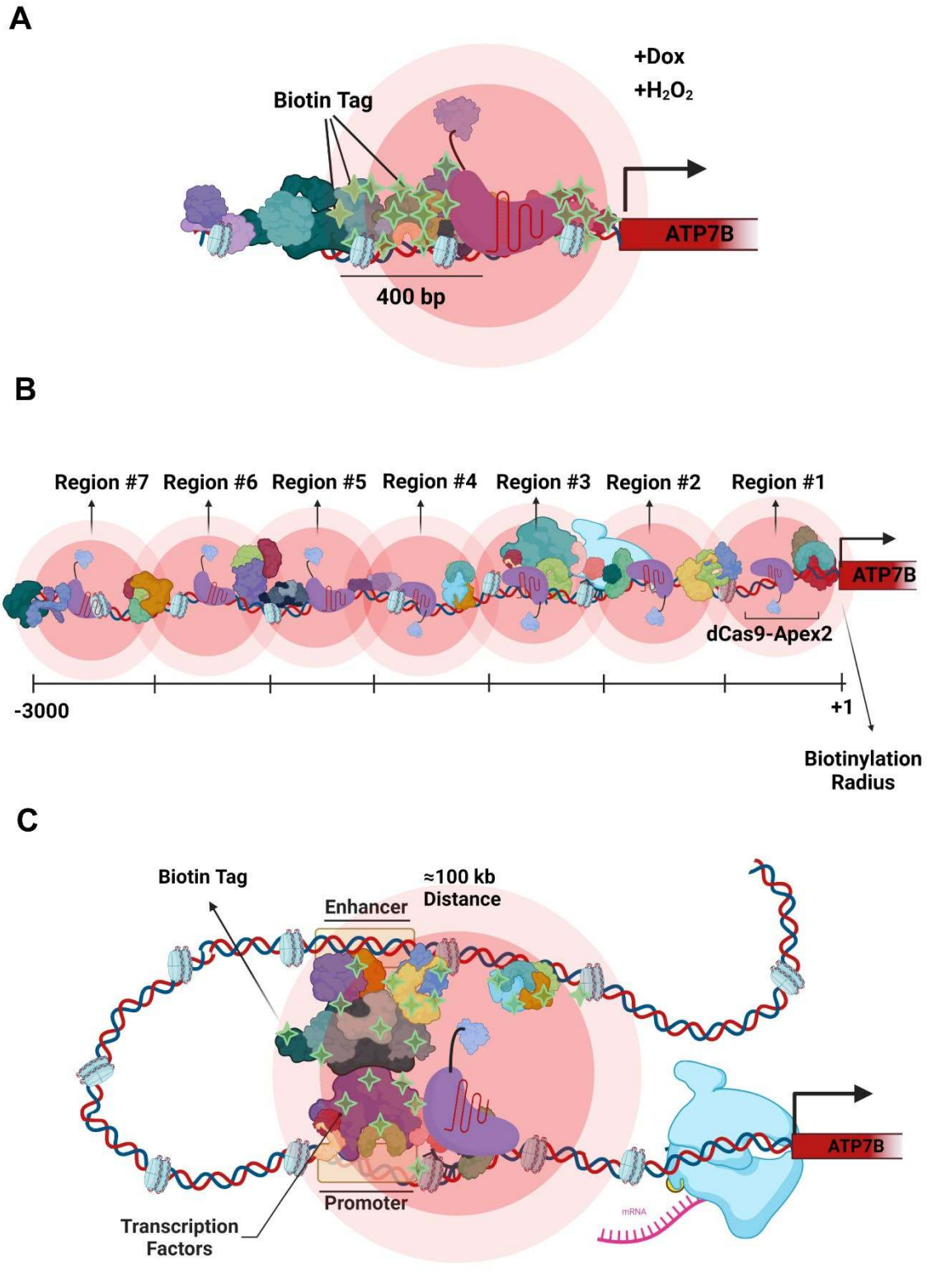

Figure 3.3 ATP7B CASPEX Labelling and Biotinylation Mechanism

A) Initiation of CASPEX transcription using an inducible system with doxycycline, followed by the rapid biotinylation process, which is completed within 1 minute upon the introduction of hydrogen peroxide (H_2O_2). Representative principle of CASPEX protein biotinylation, highlighting the proximity radius of approximately 400 base pairs (bp), which enables the selective labeling of proteins in the immediate vicinity of the targeted genomic locus.
B) Illustration of gRNA design and its targeting locations on the ATP7B promoter, displaying the precise and efficient guide RNA (gRNA) design for the CASPEX system.
C) Schematic representation of the ATP7B transcriptional machinery and biotinylation, demonstrating the involvement of transcription factors and enhancer-promoter interactions that contribute to the assembly of the RNA-Pol II transcriptional machinery for ATP7B gene expression. Figures generated with Biorender.

The CASPEX plasmid incorporates the Tet-on 3G (TRE3G) promoter, which allows for precise and controllable induction of transcriptional activation through the addition of Doxycycline(Randolph et al., 2017). This inducibility feature prevents excessive accumulation of the ATP7B promoter and reduces background interference in mass spectrometry analysis (Figure 3.3C).

Additionally, the CASPEX system includes a Piggybac transposase site, facilitating a cut-and-paste mechanism for integrating the CASPEX plasmid into the genome of HEK293T cells. By co-transfecting CASPEX and the Piggybac transposase, we generated the HEK293T-CASPEX cell line to ensure stable integration, the transfected cells underwent puromycin selection, followed by the utilization of flow cytometry to select colonies exhibiting the +GFP marker on the CASPEX cassette (Figure 3.4A). Subsequently, individual colonies were isolated and allowed to grow independently, enabling the selection of the most robust colony expressing CASPEX efficiently. This meticulous colony selection process ensures optimal biotinylation steps for subsequent mass spectrometry analysis, leading to a reduced background signal (Figure 3.4B). This experimental approach enables us to investigate the proteins associated with the ATP7B promoter in a precise and controlled manner. The combination of the CASPEX system, inducible promoter, and single-cell isolation techniques contributes to the robustness and

reliability of our analysis, providing valuable insights into the regulatory landscape surrounding ATP7B.

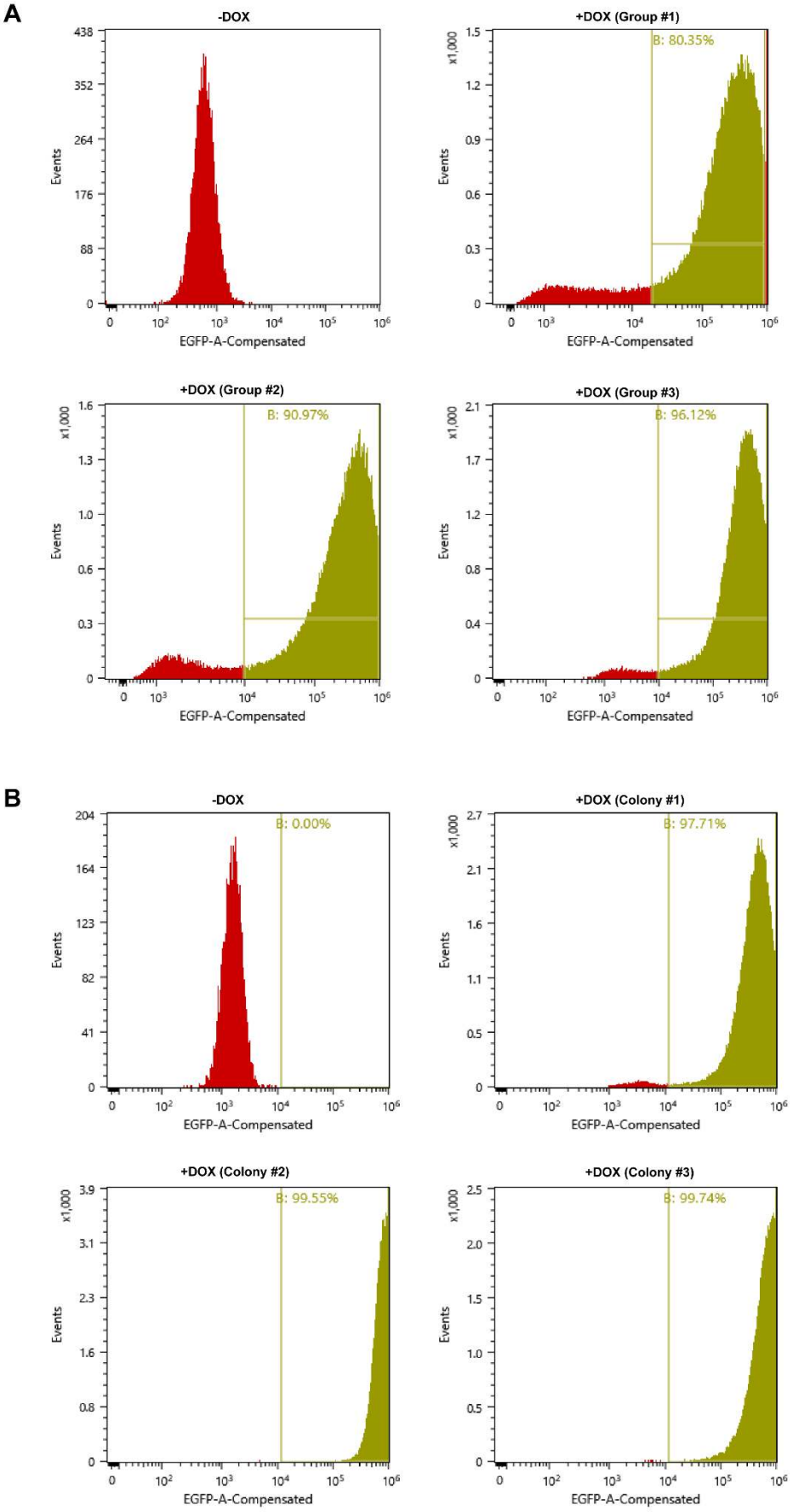
A
-DOX
+DOX (Group #1)
B: 80.35%
+DOX (Group #2)
B: 90.97%
+DOX (Group #3)
B: 96.12%
B
-DOX
B: 0.00%
+DOX (Colony #1)
B: 97.71%
+DOX (Colony #2)
B: 99.55%
+DOX (Colony #3)
B: 99.74%
Events
x1,000
EGFP-A-Compensated

Figure 3.4: HEK-CASPEX Cell Line Single Cell Sorting and GFP Confirmation.

A) Polyclonal cell population expressing the GFP marker was visually demonstrated, showing the successful introduction of the CASPEX system.

B) Single colonies exhibiting the GFP marker, which were carefully observed and isolated for subsequent investigations.

Figure generated in collaboration with Ayca Acar, MSc Student.

3.2.2 Validation of HEK-CASPEX Cells

To validate CASPEX expression in the HEK-CASPEX cell line, we assessed the efficiency of +GFP expression in single colonies. Among these colonies, colony #3 demonstrated a 99% efficiency in expressing +GFP. To further confirm CASPEX expression, we employed doxycycline induction and performed immunoprecipitation (IP) followed by Western blotting with anti-FLAG antibody. CASPEX, a 180 KDa protein, was specifically detected in Colony #3, validating its expression in the cell line (Figure 3.5A).

To investigate the localization of CASPEX, we conducted immunofluorescence (IF) assays. Notably, CASPEX contains a P2A sequence that separates GFP from FLAG-dCas9-APEX2-V5 through a self-cleaving peptide(Liu et al., 2017). After 48 hours of doxycycline induction, we utilized anti-V5 antibody to detect CASPEX localization (Figure 3.5B). The results confirmed the nuclear localization of CASPEX, indicating its presence in the appropriate cellular compartment. This localization data secured the way for further preparations involving biotinylation and targeting of the ATP7B promoter. The successful validation of CASPEX expression and its nuclear localization in the HEK-CASPEX cell line provides a solid foundation for biotinylation and ATP7B promoter targeting steps.

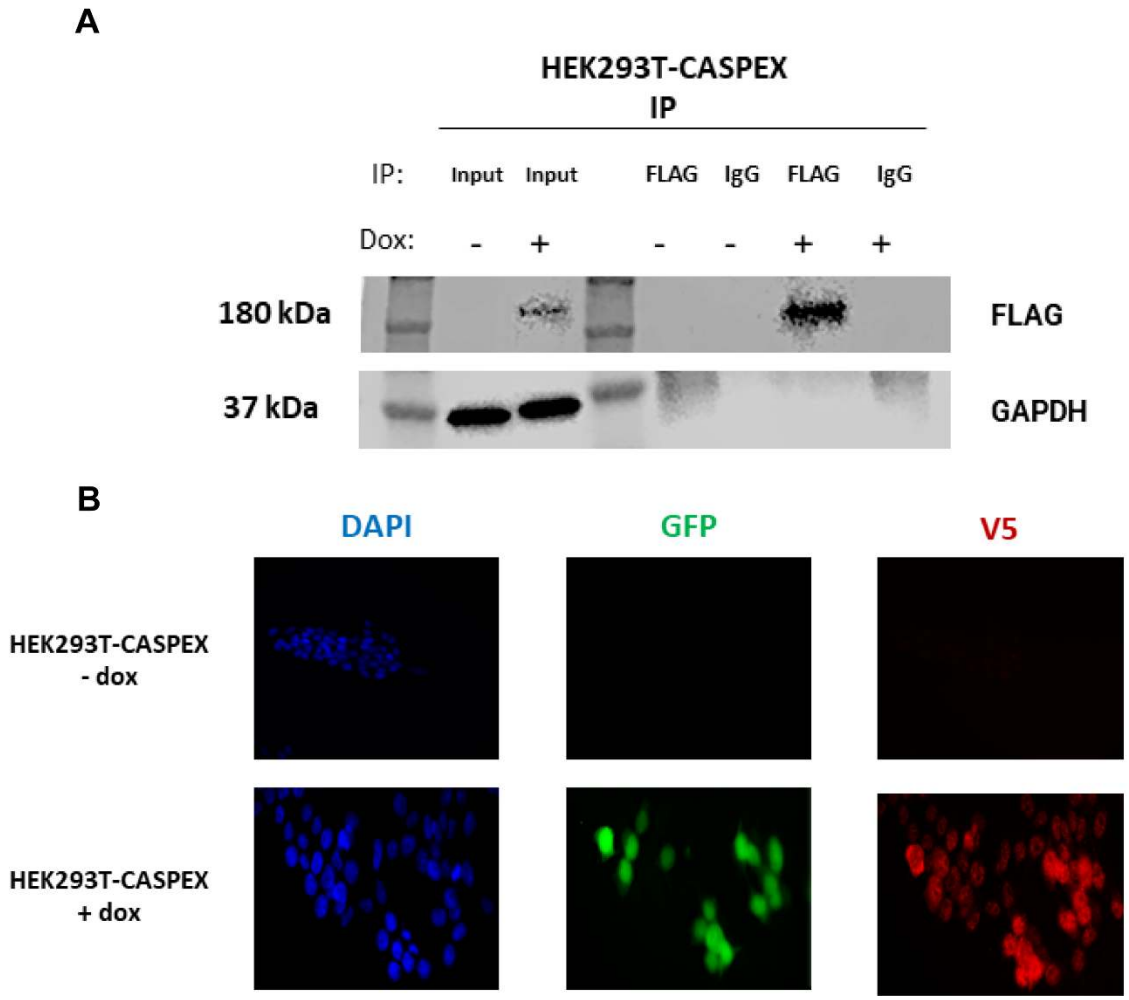

Figure 3.5 HEK-CASPEX Cell Line Verification using Immunoprecipitation (IP) and Immunofluorescence (IF).

A) Immunoprecipitation (IP) was performed using Anti-FLAG antibodies to validate the presence and expression of the CASPEX system.

B) IF analysis was conducted using Anti-V5 antibodies to visualize and confirm the expression and localization of the V5 tag in the CASPEX system.

Figure generated in collaboration with Ayca Acar, MSc Student.

3.2.3 Targeting ATP7B Promoter with 7 Different gRNAs and gRNA Efficiency

To target the ATP7B promoter effectively using the CASPEX system, we defined seven distinct regions spanning from the +1 transcription start site to -3000 base pairs. Considering the biotinylation capacity of CASPEX, which covers approximately 350 base pairs, we designed gRNAs that were optimized for on-off targeting efficiency within

each region (Hsu et al., 2013; Xiang et al., 2021). As the targeting location is the promoter region, the efficiency of gRNAs may vary. To select the most efficient gRNA from each region, we designed two gRNAs for each region and included one non-targeting gRNA as a control. These gRNAs were then cloned into the Lenti-guide (hygro) backbone, and viral particles were prepared. To assess the efficiency of gRNAs, the viral particles were delivered to HEK293T cells along with the transfection of pspCas9-GFP. The cells were allowed to incubate for 72 hours to generate indel sequences, which served as indicators of gRNA efficiency.

To validate the efficiency of gRNA targeting the ATP7B promoter in regular 293T cells, we enhanced the T7EI assay (Figure 3.6A). Based on the T7EI analyses, we selected one gRNA from each region that exhibited promising efficiency(Sentmanat et al., 2018). These selected gRNAs were then further validated for their efficiency in the HEK-CASPEX cell line (Figure 3.6B).

This detailed process of gRNA selection ensures that we identify the most efficient gRNAs for targeting the ATP7B promoter in the context of the CASPEX system. The validation of gRNA efficiency will contribute to the accuracy and reliability of subsequent experiments and biotinylation steps in investigating the transcriptional regulation of ATP7B.

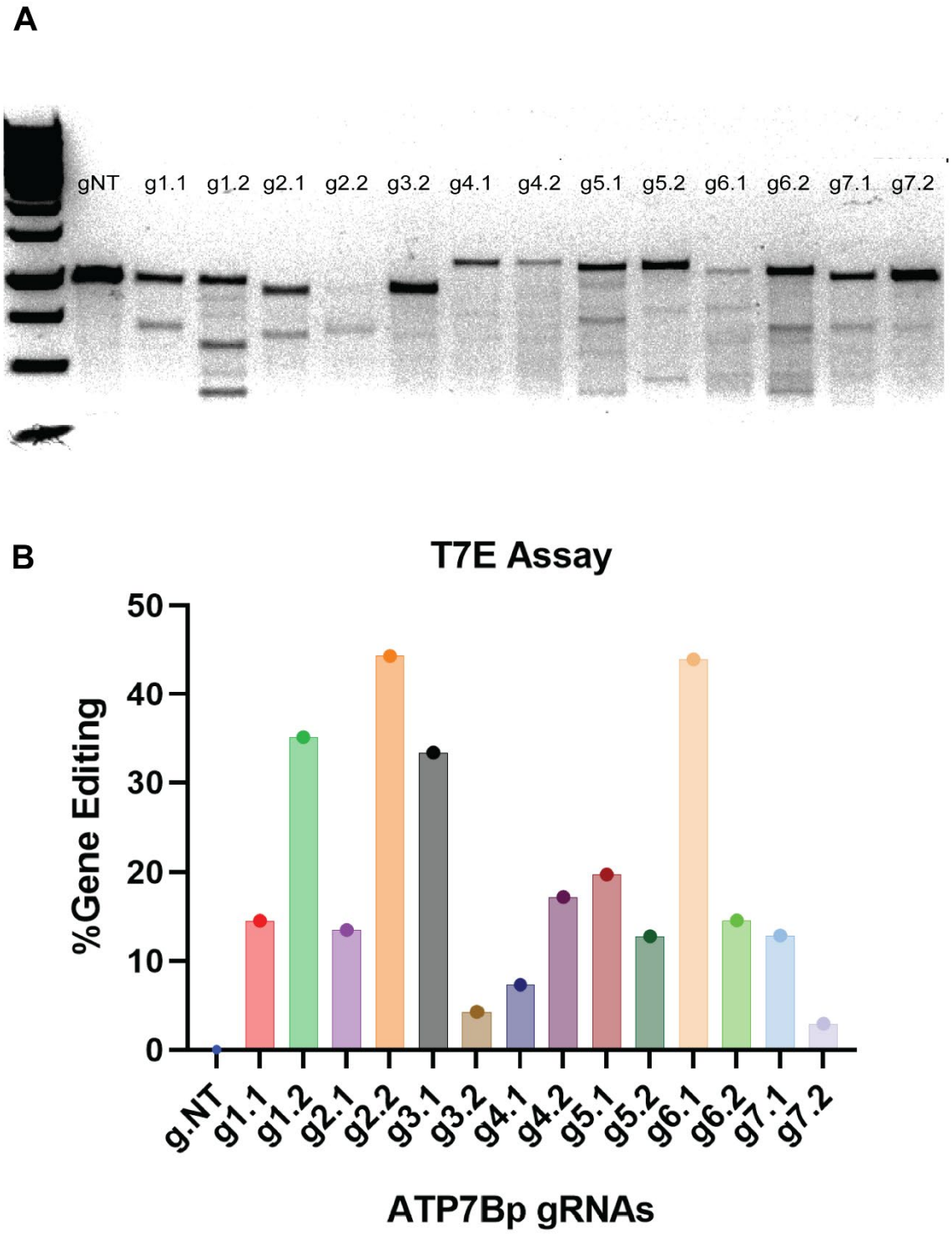

Figure 3.6 Efficiency Assessments of HEK-CASPEX gRNAs Targeting ATP7B Promoter.

A) T7E Analysis of ATP7B Promoter Targeting gRNAs: The efficiency of gRNAs targeting the ATP7B promoter region is assessed using the T7 endonuclease I (T7E)

assay. The ATP7B promoter sequences, amplified using the specific gRNAs, were subjected to T7E analysis to detect the presence of indels (insertions or deletions) resulting from CRISPR-Cas9 cleavage.

B) Quantification and Analysis of T7E Results: Image analyzed with ImageJ to determine the gene editing efficiency of each gRNA. The gene editing efficiency is calculated using the formula: Gene editing efficiency = 100 x (1 - (1 - fraction) $^{\wedge 1/2}$), where "fraction" represents the proportion of cleaved DNA fragments compared to the total amount of DNA.

Figure generated in collaboration with Ayca Acar, MSc Student.

3.2.4 Validation of Selected gRNAs and CASPEX Targeting Through ChIP on HEK-CASPEX Cells.

In the T7EI assay results, the gRNA showing higher gene editing activity was selected, and its corresponding viral particles were delivered to HEK-CASPEX cells. After 48 hours of doxycycline induction, CASPEX expression was observed, and cell pellets were prepared for ChIP experiments. Before proceeding with ChIP, we assessed the sonication capability of HEK-CASPEX cells by optimizing parameters such as cell number, sonication time, cycle number, and different buffers. Based on the sonication results, we determined that 50 cycles were optimal for obtaining 150-200 base pairs of shared DNA, which is ideal for subsequent ChIP experiments (Figure 3.7A).

For the ChIP experiments, CASPEX, which contains 3x FLAG tags at the N-terminal, was utilized for the pulldown of the targeted ATP7B promoter sequence. Anti-FLAG antibodies were employed for this purpose, while IgG was used as a negative control.

To analyze the ChIP-qPCR results, we designed primers that spanned approximately 25 base pairs of the gRNAs and additional qPCR primers spanning around 80-150 base pairs. The qPCR results were reported as Input% and Fold change, which allowed us to consider both IgG and Non-Targeting gRNA samples. Regions 1 and 2 exhibited a high percentage of Input (between 20-30%), indicating efficient pulldown. However, in other regions, the percentage of Input was not as high (Figure 3.7B). Considering the challenges in qPCR amplification such as temperature, AT rich regions, heterochromatin, and to ensure a comprehensive analysis, we considered both the Input% and Fold change values to

identify and validate the most suitable gRNA for targeting each region of the ATP7B promoter(Kurtenbach et al., 2019).

In the case of region 3, both gRNAs showed issues during the ChIP-qPCR experiments. As a result, new gRNAs were designed and successfully applied to target the ATP7B promoter, with g3.4 demonstrating a three-fold enrichment compared to the control samples (Figure 3.7C).

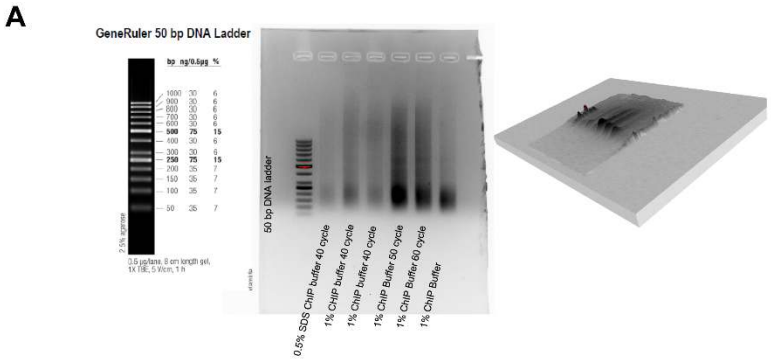
A
GeneRuler 50 bp DNA Ladder
50 bp DNA ladder
0.5% SDS ChIP buffer 40 cycle
1% ChIP buffer 40 cycle
1% ChIP buffer 40 cycle
1% ChIP Buffer 50 cycle
1% ChIP Buffer 60 cycle
1% ChIP Buffer

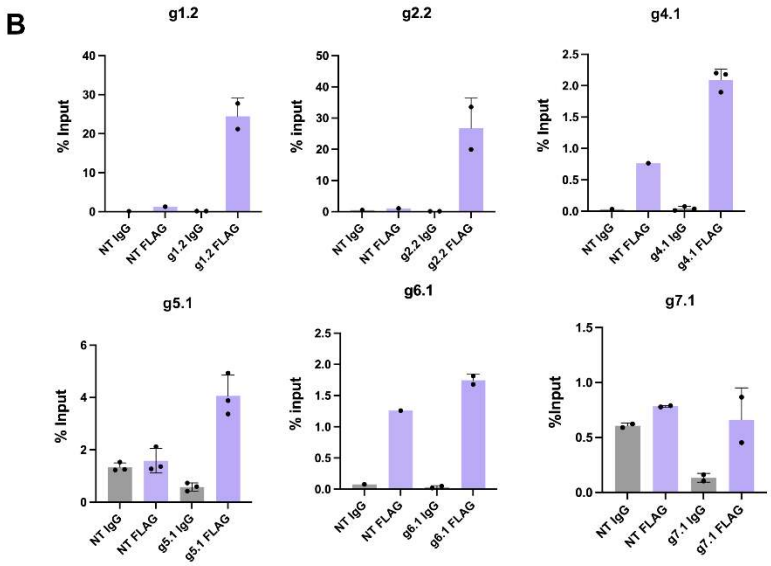
B
g1.2
g2.2
g4.1
g5.1
g6.1
g7.1
% Input
% input
%Input
NT IgG
NT FLAG
g1.2 IgG
g1.2 FLAG
g2.2 IgG
g2.2 FLAG
g4.1 IgG
g4.1 FLAG
g5.1 IgG
g5.1 FLAG
g6.1 IgG
g6.1 FLAG
g7.1 IgG
g7.1 FLAG

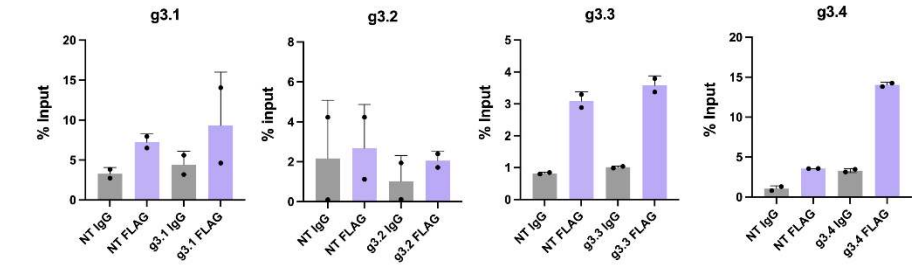
C
g3.1
g3.2
g3.3
g3.4
% Input
% input
NT IgG
NT FLAG
g3.1 IgG
g3.1 FLAG
g3.2 IgG
g3.2 FLAG
g3.3 IgG
g3.3 FLAG
g3.4 IgG
g3.4 FLAG

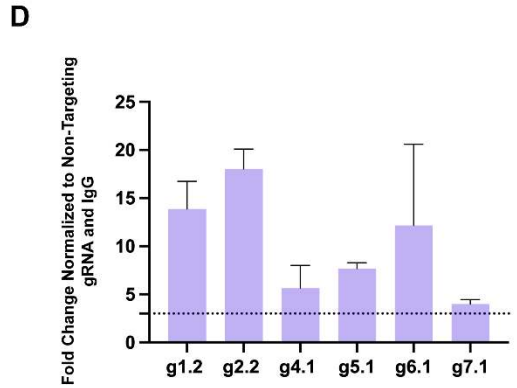
D
Fold Change Normalized to Non-Targeting gRNA and IgG
g1.2
g2.2
g4.1
g5.1
g6.1
g7.1

Figure 3.7 Targeting Efficiency of gRNAs to ATP7B Promoter via ChIP-qPCR.

A) Sonication Optimization of ChIP: Different sonication conditions were tested to determine the optimal settings that result in appropriately 150-200 bp sized chromatin fragments for subsequent ChIP experiments.

B) ChIP-qPCR of gRNAs Targeting ATP7B Promoter on HEK-CASPEX Cells with Input% Demonstration: CASPEX pulldown performed with anti-FLAG antibody and Mouse IgG used as a control

C) Region-3 gRNAs: Trouble shooting with the design and ChIP-qPCR of 4 different gRNAs on region-3.

D) Fold Calculation and Demonstration of Each Region: The fold enrichment of each gRNA is calculated based on the ChIP-qPCR results.

Figure generated with Ayca Acar, MSc Student.

Following the successful confirmation of all gRNAs for targeting the ATP7B promoter, the HEK-CASPEX cell line, along with the eight different cell lines each containing a specific gRNA, were prepared for biotinylation and subsequent mass spectrometry analysis (Figure 3.7D). This approach aims to delve deeper into the transcriptional regulation of ATP7B by identifying and characterizing the proteins associated with the targeted regions.

3.3 Identification of Transcriptional Regulators of ATP7B via Mass Spectrometry

3.3.1 Biotinylation of Transcriptional Regulators of ATP7B

HEK-CASPEX cells harboring confirmed gRNAs (validated through T7EI and ChIP assays) were induced with doxycycline for 48 hours to initiate APEX2 biotinylation. To confirm the biotinylation signal and reduce background noise during subsequent mass spectrometry analysis, cell lysates were divided into cytoplasmic and nuclear fractions for biotinylation background confirmation. Given the abundance and localization of transcription factors within the cell, nuclear protein extraction was prioritized. To minimize protein misidentification during LC-MS/MS analysis, streptavidin-coated magnetic beads were utilized for efficient and selective enrichment of the biotinylated

proteins (Figure 3.8A). Next, biotinylation was performed on the first three regions of interest, and the extent of biotinylation was assessed by comparing it to the non-targeting gRNA using streptavidin-horseradish peroxidase (HRP) blotting (Figure 3.8B). To optimize the pull-down efficiency using streptavidin beads, we compared streptavidin-HRP agarose beads to streptavidin-magnetic beads. While agarose beads exhibit stronger binding to biotinylated proteins, magnetic beads offer greater precision and are more suitable for mass spectrometry-based identification (Figure 3.8C). Therefore, we continued the pull-down process using magnetic beads to prepare our biotinylated samples for subsequent mass spectrometry analysis.

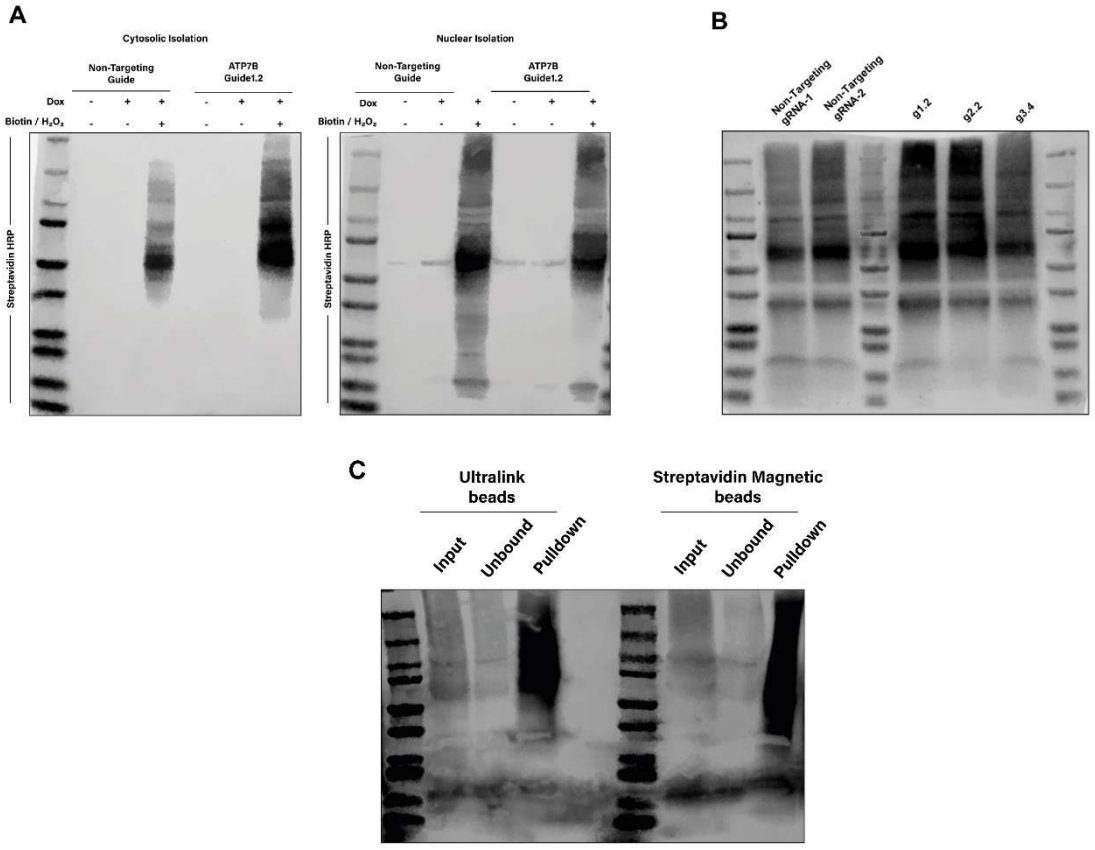

Figure 3.8 CASPEX Proximity Biotinylation and Enrichment of HEK-CASPEX Cell Lines.

A) Comparison of Cytosolic and Nuclear Proximity Biotinylation using Streptavidin-HRP Blot

B) Streptavidin-HRP Blot of Non-Targeting gRNA and ATP7B Promoter Regions:

C) Comparison of Agarose Beads and Magnetic Beads for Protein Enrichment:

These experiments provide essential information about the specificity and efficiency of CASPEX proximity biotinylation and protein enrichment, allowing us to identify proteins in close proximity to the targeted genomic regions of the ATP7B promoter. The results shed light on potential transcriptional regulators and other factors involved in ATP7B regulation and cisplatin resistance mechanisms.

Figure generated with Ayca Acar, MSc Student.

3.3.2 Mass Spectrometry Results of HEK-CASPEX ATP7B Promoter

Following the successful CASPEX biotinylation of the eight HEK-CASPEX cell lines containing targeting gRNAs and the non-targeting gRNA as a negative control, protein samples were meticulously prepared for pulldown experiments and subsequent Label-Free Quantification (LFQ).

The biotinylated protein samples from each cell line were subjected to pulldown assays to selectively isolate the biotinylated proteins of interest. This step aimed to enrich the transcription factors associated with the ATP7B promoter region. Subsequently, Label-Free Quantification (LFQ) analysis was performed on the HEK-CASPEX samples(Tyanova et al., 2016). According to the statistical analysis, raw intensity distributions were examined and compared among the seven samples containing the targeting gRNAs, along with the control sample (Figure 3.9) (Varnavides et al., 2022). Notably, the raw intensity distributions showed striking similarities between the peaks of the seven targeting gRNA samples when compared to the control sample.

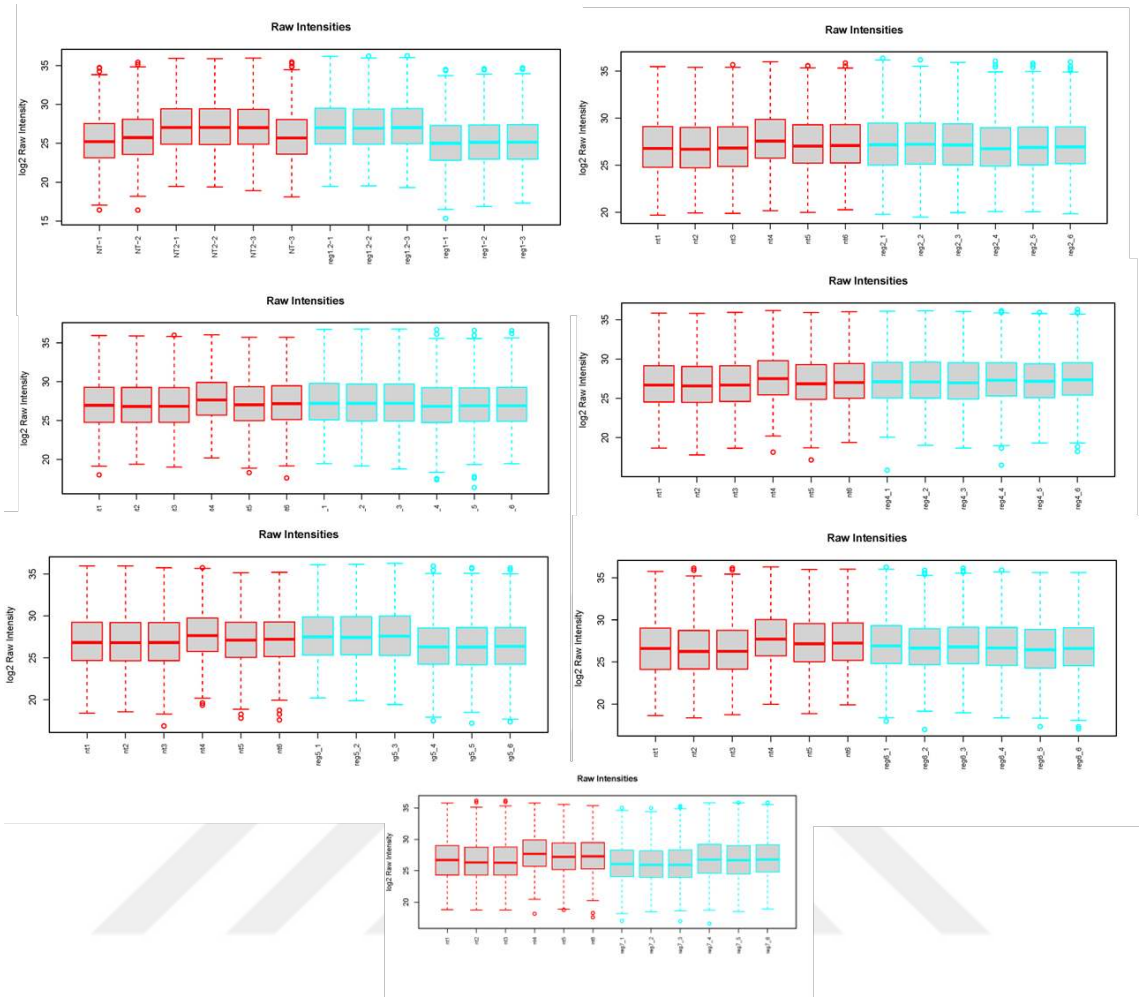

Figure 3.9 Raw Intensities and Distributions of 7 Regions Compared to Non-Targeting gRNA.

The distributions of intensities for each region are plotted to visualize the variability and spread of protein abundance in the proximity of the targeted genomic loci. By comparing these distributions to the non-targeting gRNA, we can assess the specificity and efficiency of CASPEX proximity biotinylation for each specific region of interest.

IBAQ (Intensity-Based Absolute Quantification) values revealed the identification of top proteins in region 1, with HISTH3A, PRSS1, and RPL8 emerging as representative proteins (Figure 3.10A). To refine our analysis and exclude potential contaminant proteins, further selection criteria were applied. Contaminant proteins such as PRSS1, ACTB, and histone variants were identified and targeted for exclusion from our analysis (Figure 3.10B). By implementing these additional selection analyses, we aimed to ensure

a more accurate and focused identification of the proteins specifically associated with the transcriptional regulation of the ATP7B promoter in region 1.

A)

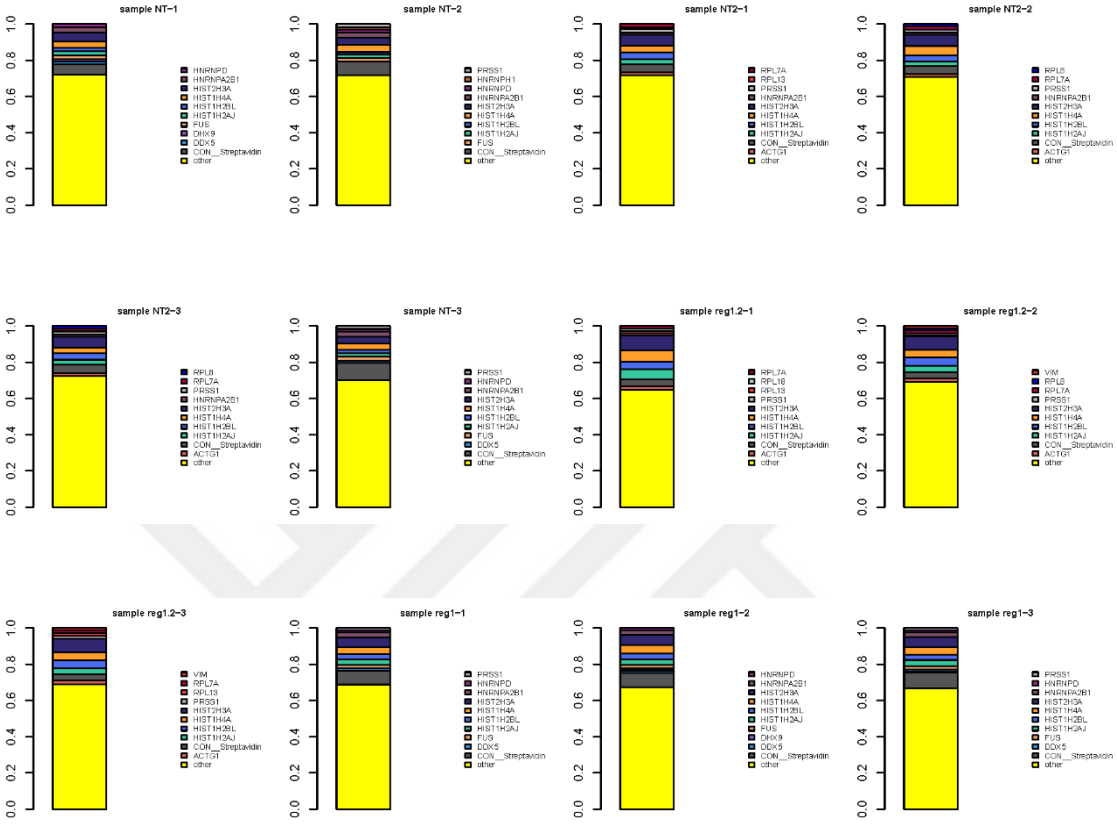

B)

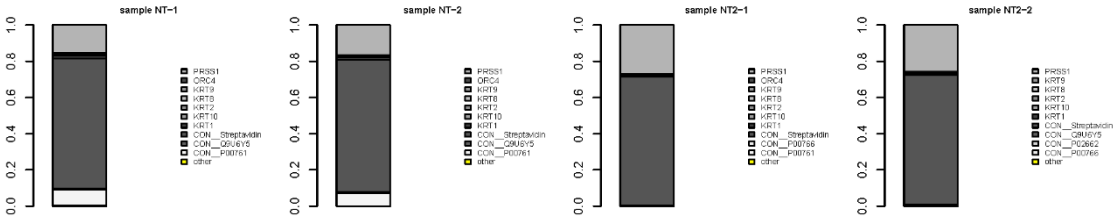

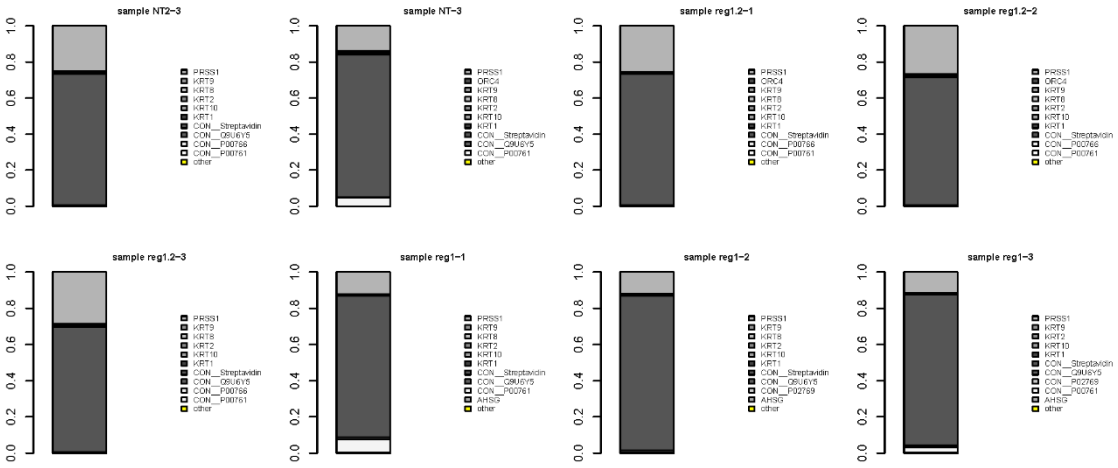

Figure 3.10 Region 1 - Top Identified Proteins and Contaminants Based on IBAQ Values from Mass Spectrometry Analysis.

A) Top identified proteins in region 1, as determined by their respective IBAQ values. The IBAQ values provide a quantitative measure of protein abundance, allowing us to rank the proteins based on their relative levels in the sample. These top identified proteins are potential candidates involved in ATP7B regulation and cisplatin resistance mechanisms in this specific region.

B) The top contaminant proteins identified in Region 1, based on their IBAQ values.

Figure generated with Dr. Selahattin Can Ozcan.

3.3.3 Identification of the Transcription Factors Regulating ATP7B

To focus specifically on transcription factors and streamline our data analysis by excluding other proteins, we conducted a comparative analysis of our results with transcription factor databases. Specifically, we compared our data with the Human Transcription Factor Database and MORF (Mulplexed Ox of the Regulatory Factors) library which contains 1500 to 1800 transcriptional regulators (Joung et al., 2023; S. A. Lambert et al., 2018). By performing these comparisons, we aimed to identify and highlight the presence of transcription factors, as well as chromatin and epigenetic regulators, within each region of interest. This approach allowed us to narrow down our focus to the key regulatory factors that potentially play a role in the transcriptional regulation of the ATP7B gene.

The utilization of these transcription factor databases provided valuable insights and served as a valuable resource in our analysis. By aligning our data with established knowledge on transcription factors and regulatory elements, we gained a deeper understanding of the potential transcriptional regulatory network associated with the ATP7B gene (http://humantfs.ccbr.utoronto.ca/). To refine our selection of transcriptional regulators, we implemented cutoffs based on statistical analysis. Several factors were considered, including LogFC (logarithmic fold change), p-values, the presence of transcription factor information in the databases, and the availability of the MORF library (Figure 3.11A).

Based on these criteria, we aimed to identify the most significant transcriptional regulators associated with the ATP7B gene. The statistical analysis allowed us to prioritize regulators that exhibited significant changes in expression levels (LogFC) and provided a measure of confidence in the observed differences (p-values) (Figure 3.11).

This comprehensive comparison and analysis of our data with transcription factor databases contributed to the identification and characterization of the key regulatory factors involved in ATP7B gene expression, further enhancing our understanding of its transcriptional regulation mechanisms.

In our research, we successfully detected several predicted and hypothesized transcription factors, including TP53, ATF3, HOXD13, LEF1, MAZ, PAX6, and YY1, during the in stage of our CASPEX project (Figure 3.11).

Subsequently, we utilized seven volcano plots to identify potential transcriptional regulators associated with the ATP7B promoter. We would like to assess the presence and overlap of these regulators across the various regions of interest. In this analysis, we discovered that GATA6, HOXB6, NR2F1, NFIC, NME2, TOX4, POU3F2 were top identified transcriptional regulators in multiple regions, indicating their presence in overlapping regions of the ATP7B promoter. This finding suggests a potential role for these transcriptional regulators in the regulation of ATP7B expression (Figure 3.12).

Given the considerable number of transcriptional regulators identified in this analysis (over 150), it becomes crucial to validate their credibility as regulators of ATP7B through further in-vitro confirmations. Consequently, we will employ additional assays and experiments to assess the functional relevance and significance of these regulators in the transcriptional regulation of ATP7B.

By systematically reducing the number of identified transcriptional regulators and subjecting them to rigorous validation processes, we aim to establish a more refined and credible set of regulators that are directly involved in the control of ATP7B expression. Notably, according to the TRANSFAC database, we identified over 150 transcription factors that have the potential to bind to the ATP7B gene, ranging from the +1 transcription start site to -3000 base pairs. Through in silico analysis, we further determined the specific base pairs to which these factors bind on the DNA. These comprehensive results highlight the powerful and precise nature of our CASPEX system. The successful detection of these transcription factors serves as a significant milestone in our CASPEX project, indicating our system's ability to effectively identify and characterize transcription factors.

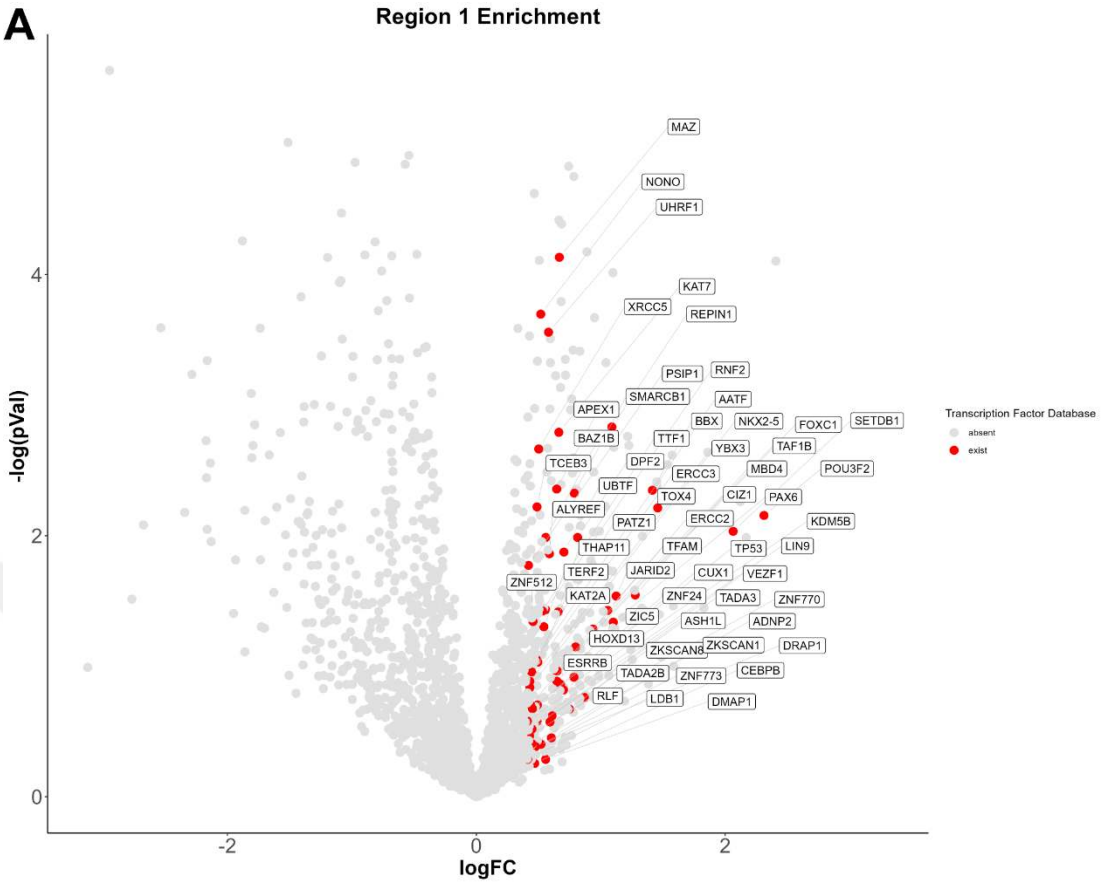
A
Region 1 Enrichment
-log(pVal)
logFC
Transcription Factor Database
absent
exist
MAZ
NONO
UHRF1
KAT7
XRCC5
REPIN1
PSIP1
RNF2
SMARCB1
AATF
APEX1
BBX
NKX2-5
FOXC1
SETDB1
BAZ1B
TTF1
YBX3
TAF1B
TCEB3
DPF2
ERCC3
MBD4
POU3F2
UBTF
TOX4
CIZ1
PAX6
ALYREF
PATZ1
ERCC2
KDM5B
THAP11
TFAM
TP53
LIN9
ZNF512
TERF2
JARID2
CUX1
VEZF1
KAT2A
ZNF24
TADA3
ZNF770
ZIC5
ASH1L
ADNP2
HOXD13
ZKSCAN8
ZKSCAN1
DRAP1
ESRRB
TADA2B
ZNF773
CEBPB
RLF
LDB1
DMAP1

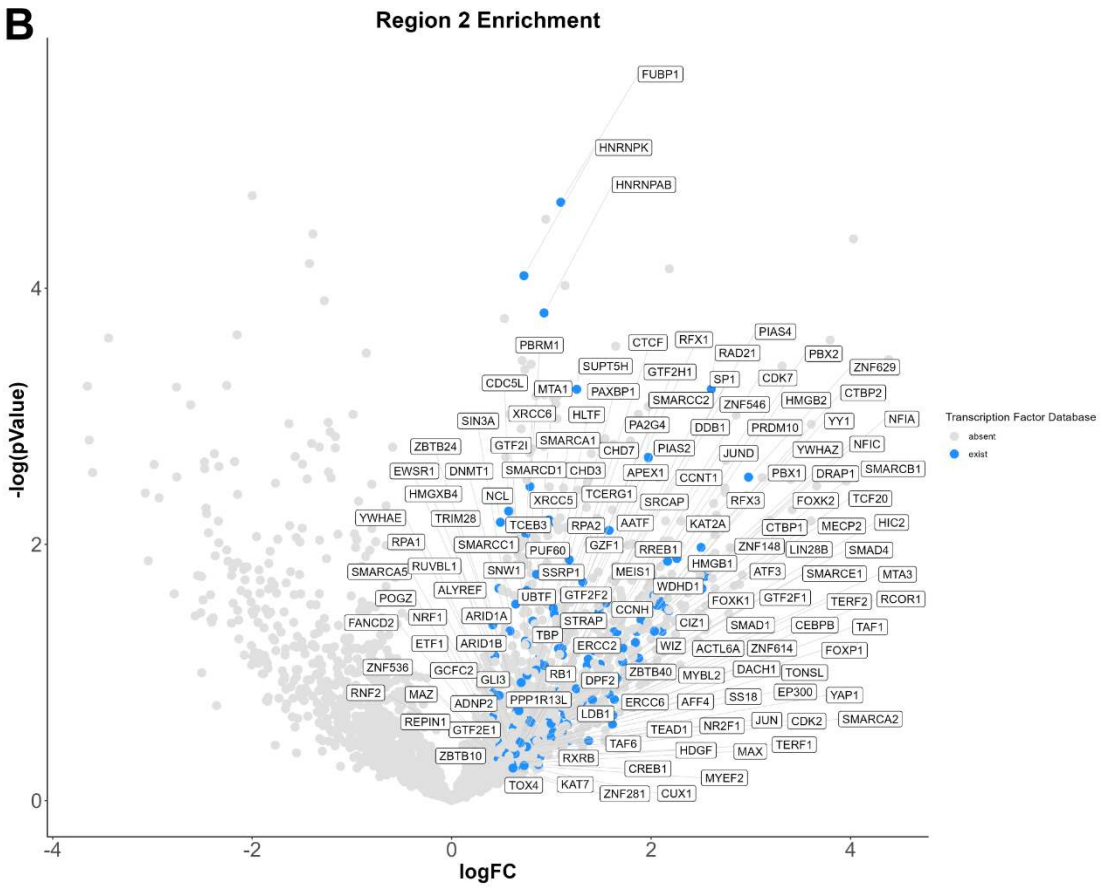
B
Region 2 Enrichment
-log(pValue)
logFC
Transcription Factor Database
absent
exist
FUBP1
HNRNPK
HNRNPAB
PBRM1
CTCF
RFX1
PIAS4
RAD21
PBX2
SUPT5H
GTF2H1
ZNF629
CDC5L
MTA1
PAXBP1
SP1
CDK7
SMARCC2
ZNF546
HMGB2
CTBP2
SIN3A
XRCC6
HLTF
PA2G4
DDB1
PRDM10
YY1
NFIA
ZBTB24
GTF2I
SMARCA1
CHD7
PIAS2
JUND
YWHAZ
NFIC
EWSR1
DNMT1
SMARCD1
CHD3
APEX1
CCNT1
PBX1
DRAP1
SMARCB1
HMGXB4
NCL
XRCC5
TCERG1
SRCAP
RFX3
FOXK2
TCF20
YWHAE
TRIM28
TCEB3
RPA2
AATF
KAT2A
CTBP1
MECP2
HIC2
RPA1
SMARCC1
PUF60
GZF1
RREB1
ZNF148
LIN28B
SMAD4
SMARCA5
RUVBL1
SNW1
SSRP1
MEIS1
HMGB1
ATF3
SMARCE1
MTA3
POGZ
ALYREF
UBTF
GTF2F2
WDHD1
FOXK1
GTF2F1
TERF2
RCOR1
FANCD2
NRF1
ARID1A
STRAP
CCNH
CIZ1
SMAD1
CEBPB
TAF1
ETF1
ARID1B
TBP
ERCC2
WIZ
ACTL6A
ZNF614
FOXP1
ZNF536
GCFC2
GLI3
RB1
DPF2
ZBTB40
MYBL2
DACH1
TONSL
RNF2
MAZ
ADNP2
PPP1R13L
ERCC6
AFF4
SS18
EP300
YAP1
REPIN1
GTF2E1
LDB1
TEAD1
NR2F1
JUN
CDK2
SMARCA2
ZBTB10
TAF6
HDGF
MAX
TERF1
RXRB
CREB1
MYEF2
TOX4
KAT7
ZNF281
CUX1

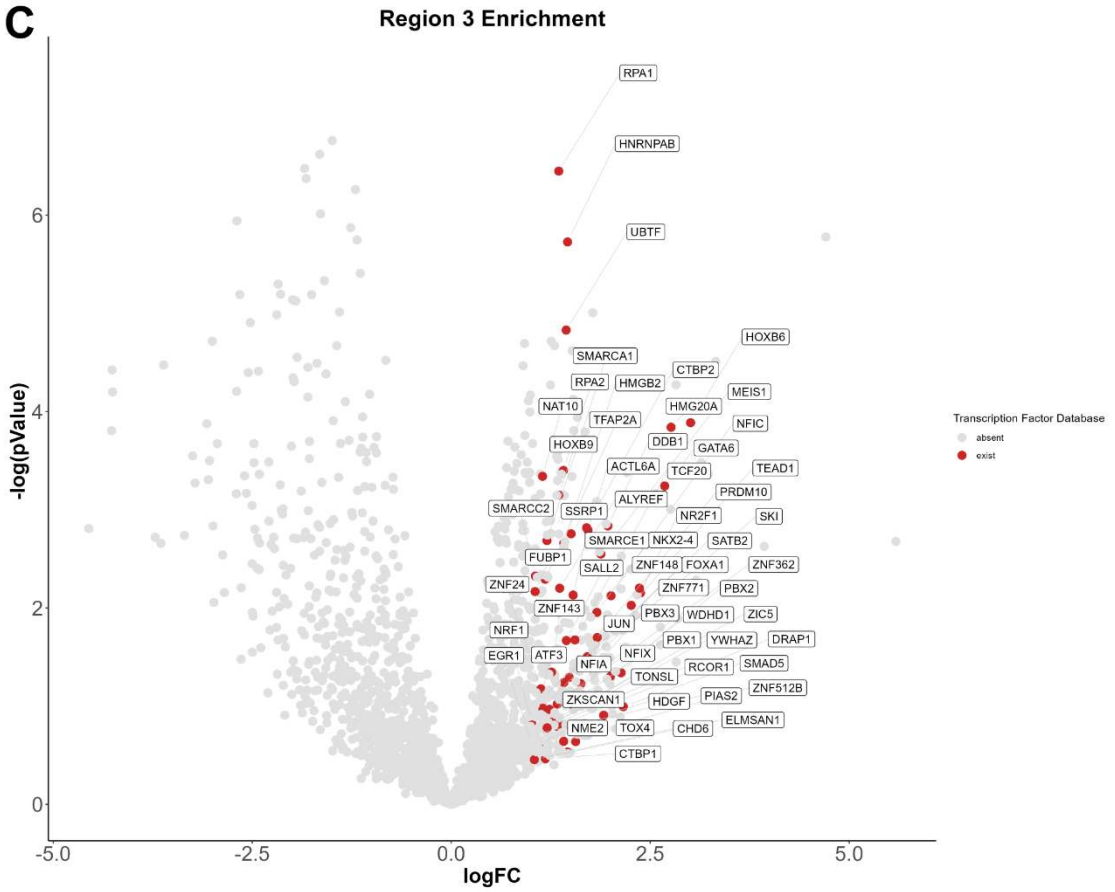
C
Region 3 Enrichment
-log(pValue)
logFC
RPA1
HNRNPAB
UBTF
HOXB6
SMARCA1
CTBP2
RPA2
HMGB2
MEIS1
NAT10
HMG20A
TFAP2A
NFIC
HOXB9
DDB1
GATA6
ACTL6A
TCF20
TEAD1
ALYREF
PRDM10
SMARCC2
SSRP1
NR2F1
SKI
SMARCE1
NKX2-4
SATB2
FUBP1
SALL2
ZNF148
FOXA1
ZNF362
ZNF24
ZNF771
PBX2
ZNF143
PBX3
WDHD1
ZIC5
JUN
NRF1
PBX1
YWHAZ
DRAP1
EGR1
ATF3
NFIX
NFIA
RCOR1
SMAD5
TONSL
ZNF512B
ZKSCAN1
HDGF
PIAS2
NME2
TOX4
CHD6
ELMSAN1
CTBP1
Transcription Factor Database
absent
exist

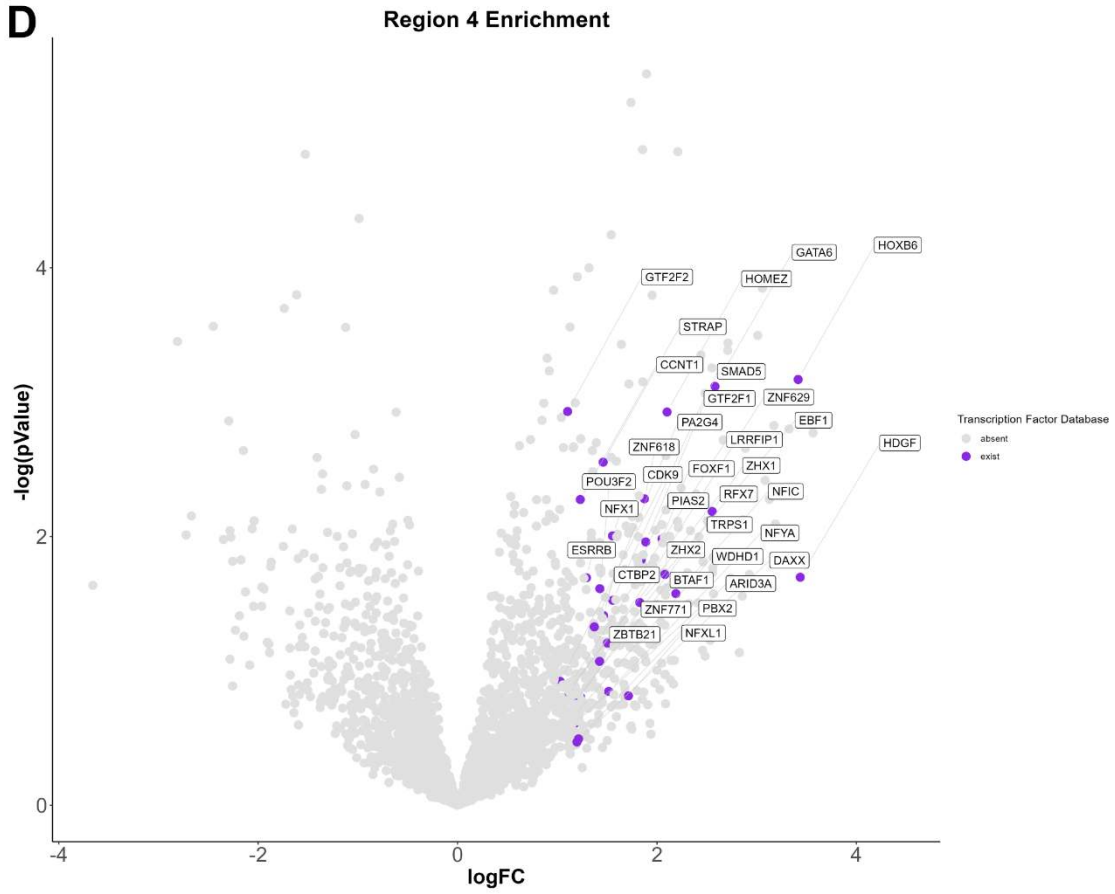
D
Region 4 Enrichment
-log(pValue)
logFC
GATA6
HOXB6
GTF2F2
HOMEZ
STRAP
CCNT1
SMAD5
GTF2F1
ZNF629
PA2G4
EBF1
HDGF
ZNF618
LRRFIP1
FOXF1
ZHX1
CDK9
POU3F2
RFX7
NFIC
NFX1
PIAS2
TRPS1
NFYA
ESRRB
ZHX2
WDHD1
DAXX
CTBP2
BTAF1
ARID3A
ZNF771
PBX2
ZBTB21
NFXL1
Transcription Factor Database
absent
exist

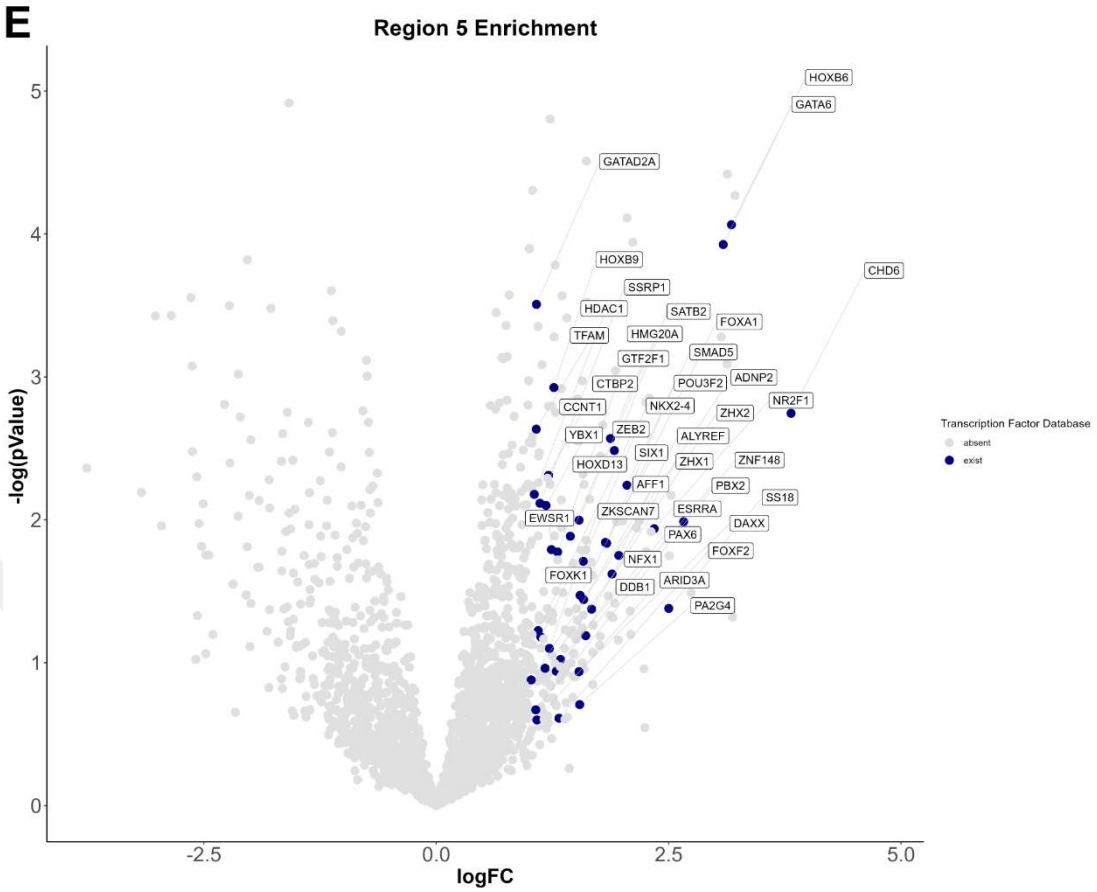
E
Region 5 Enrichment
-log(pValue)
logFC
HOXB6
GATA6
GATAD2A
HOXB9
CHD6
SSRP1
HDAC1
SATB2
FOXA1
TFAM
HMG20A
SMAD5
GTF2F1
CTBP2
POU3F2
ADNP2
NR2F1
CCNT1
NKX2-4
ZHX2
YBX1
ZEB2
ALYREF
SIX1
HOXD13
ZHX1
ZNF148
AFF1
PBX2
SS18
ZKSCAN7
ESRRA
EWSR1
DAXX
PAX6
FOXF2
NFX1
FOXK1
ARID3A
DDB1
PA2G4
Transcription Factor Database
absent
exist

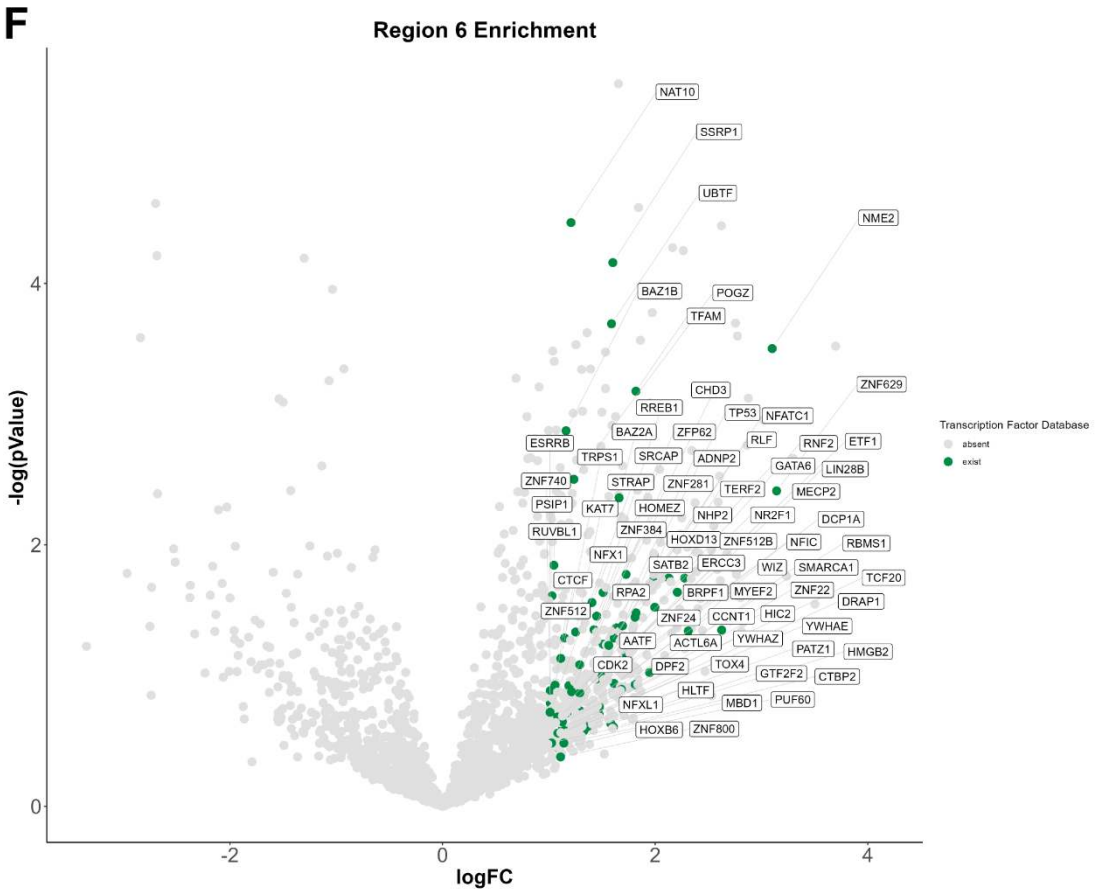
F
Region 6 Enrichment
-log(pValue)
logFC
NAT10
SSRP1
UBTF
NME2
BAZ1B
POGZ
TFAM
ZNF629
CHD3
RREB1
TP53
NFATC1
BAZ2A
ZFP62
ESRRB
RLF
RNF2
ETF1
TRPS1
SRCAP
ADNP2
GATA6
LIN28B
ZNF740
STRAP
ZNF281
TERF2
MECP2
PSIP1
KAT7
HOMEZ
NHP2
NR2F1
DCP1A
RUVBL1
ZNF384
HOXD13
ZNF512B
NFIC
RBMS1
NFX1
SATB2
ERCC3
WIZ
SMARCA1
TCF20
CTCF
RPA2
BRPF1
MYEF2
ZNF22
DRAP1
ZNF512
ZNF24
CCNT1
HIC2
YWHAE
AATF
ACTL6A
YWHAZ
PATZ1
HMGB2
CDK2
DPF2
TOX4
GTF2F2
CTBP2
HLTF
NFXL1
MBD1
PUF60
HOXB6
ZNF800
Transcription Factor Database
absent
exist

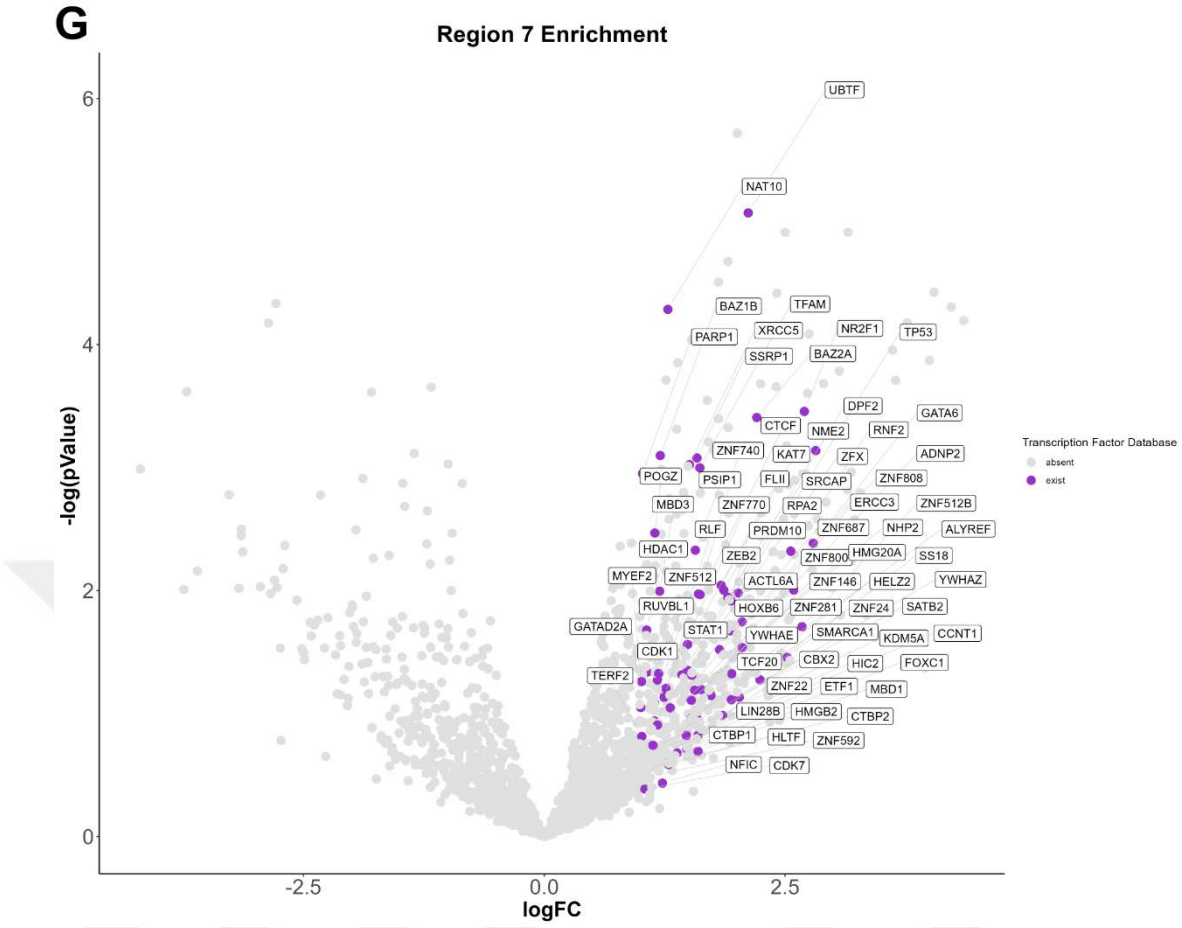

Figure 3.11 Enrichment of Transcriptional Regulators of ATP7B From CASPEX Proteome Compared to Non-Targeting gRNA. Highlighted protein are transcription factors and all of them passed to the LogFC > 1 (LogFC > 0.5 for region-2 to demonstrate abundance of identified transcriptional regulators)

A) Enrichment of transcriptional regulators in Region 1 compared to the non-targeting gRNA. B) Region-2 C) Region-3 D) Region-4 E) Region-5 F) Region-6 G) Region-7

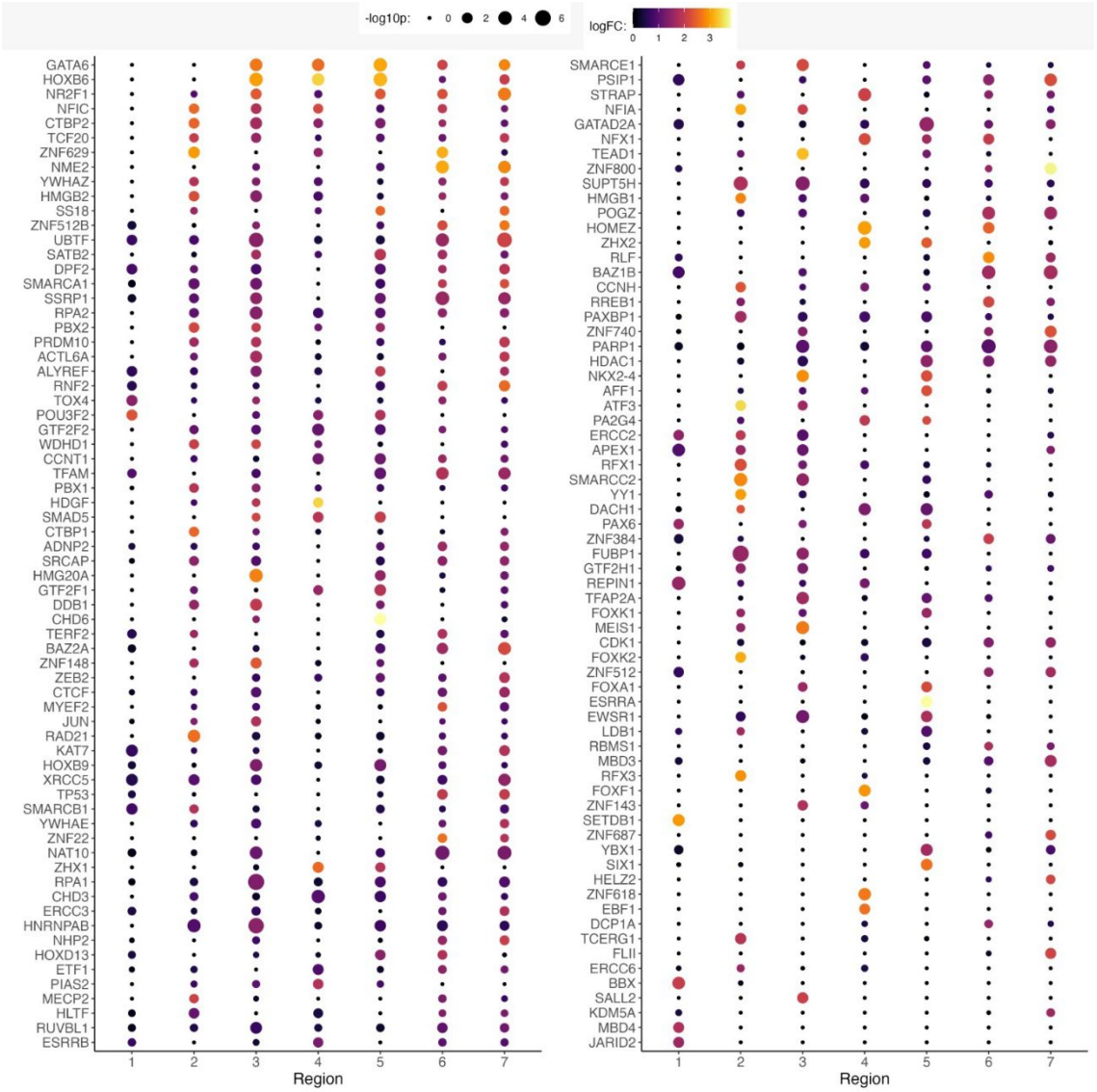

Figure 3.12 Promoter Mapping of CASPEX Proteome Enrichment and Localization of Transcriptional Regulators on ATP7B Promoter in 7 Regions.

To investigate the regulatory landscape of ATP7B, CASPEX proteome enrichment was performed across seven distinct regions of the ATP7B promoter. The relative abundance of transcriptional regulators in each region was assessed, and LogFC > 1 and p-Value < 0.05 were used as cut-off thresholds to identify significant enrichments.

Figure generated with Dr. Selahattin Can Ozcan.

3.4 Selection of Transcription Factor Candidates from CASPEX Mass Spectrometry

To uncover the transcriptional regulators of ATP7B, it was crucial to carefully select the appropriate transcription factors for further investigation. Several criteria were employed to guide this selection process, including the detection of a transcription factor in multiple regions, the identification of distinct peptides in mass spectrometry analysis, and consideration of the correlation between the transcription factor and ATP7B expression in different cancers (Figure *3.13*) (T. Li et al., 2020). Based on specific criterias, including their presence in multiple regions, detection of distinct peptides in mass spectrometry analysis, and correlation with ATP7B expression, and ChIP-seq correlations on ATP7B promoter, four transcription factors were chosen: ATF3, LEF1, TOX4, and TP53. These transcription factors demonstrated strong potential based on the established criteria, previous literature and will be subjected to comprehensive experimental validation to elucidate their role as transcriptional regulators of ATP7B.

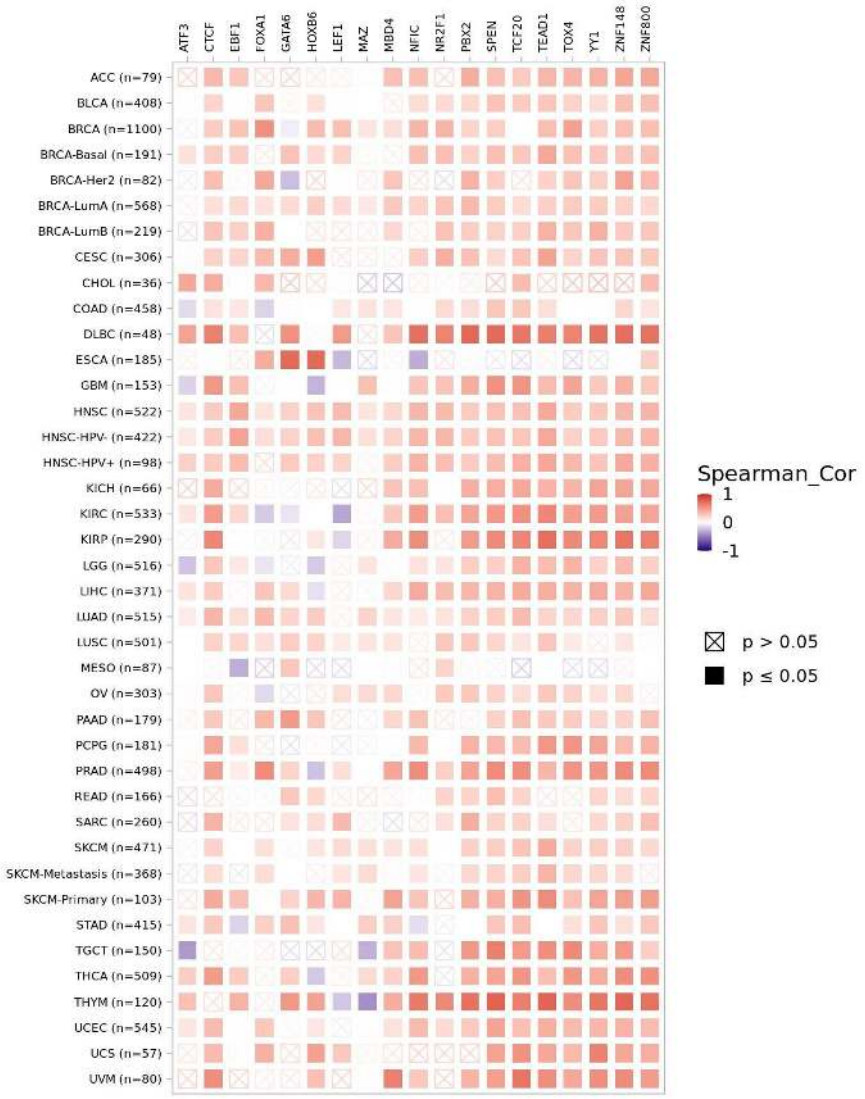

Figure 3.13 Correlation of ATP7B with 20 Transcription Factors in Different Cancers

To investigate the potential regulatory network of ATP7B in various cancer types, we analyzed the correlation between ATP7B expression and 20 selected transcription factors using data from the TIMER 2.0 database. The correlation analysis was performed using Spearman's correlation coefficient, and p-values were considered for significance.

3.4.1 ATF3

Activating Transcription Factor-3 (ATF3) is a member of the cAMP binding protein family and plays a significant role in regulating various metabolic pathways, particularly glucose metabolism. It is characterized by its ability to interact with other proteins through a bZip domain. In the cancer perspective, ATF3 is a crucial regulator in chemotherapy, particularly in the context of cisplatin therapy (Ku & Cheng, 2020).

In lung cancer cell lines, ATF3 expression is predominantly upregulated following cisplatin treatment. This upregulation suggests a potential involvement of ATF3 in the cellular response to cisplatin-induced stress. ATF3 also linked closely with the P53 as a stabilizor of the protein (Yan & Boyd, 2006). Conversely, in liver cancers, ATF3 levels are observed to be decreased when compared to normal liver tissue. This dysregulation of ATF3 expression in liver cancers may contribute to the pathogenesis of hepatocellular carcinoma (HCC) (St. Germain et al., 2010).

Interestingly, increased levels of ATF3 have been found to induce cell death in HCC through apoptosis. This suggests that ATF3 may serve as a potential therapeutic target for promoting apoptosis in HCC cells. Further investigations into the mechanisms underlying ATF3-mediated apoptosis could provide valuable insights into the development of novel therapeutic strategies for HCC (J. Shen et al., 2016).

ATF3 exhibits distinct expression patterns and functional implications in different cancer types, highlighting its complex and context-dependent roles in tumorigenesis and chemotherapy response. In our CASPEX Mass Spectrometry analysis, ATF3 demonstrated significant enrichment in region 2-3 and exhibited more than a 2-fold change compared to the non-targeting gRNA (Figure 3.11B-C, Figure 3.12). Interestingly, ATF3 showed a lower correlation with ATP7B across different cancers (Figure 3.13). However, considering its role as a stress factor, we hypothesized that the correlation of ATF3 with ATP7B may be influenced by the treatment of cisplatin on cells.

The low level of correlation between ATF3 and ATP7B in various cancers suggests that their regulatory interactions may be context-dependent and influenced by specific cellular conditions (Huo et al., 2023). As ATF3 is known to be involved in stress responses, it is possible that its correlation with ATP7B could be modulated by the presence of cisplatin, a chemotherapy drug. The induction of ATF3 in response to cisplatin-induced stress might affect its relationship with ATP7B, highlighting the

intricate interplay between transcription factors and their target genes in response to therapeutic interventions.

To investigate the role of ATF3 in the regulation of ATP7B expression, we generated an ATF3 Ko cell line in HEK293T cells, where we previously identified ATF3 on the ATP7B promoter through CASPEX proteome analysis (Figure 3.14). Subsequently, we observed a significant decrease in ATP7B expression in the ATF3 Ko cell line compared to the non-targeting gRNA control, with a 70% reduction in the ATF3 mRNA expression. To further elucidate the regulatory role of ATF3 on ATP7B, we also established a stable ATF3 Ox cell line, which led to a 1.63-fold increase in ATP7B expression (Figure 3.14B).

To validate the influence of ATF3 on ATP7B expression in a different cellular context, we employed a hepatocellular carcinoma cell line, HUH7. As in our findings in HEK293T cells, we observed a significant reduction in ATP7B expression in the ATF3 Ko HUH7 cells, with a 55% of difference compared to the control (Figure 3.14C). Conversely, the stable Ox of ATF3 in HUH7 cells resulted in a 2.12-fold increase in ATP7B expression (Figure 3.14D). It is worth noting that the observed differences in ATP7B expression between the two cell lines may be attributed to inherent variations in the basal regulatory mechanisms of ATP7B expression, as ATP7B is known to be highly expressed in HEK293T cells compared to HUH7 cells.

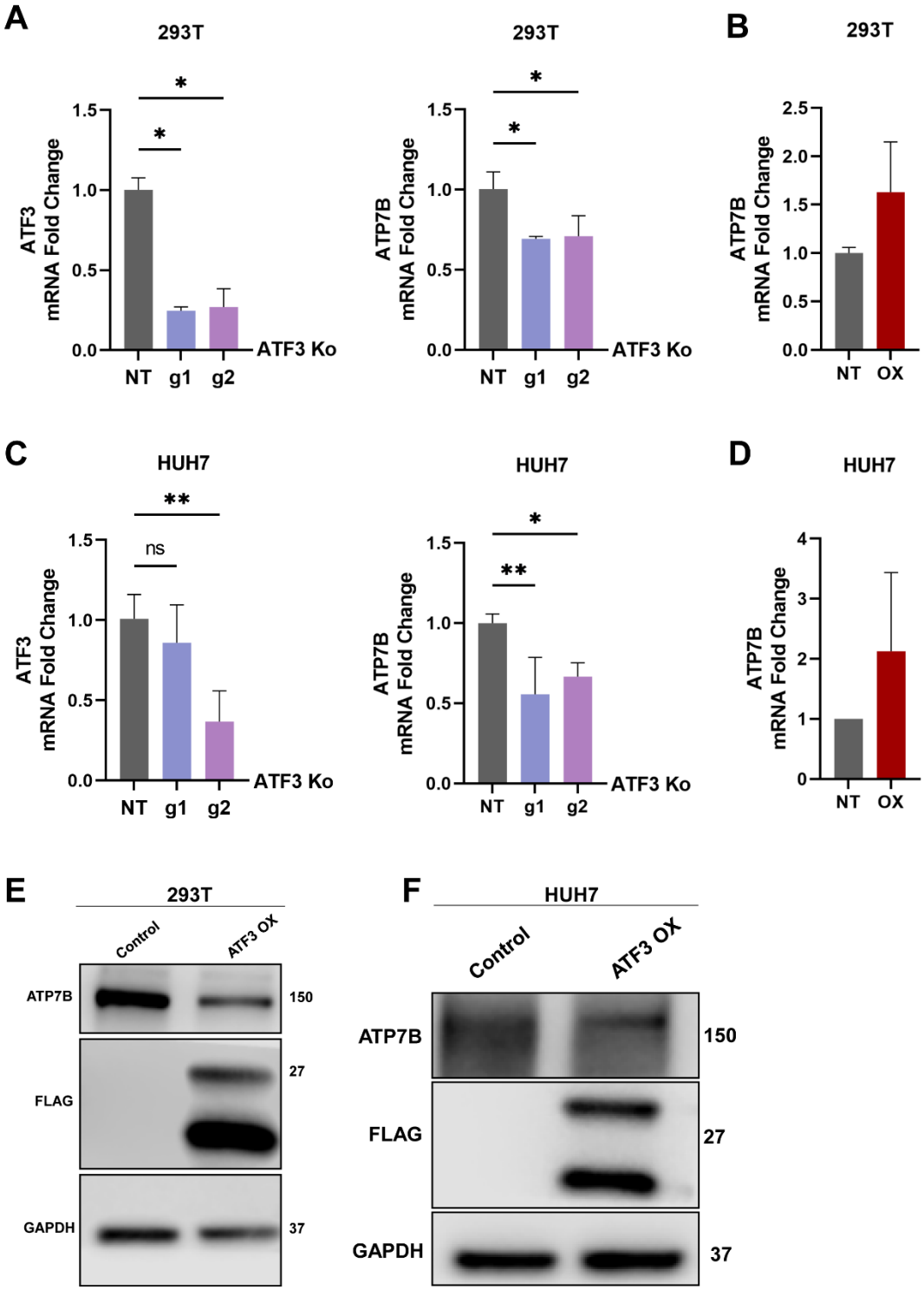

Figure 3.14 Effects of ATF3 Expression on ATP7B Expression in HEK293T and Huh7 Cell Lines.

A) Ko of ATF3 and its effect on ATP7B expression on HEK293T cells. B) HEK-ATF3 Ox. C) Huh7-ATF3 Kos. D) Huh7-ATF3 Ox. E) Western blot of ATF3 Ox effects on ATP7B on HEK293T. F) Huh7-ATF3 Ox. Western blot.

In a surprising contrast to the observed increase in ATF3 mRNA levels and its role as a transcriptional regulator, Ox of ATF3 at the protein level resulted in a slight reduction in ATP7B protein levels in HEK293T cells (Figure 3.14E). The discrepancy between the molecular weight of ATF3 (27 kDa) and ATP7B (150 kDa) suggests that the reduction in ATP7B protein levels may not be directly mediated by ATF3. Other regulatory mechanisms or interactions between ATF3 and ATP7B may be responsible for this observation. In contrast, the protein level of ATP7B remained stable upon ATF3 Ox in HUH7 cells (Figure 3.14F). This consistency in ATP7B protein levels suggests a cell line-specific response, indicating that the interplay between ATF3 and ATP7B may be influenced by the cellular context of HUH7 cells.

3.4.2 Promoter Strength of ATP7B

To investigate the promoter strength of ATP7B, we constructed luciferase reporter plasmids containing various lengths of the ATP7B promoter region, ranging from +1 TSS to -200, -500, -1000, -2000, and -3000 bp (Figure 3.15A). These constructs were transiently transfected into cells to assess their ability to drive luciferase expression, serving as a proxy for promoter strength.

Our results revealed that the ATP7B promoter exhibited the highest activity within the region spanning -1000 to -2000 bp. These regulatory regions play a crucial role in modulating the activity of the ATP7B promoter, potentially by interacting with cis-regulatory elements in proximity to the +1 TSS (Figure 3.15B).

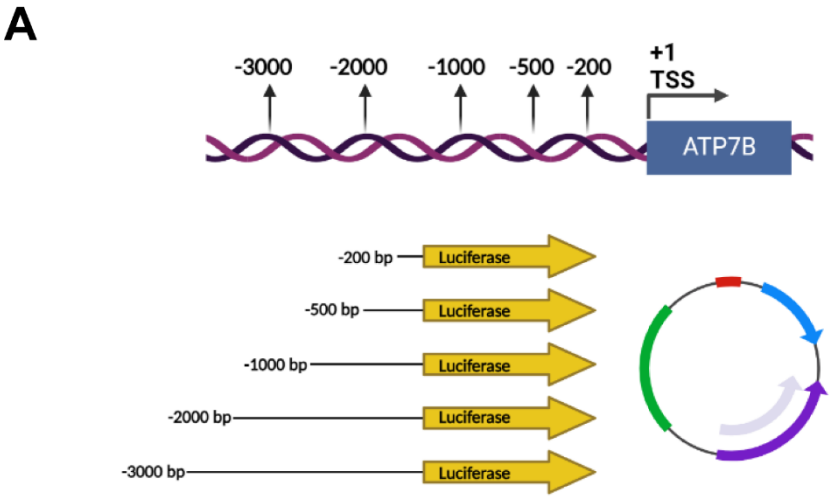
A
-3000
-2000
-1000
-500
-200
+1
TSS
ATP7B
-200 bp
-500 bp
-1000 bp
-2000 bp
-3000 bp
Luciferase
Luciferase
Luciferase
Luciferase
Luciferase

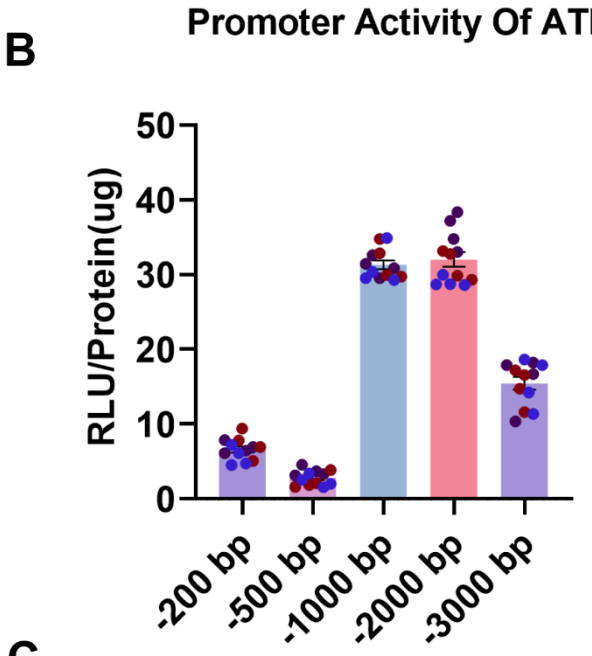
B
Promoter Activity Of ATP7B
RLU/Protein(ug)
50
40
30
20
10
0
-200 bp
-500 bp
-1000 bp
-2000 bp
-3000 bp

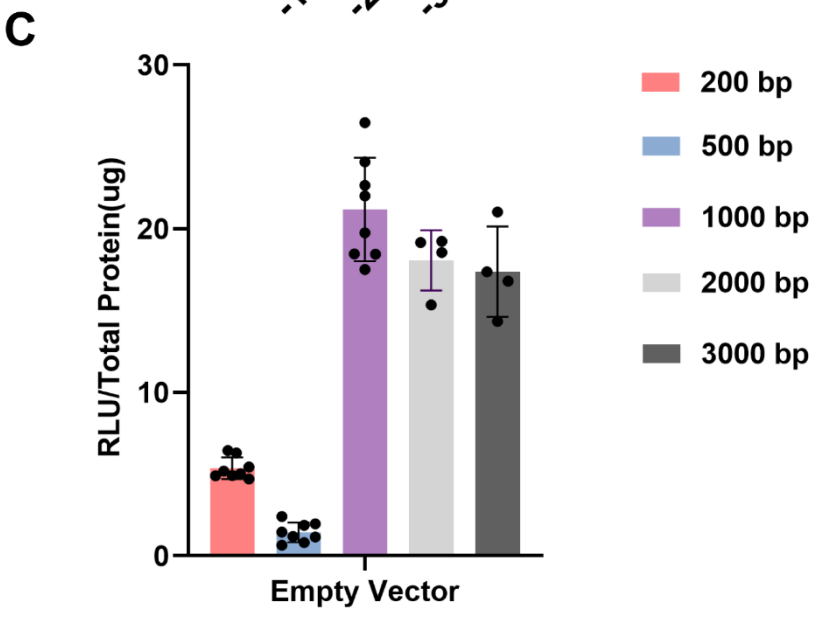
C
RLU/Total Protein(ug)
30
20
10
0
Empty Vector
200 bp
500 bp
1000 bp
2000 bp
3000 bp

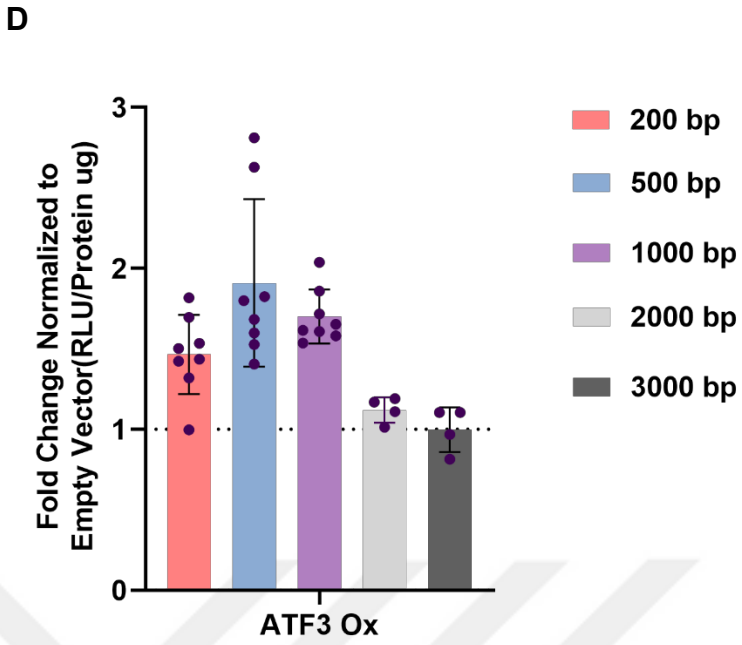

Figure 3.15 Promoter Strength of ATP7B and the Effects on Control and ATF3 Ox.

A) The ATP7B promoter was isolated and cloned onto a luciferase backbone, allowing for the evaluation of its transcriptional activity. B) Promoter assay of ATP7B was performed using various lengths of the luciferase constructs (200, 500, 1000, 2000, and 3000 bp). C) A promoter assay was carried out in stable HEK-3x FLAG Empty Vector Cell line to provide a baseline measurement of ATP7B promoter activity. D) Promoter assay on HEK-ATF3 Ox cells was conducted to examine the impact of ATF3 Ox on the ATP7B promoter activity and normalized to the Empty Vector values as previously described.

These regulatory regions may contain essential transcription factors and other regulatory elements as GC/AT box elements and RNA Poll II binding sites etc. that contribute to the precise control of ATP7B expression.

Considering the observed increase in ATP7B expression upon ATF3 Ox in qPCR experiments, we aimed to identify specific cis-regulatory regions within the ATP7B promoter that are targeted by ATF3. To this end, we generated a control construct containing the backbone of the ATF3 Ox vector without any specific regulatory elements (3xFLAG Empty construct). Additionally, we established a stable cell line serving as the control for comparative analyses.

Upon transfection of these constructs into both the HEK-Control and HEK-ATF3 Ox cell lines, we observed that ATF3 Ox led to an increase in luciferase expression specifically from the -200, -500, and -1000 bp regions of the ATP7B promoter (Figure 3.15C). This suggests that ATF3 may interact with these cis-regulatory regions, thereby enhancing the transcriptional activity of the ATP7B promoter.

To directly investigate the binding sites of ATF3 on the ATP7B promoter and confirm its regulatory role, we performed ChIP assay. We utilized HEK293T and HUH7 cell lines overexpressing ATF3 (ATF3 Ox) for these experiments, along with an IgG control for comparison (Figure 3.16). Using specific ChIP-qPCR primers designed to target seven regions identified through CASPEX analysis, we assessed the binding of ATF3 to the ATP7B promoter. Among these regions, we focused on regions 1, 2, and 6 to provide evidence of ATF3 binding and its impact on ATP7B expression regulation (Figure 3.16A). The enrichment scores (%Input) for these regions were relatively high, indicating a strong binding of ATF3 to the ATP7B promoter in this cell line. However, in HUH7 cell line, we observed relatively lower enrichment scores for ATF3 binding, suggesting that the regulatory mechanism of ATF3 on ATP7B expression may vary in different cell lines. This difference in enrichment scores suggests that ATF3 may still have a regulatory effect on ATP7B expression in HUH7 cells, but the extent of binding and enrichment may differ compared to HEK293T cells (Figure 3.16B).

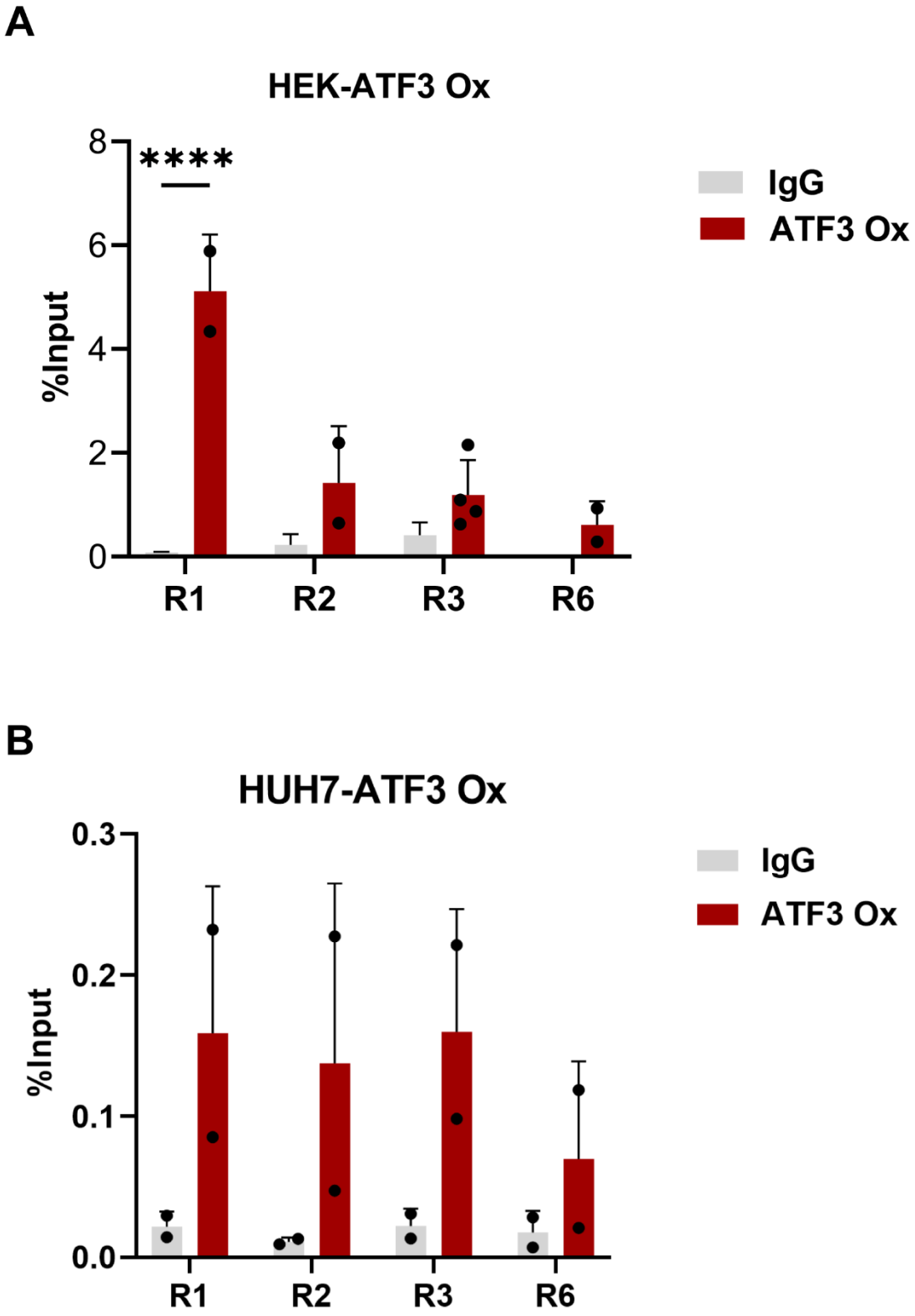

Figure 3.16 ChIP-qPCR of ATF3 on ATP7B Promoter Regions.

A) ChIP-qPCR analysis was performed in the HEK-ATF3 Ox cell line using CASPEX ChIP-qPCR primers targeting Region 1 (R1), Region 2 (R2), Region 3 (R3), and Region

6 (R6) of the ATP7B promoter. The enriched DNA fragments from each region were quantified using qPCR %Input, providing valuable insights into the direct interaction between ATF3 and these regulatory elements on the ATP7B promoter.
B) Similarly, ChIP-qPCR was carried out in the Huh7-ATF3 Ox cell line, focusing on Region 1 (R1), Region 2 (R2), Region 3 (R3), and Region 6 (R6) of the ATP7B promoter.

Through the ChIP-qPCR assays, we confirmed the specific binding of ATF3 to these regions of the ATP7B promoter. The enrichment of ATF3 at these sites further supports its role in the regulation of ATP7B expression. These findings provide valuable insights into the direct interaction between ATF3 and the ATP7B promoter, shedding light on the underlying regulatory mechanisms involved.
These findings highlight the significance of cis-regulatory elements and the potential involvement of ATF3 in the regulation of ATP7B expression. Further investigations are needed to elucidate the precise mechanisms by which ATF3 interacts with these regulatory regions and modulates ATP7B promoter activity.

Furthermore, we conducted viability assays to assess the effect of ATF3 on ATP7B and its relation to cisplatin. We utilized stable cell lines with ATF3 Ko - HEK-ATF3 Ko-1 and HEK-ATF3 Ko-2 (corresponding to gRNA 1 and gRNA 2) - to examine the response to cisplatin in the absence of ATF3 (Figure 3.17). The ATF3 Ko cells displayed increased stability and higher viability when exposed to different doses of cisplatin compared to the HEK-Non-Targeting gRNA control cells. The IC50 dose of the control group was 3.38-fold lower than that of HEK-ATF3 Ko-1 and 2.18-fold lower than that of ATF3 Ko-2. Conversely, in our experiments, the cisplatin response assay conducted on HEK-ATF3 Ox cells, where ATF3 was overexpressed, revealed a notable decrease in cell viability (Figure 3.17B). Contrary to the Ko responses, the viability of ATF3 Ox cells was reduced on the cisplatin response curve. In accordance with the expected results in response to cisplatin, reduced ATF3 expression increased the resistance of HEK293T cells to become more viable, while ATF3 Ox resulted in sensivity against copper (Figure 3.18).

Then, we assessed cellular response to cisplatin and copper on the HUH7 cell line to evaluate viability. We found that ATF3 Ko cells exhibited greater protection against cisplatin, leading to increased resistance. However, in the case of copper, ATF3 Ko cells showed reduced viability and increased sensitivity (Figure 3.17C).

Based on our findings, we can speculate that ATF3 plays a context-dependent role in cell lines with respect to ATP7B and the response to cisplatin and copper (Figure 3.17). In HEK293T cells, ATF3 Ko led to increased stability and viability in the presence of cisplatin, indicating a potential protective effect of ATF3 against cisplatin-induced cytotoxicity. Conversely, ATF3 Ox resulted in reduced cell viability upon cisplatin exposure. These observations suggest that ATF3 may act as a modulator of cisplatin response in HEK293T cells. In the HUH7 cell line, ATF3 Ko cells exhibited enhanced resistance to cisplatin, suggesting a potential role of ATF3 in sensitizing HUH7 cells to cisplatin-induced cell death. On the other hand, ATF3 Ko cells showed reduced viability and increased sensitivity to copper. This suggests that ATF3 may play a complex role in regulating cellular responses to different cytotoxic agents, with varying effects on cell viability depending on the specific context.

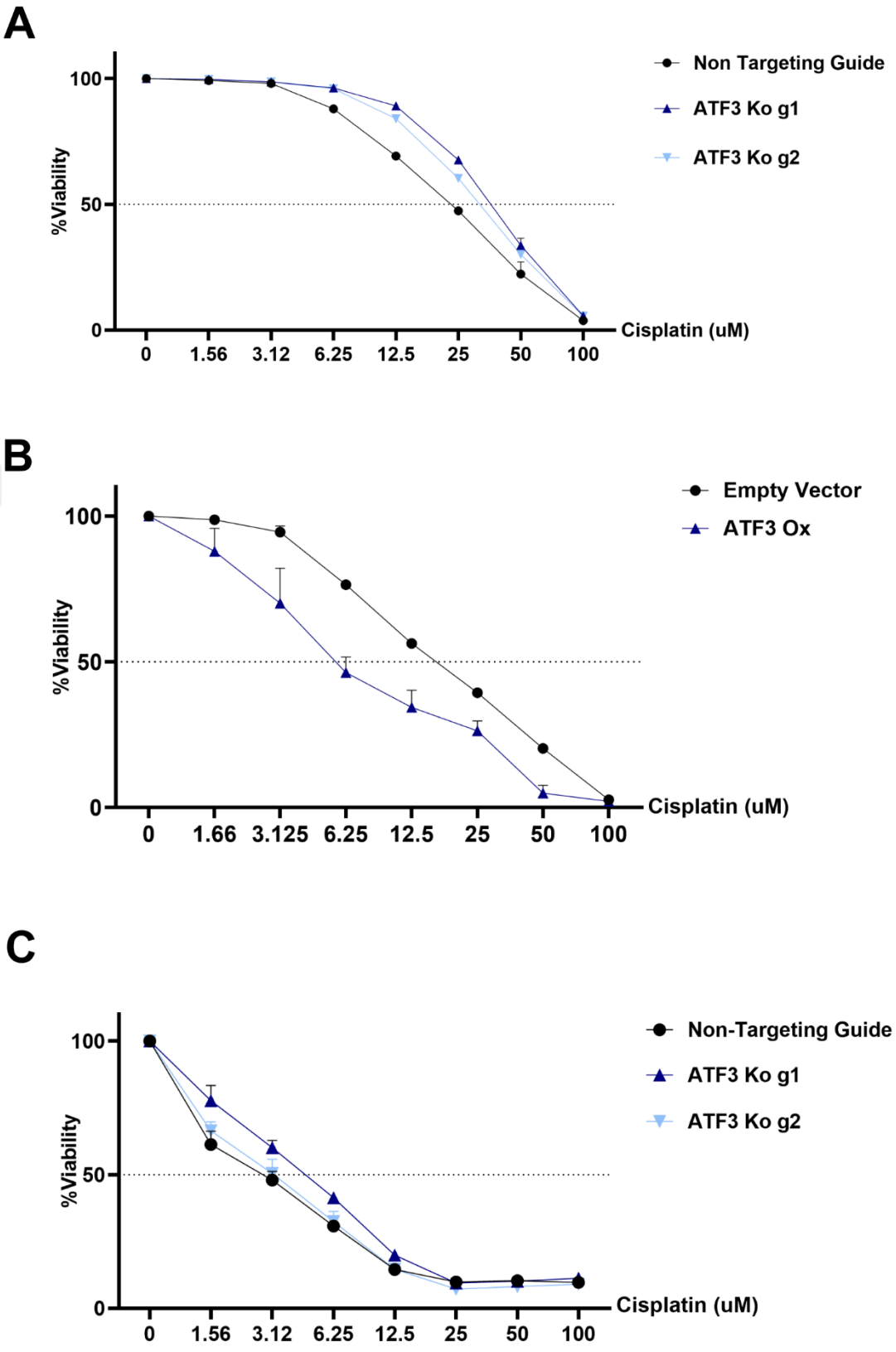
A
100
50
0
%Viability
0
1.56
3.12
6.25
12.5
25
50
100
Cisplatin (uM)
Non Targeting Guide
ATF3 Ko g1
ATF3 Ko g2
B
100
50
0
%Viability
0
1.66
3.125
6.25
12.5
25
50
100
Cisplatin (uM)
Empty Vector
ATF3 Ox
C
100
50
0
%Viability
0
1.56
3.12
6.25
12.5
25
50
100
Cisplatin (uM)
Non-Targeting Guide
ATF3 Ko g1
ATF3 Ko g2

Figure 3.17 Effects of ATF3 Expression on Cisplatin Sensitivity.

A) Cisplatin response of HEK-ATF3 Kos. Viability performed with SRB Assay with NT gRNA stable cell line as a control. B) Cisplatin response of HEK-ATF3 Ox. HEK-3x FLAG Empty cell line used as control. C) Cisplatin response of HUH7-ATF3 Kos.

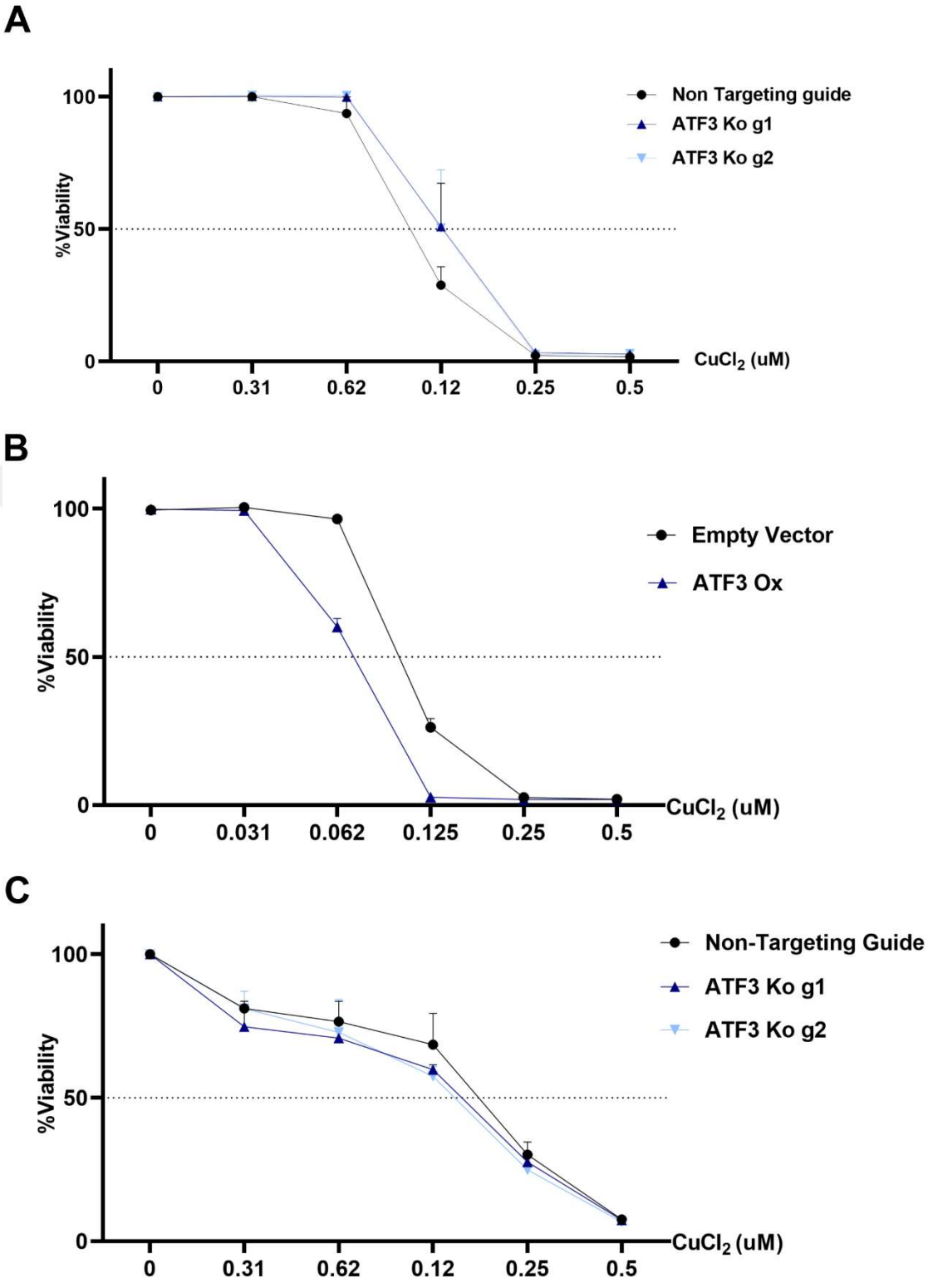

Figure 3.18 Effects of ATF3 Expression on Copper Sensitivity.

A) ATF3 Ko in HEK293T cells: The effects of ATF3 Ko on copper sensitivity in HEK293T cells were assessed. B) Copper response of HEK-ATF3 Ox. C) Copper response of Huh7-ATF3 Kos.

3.4.3 LEF1

The transcription factor Lymphoid-enhancer binding factor 1 (LEF1) plays a crucial role in the canonical Wnt/β-Catenin pathway. LEF1 has been specifically implicated in epithelial-mesenchymal transition (EMT), a process recognized as a hallmark of cancer migration and invasion (Mu et al., 2019; Santiago et al., 2017; Zhao et al., 2019). Our in-silico analysis successfully identified LEF1, specifically locating it on the 5th region of ATP7B CASPEX Proteome. Despite its distance from the promoter region, we aimed to explore the potential effects of LEF1 on ATP7B.

To investigate this, we initiated the cloning of LEF1 Kos and generated stable cell lines using both HEK-293T and HUH7 cell lines. On HEK-293T, LEF1 Ko gRNA-1 reduced the LEF1 by 2-fold comparing to the non-target, however, it doesn't affect the ATP7B expression (Figure 3.19). Additionally, alongside the Kos, we also generated LEF1 Ox constructs to investigate the consequences of LEF1 Ox in relation to ATP7B. Ox of LEF1 increases the ATP7B expression by 1.3-fold on 293Ts (Figure 3.19B).

In the HUH7 cell line, the delivery of LEF1 Ko gRNA (LEF1 Ko g1) led to a significant reduction in LEF1 mRNA expression compared to the non-targeting gRNA, with a fold change of 0.5. Interestingly, the mRNA expression of ATP7B, the target gene of interest, also showed a 60% reduction on mRNA level (Figure 3.19C). These findings indicate a potential correlation between LEF1 expression and ATP7B regulation in HUH7 cells.

Furthermore, when LEF1 was overexpressed in the HUH7 cell line, ATP7B mRNA expression showed a substantial increase, with a fold change of 2.5. This suggests that elevated LEF1 expression may positively influence ATP7B expression levels (Figure 3.19D)

To evaluate the effects of LEF1 Ox at the protein level, we examined two cell lines: HEK-3x FLAG empty (control) and HEK-LEF1 Ox (Figure 3.19E). Interestingly, in the HEK-LEF1 Ox cells, the protein level of ATP7B exhibited a slight reduction compared

to the control, contrary to the transcriptional level findings. This observation suggests that LEF1 may potentially interact with protein partners involved in ATP7B regulation, leading to alterations in ATP7B protein levels.

In the HUH7 cell line, consistent with the mRNA expression results, we also observed a decrease in ATP7B protein levels. This suggests that the reduction in ATP7B expression occurs at both the transcriptional and translational levels in HUH7 cells (Figure 3.19F).

Taken together, these findings imply that LEF1 may have a complex role in regulating ATP7B, potentially involving protein-protein interactions. It is important to note that these results highlight the influence of cell line variations on the observed effects. Therefore, the differences observed between cell lines should be taken into consideration when interpreting the relationship between LEF1 expression and ATP7B regulation.

Previously, we generated various lengths of ATP7B promoter constructs, including 200, 500, 1000, 2000, and 3000 base pairs (bp) fused to a luciferase reporter (Figure 3.14A-B). These constructs were transfected into two cell lines: HEK-Control and HEK-LEF1 Ox. Our results indicate that LEF1 Ox has a notable effect on enhancing luciferase expression when utilizing ATP7B promoter constructs. Specifically, we observed significant increases in luciferase activity with the 500, 1000, and 3000 bp constructs.

These findings suggest that LEF1 may play a crucial role in promoting the utilization of ATP7B promoter regions of these lengths, leading to enhanced luciferase expression. This data supports the hypothesis that LEF1 positively influences the activity of ATP7B promoter regions, particularly those with lengths of 500, 1000, and 3000 bp (Figure 3.20). These results provide valuable insights into the specific impact of LEF1 on ATP7B promoter-driven gene expression in the context of luciferase reporter assays.

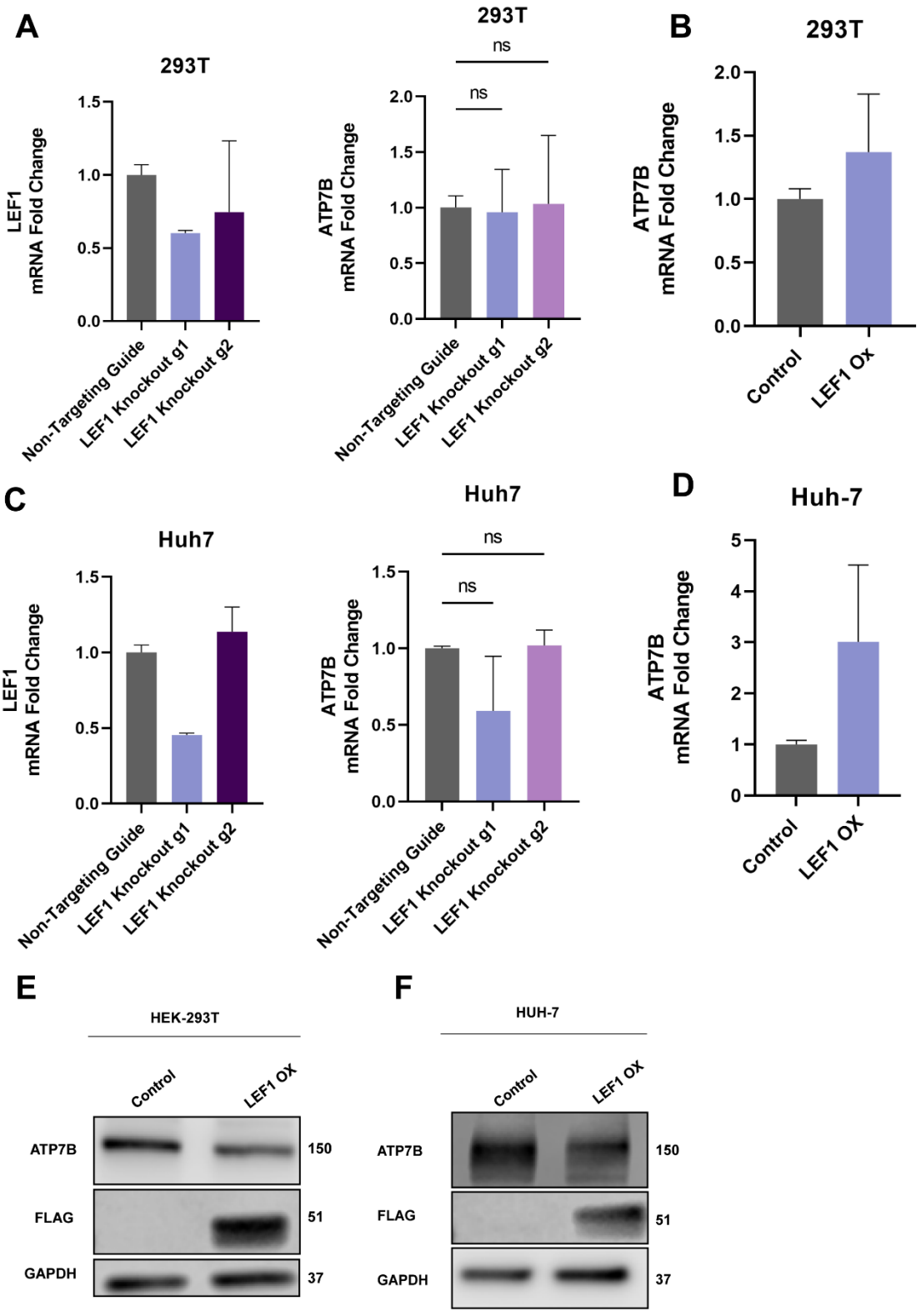

Figure 3.19 LEF1 Expression Effects on ATP7B.

A) Transcriptional changes of HEK-LEF1 Ko (g1-g2) and ATP7B. B) ATP7B mRNA fold change on HEK-LEF1 Ox. C) Transcriptional changes of HUH7-

LEF1 Ko (g1-g2) and ATP7B. D) ATP7B mRNA fold change on HUH7-LEF1 Ox. E) HEK-LEF1 Ox western blotting, LEF1 Ox plasmid contains 3x FLAG epitope which used to blot on 51 KDa. F) HUH7-LEF1 Ox western blotting.

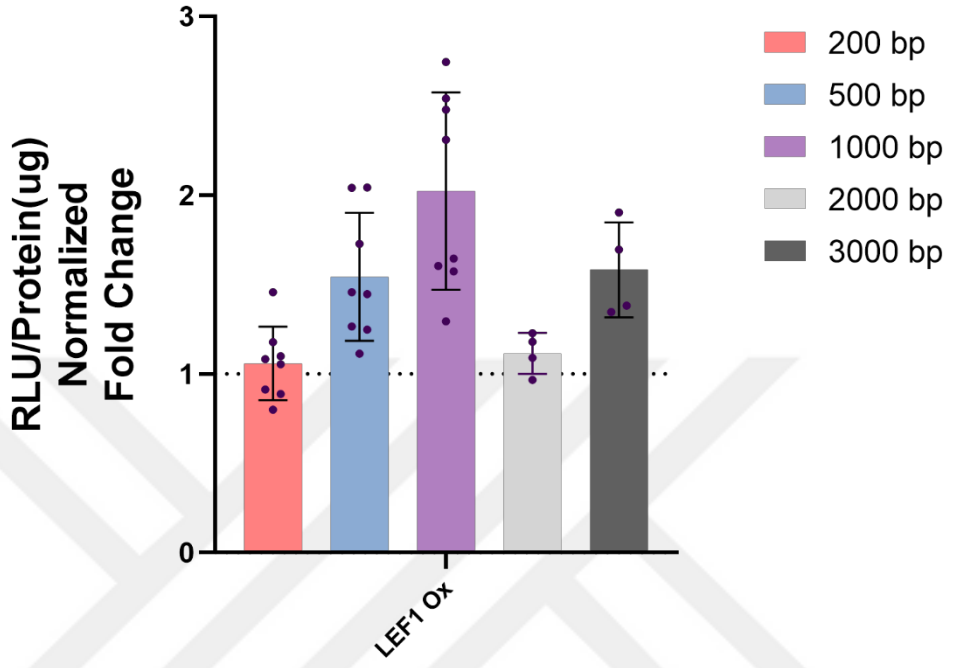

Figure 3.20 ATP7B Promoter Assay on LEF1 Ox. Putative ATP7B promoters transfected on both HEK-Empty Vector cells and HEK-LEF1 Ox cells. LEF1 Ox results normalize to the Empty vector values.

To further investigate the impact of LEF1 expression, we conducted viability assays using Cisplatin and Copper treatments to examine any correlation with ATP7B. In HEK293T cells, we unexpectedly observed that LEF1 Kos resulted in increased cell viability, which was not correlated with ATP7B expression (Figure 3.21A). Conversely, Ox of LEF1 Ox did not significantly affect the viability of HEK293T cells (Figure *3.21*B).

Additionally, we examined the response to copper treatment and found a significant increase in cell viability in LEF1 Kos of the HEK293T cell line (Figure 3.20C-D). This increase in viability may be attributed to alternative targets of LEF1 rather than ATP7B. On the other hand, there was no change when LEF1 was overexpressed in the viability of HEK293T cells upon copper treatment.

During our investigation into the effects of LEF1 expression on HUH7 cells, we observed similar trends as seen in HEK293T cells. Specifically in LEF1 Kos, resulted in a marginal increase in cell viability following cisplatin treatment, while Ox of LEF1 did not exert a significant impact on cell viability under the same conditions (Figure 3.22).

These findings indicate that LEF1 expression may influence the cellular response to cisplatin, regardless of ATP7B involvement.

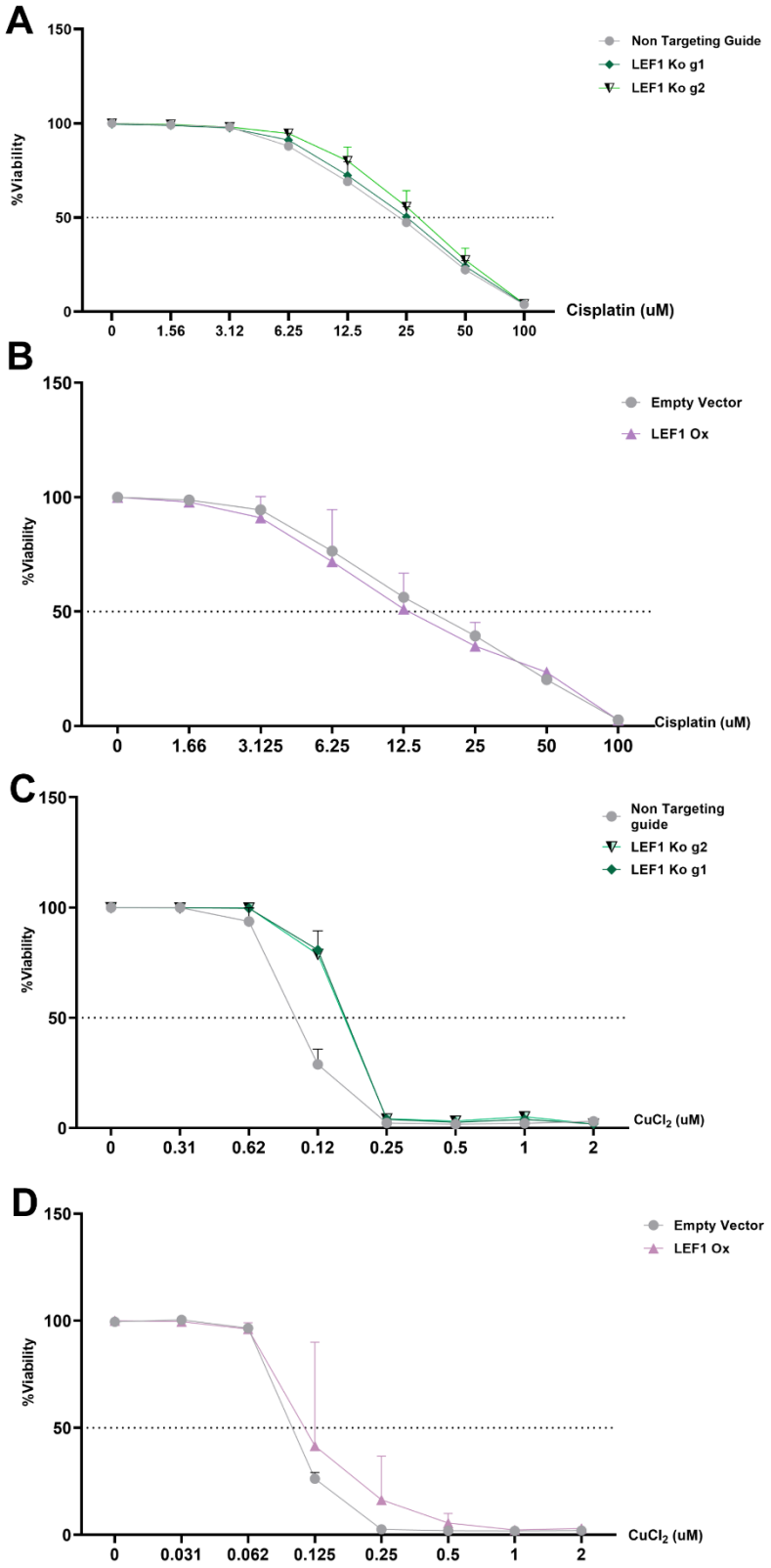

Figure 3.21 Cisplatin and Copper Responses of LEF1 Expression.

A) Cisplatin response of LEF1 Kos on HEK293T. B) Cisplatin response of LEF1 Ox on HEK293T. C) Copper response of LEF1 Kos on HEK293T. D) Copper response of LEF1 Ox on HEK293T.

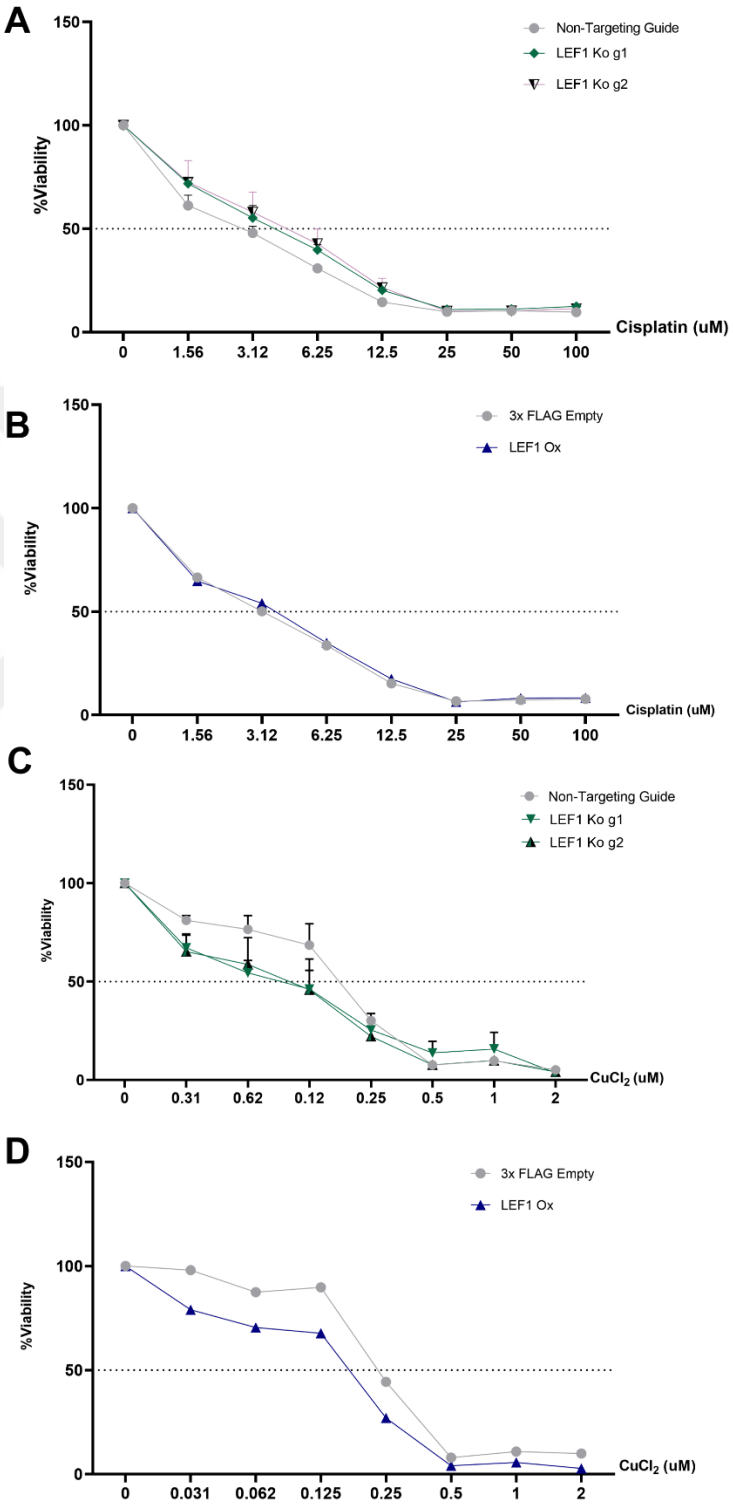

Figure 3.22 LEF1 Expression Effect on Cisplatin and Copper Response.

A) Cisplatin response of LEF1 Ko on HUH7. B) Cisplatin response of LEF1 Ox on HUH7. C) Copper response of LEF1 Kos on HUH7. D) Copper response of LEF1 Ox on HUH7.

Furthermore, in the case of copper treatment, both LEF1 Kos and Ox resulted in a significant decrease in cell viability in HUH7 cells (Figure 3.22). These findings indicate that LEF1 expression can influence the cellular response to copper, suggesting a more complex context in which LEF1 may interact with other factors or pathways beyond ATP7B regulation.

Taken together, our results demonstrate that LEF1 expression can impact the cellular response to cisplatin and Copper in HUH7 cells, suggesting that its effects are not solely reliant on ATP7B but rather involve intricate and multifaceted cellular mechanisms.

3.4.4 P53

P53 is a well-known protein that plays a crucial role in apoptosis and is extensively studied in the context of cancer treatment. Mutations in P53 can lead to the development of drug resistance in cancer cells (Chee et al., 2013; Di Pietro et al., 2012; Han et al., 1999). In our CASPEX Proteome analysis, we identified P53 in regions 1, 6, and 7, highlighting its potential involvement in the regulation of ATP7B and its response to cisplatin treatment (Figure 3.11).

To further investigate the properties of P53 in relation to ATP7B and cisplatin, we performed Ox experiments in both the HEK293T and HUH7 cell lines. In HEK293T cells, Ox of TP53 led to a significant increase in ATP7B mRNA levels, indicating its role in upregulating ATP7B expression (Figure 3.23). However, in the HUH7 cell line, which harbors a mutated form of p53, Ox of TP53 resulted in apoptotic cell death rather than an increase in ATP7B expression.

We generated two different stable cells that overexpress p53 (abbrevieated as p53 ox-1 and 2 on Figure 3.23). While, in p53 ox-1, there was little change in ATP7B protein levels. However, in p53 ox-2, there was a significant increase in ATP7B protein levels (Figure 3.22B). To solve this inconsistency, we conducted western blot analysis on HEK-P53 Ox-2 cells and observed that ATP7B levels were restored to normal levels. These results

imply the existence of protein-protein interactions that aid in maintaining the balance of ATP7B expression following transcriptional activation (Figure 3.22C).

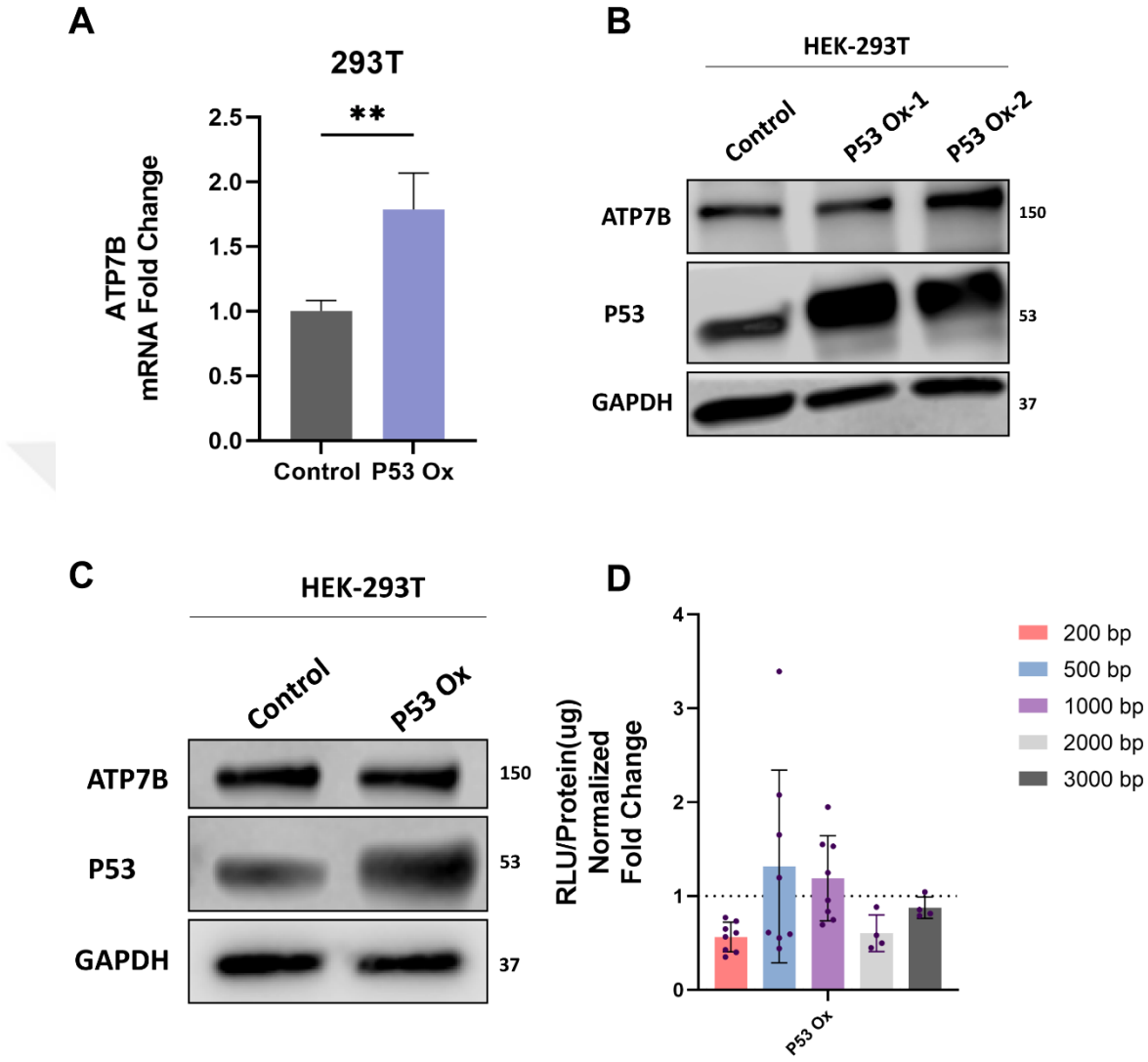

Figure 3.23 P53 Ox Effect on ATP7B.

A) ATP7B mRNA fold change on P53 Ox on HEK293T. B) Western Blotting of ATP7B on P53 Ox on HEK293T with 2 biological replicates. C) Westernblot of P53-Ox-2. D) Luciferase change of HEK-P53 Ox cell line with ATP7B promoter contructs.

These findings highlight the intricate relationship between P53, ATP7B, and cisplatin response, emphasizing the importance of studying the protein-protein interactions and regulatory mechanisms that modulate ATP7B expression in the context of P53 activation.

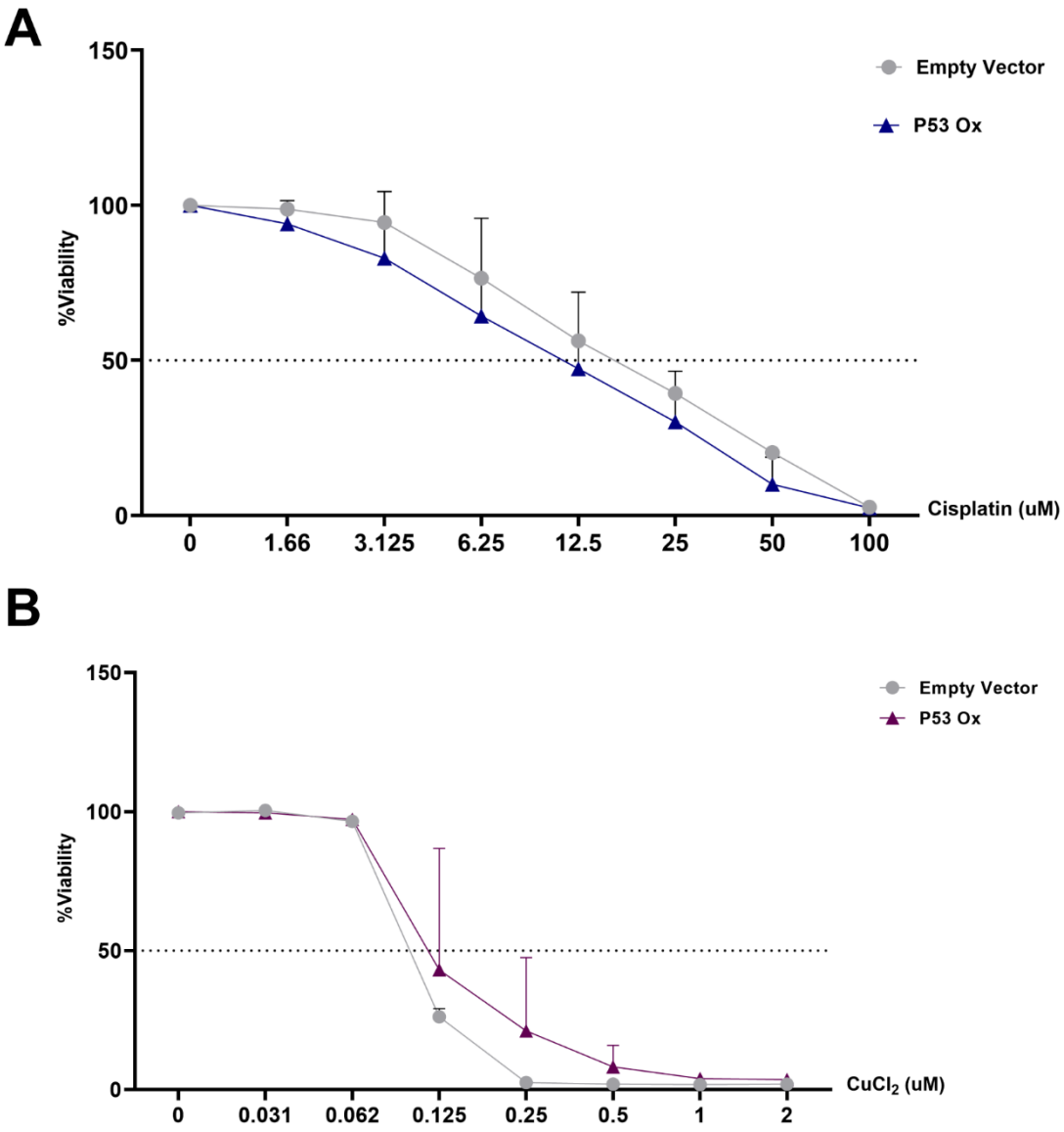

Figure 3.24 Cisplatin and Copper Responses of P53 Ox.

A) Effect of P53 Ox on Cisplatin response of HEK293T. B) Copper Response of HEK-P53 Ox.

Furthermore, we conducted viability experiments to evaluate the response of P53 Ox to cisplatin and copper. Surprisingly, we observed that P53 Ox did not significantly affect the viability of the HEK-P53 Ox cells in both cisplatin and copper treatments (Figure 3.24).

3.5 TOX4 as a Novel Regulator of ATP7B and Cisplatin Resistance.

TOX4, also referred to as TOX High Mobility Group Box Family Member 4, is a transcription factor that has been identified as a constituent of two distinct protein complexes, namely the protein phosphatase complex 1 and the PAF1C complex. Previous studies have reported that TOX4, along with its binding partners, recognize platinylated DNA, which in turn facilitates the recruitment and maintenance of other transcription factors involved in DNA repair mechanisms at the specific binding site (Puch et al., 2011; T. Wang et al., 2023).

TOX4 possesses a nuclear localization signal and a high mobility box group, which contribute to its structure and mechanism of activation as a transcription factor(T. Wang et al., 2023). The nuclear localization signal enables TOX4 to be transported into the nucleus, where it exerts its transcriptional regulatory functions (Figure 1.1). Meanwhile, the high mobility box group, which is a characteristic feature of TOX4, is involved in DNA binding and protein-protein interactions. This structural element enables TOX4 to interact with specific DNA sequences and other transcriptional factors, thereby influencing gene expression. The combined action of the nuclear localization signal and the high mobility box group allows TOX4 to effectively modulate transcriptional processes and contribute to the regulation of cellular functions (Ding et al., 2015; L. Wang et al., 2022).

TOX4, a candidate regulator of ATP7B, was identified in multiple regions of the HEK-CASPEX ATP7B proteome analysis. Notably, region-1 exhibited a 1.47-fold change, region-2 showed a 0.63-fold change, region-3 demonstrated a 1.56-fold change, and region-6 displayed a 1.47-fold change in enrichment, as determined by statistical analysis after mass spectrometry. These findings suggest that TOX4 may play a role in the regulation of ATP7B and in cisplatin resistance.

To further investigate the relationship between ATP7B and TOX4, we examined their expression correlations across various cancer types. Our analysis demonstrated a consistent and significant correlation between the expression levels of ATP7B and TOX4 across a wide range of cancer types. In over 20 different cancers, including breast, kidney, liver, and prostate, we observed a strong positive association between the expression of ATP7B and TOX4. These findings were supported by data obtained from large-scale cancer databases such as TCGA and Timer-Cistrome (Figure *3.13*). This consistent

upregulation of TOX4 alongside ATP7B in diverse cancer types implies a potential co-regulatory mechanism or functional association between the two.

In order to explore, we specifically investigated the expression of TOX4 in breast, kidney, liver, and prostate cancers. In these cancer types, we observed a positive correlation between TOX4 and ATP7B expression (Figure 3.32). This positive correlation further supports the notion that TOX4 may contribute to the regulation of ATP7B expression in a context-specific manner within these cancer types.

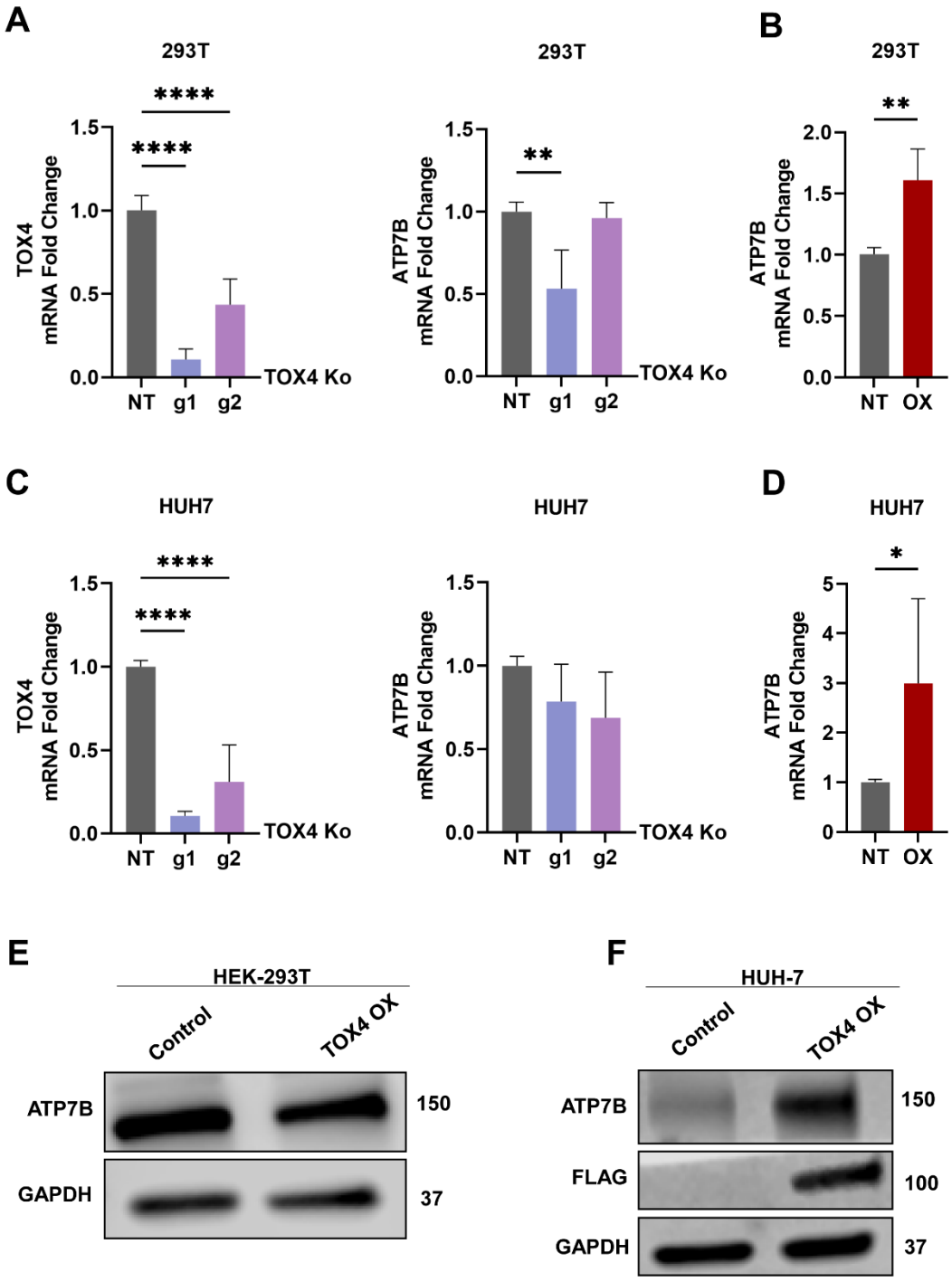

Figure 3.25 The Effects of TOX4 Expression on ATP7B at Transcriptional and Protein Level.

A) HEK-TOX4 Ko g1 and g2: The mRNA fold change of TOX4 and ATP7B in HEK-TOX4 Ko cells (g1 and g2) was measured. B) HEK-TOX4 Ox: The effects of TOX4 Ox on ATP7B. C) HUH7-TOX4 Ko g1 and g2. D) HUH7-TOX4 Ox: The impact of TOX4 Ox on ATP7B transcriptional change in HUH7 cells. E) HEK-TOX4 Ox Western Blot. (TOX4-FLAG) F) HUH7-TOX4 Ox Western Blot.

To investigate the role of TOX4 in the regulation of ATP7B, we generated TOX4 Ko cell lines to examine its impact on ATP7B expression (3.19A). We observed a significant reduction in ATP7B expression in TOX4-Ko cell line g1, indicating the involvement of TOX4 in the regulation of ATP7B (Figure 3.19B). Conversely, when TOX4 was overexpressed in HEK293T cells, we observed a 1.5-fold increase in ATP7B expression, suggesting a regulatory mechanism between TOX4 and ATP7B at the promoter level.

Additionally, we generated TOX4 Ko HUH7 cells and observed a significant decrease in TOX4 mRNA levels, resulting in a reduction of ATP7B expression (Figure 3.25). However, the magnitude of change in ATP7B expression was lower compared to that in HEK293T cells. Subsequently, stable Ox of TOX4 in HUH7 cells led to a 3-fold increase in ATP7B expression compared to the control (Figure 3.19D). Then, we blotted ATP7B (150 kDa), TOX4 Ox which has 3xFLAG epitope (100 KDa) to assess TOX4 Ox effects on ATP7B protein level. Interestingly, when assessing protein levels, we observed minimal changes in ATP7B expression level of TOX4 Ox in both HEK293T and HUH7 cell lines (Figure 3.25). However, there was a significant increase in ATP7B protein levels in the HUH7 cell line. These observations suggest that the effects of TOX4 on ATP7B expression may be cell line-specific and could be influenced by the baseline expression levels of ATP7B, which are higher in HEK293T cells and relatively lower in HUH7 cells. Results suggest that TOX4 expression effects ATP7B independent from the cell line context, comparing these two HEK293T and HUH7 cell lines.

To investigate the specific cis-regulatory regions targeted by TOX4 within the ATP7B promoter, we conducted a series of experiments. Initially, we assessed the effect of TOX4 Ox on ATP7B expression using promoter assay, which revealed an increase in ATP7B expression (Figure 3.26) Building upon these findings, our aim was to identify the specific regions within the ATP7B promoter that interact with TOX4.

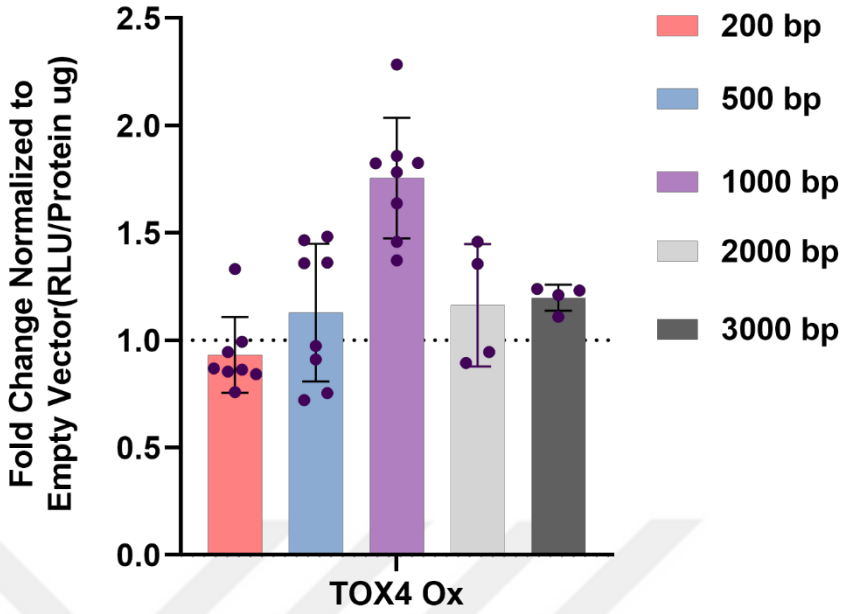

Figure 3.26 TOX4 Ox Increases Luciferase Activity on ATP7B Promoter.

Transfection of ATP7B Promoter Constructs with Luciferase: HEK-3x FLAG Empty (Control) and HEK-TOX4 Ox cell lines were transfected with ATP7B promoter constructs fused to luciferase. The luciferase activity was measured using Relative Luminescence Units (RLU) per microgram of protein (ug). The data compare luciferase activity levels in the control and TOX4 overexpressing cells. HEK-TOX4 Ox Fold Change Normalized to HEK-3x FLAG Empty Control: The fold change in luciferase activity in HEK-TOX4 Ox cells was calculated and normalized to the luciferase activity in HEK-3x FLAG Empty (Control) cells. The results highlight the relative increase in luciferase activity upon TOX4 Ox compared to the control.

To achieve this, we generated a control construct containing the backbone of the TOX4 Ox vector (3xFLAG Empty construct) and established a stable cell line as a control for comparative analyses. We then transfected different sizes of ATP7B promoter constructs (ranging from 200 to 3000 bp) into both the HEK-Control and HEK-TOX4 Ox cell lines (Figure 3.26). Our luciferase assay results indicated that TOX4 Ox specifically enhanced luciferase expression from the -1000 bp region of the ATP7B promoter,

suggesting that TOX4 interacts with this specific cis-regulatory region, thereby increasing the transcriptional activity of the ATP7B promoter (Figure 3.26).

To further investigate the binding sites of TOX4 on the ATP7B promoter and confirm its regulatory role, we performed ChIP assays. For this purpose, we utilized TOX4-overexpressing cell lines (HEK293T and HUH7) and included an IgG control for comparison (Figure 3.27). Using specific ChIP-qPCR primers designed to target seven regions identified through CASPEX analysis, we assessed the binding of TOX4 to the ATP7B promoter. We focused our analysis on regions 1, 2, 3, and 6 to provide evidence of TOX4 binding and its impact on ATP7B expression regulation (Figure 3.27). The enrichment scores (%Input) for these regions were relatively high in the HEK-TOX4 Ox cell line, indicating a strong binding of TOX4 to the ATP7B promoter especially on Region-1: 0.16, Region-2: 0.27, Region-6: 0.17 which are considerebly good enrichments in terms of transcription factor binding on enhancing regions, however on Region-3: 1.26 which states that a strong indication of binding. Additionaly, Region-4 binding of TOX4 is negative.

As having identified TOX4 on CASPEX proteome analysis in regions 1, 2, 3, and 6 of the ATP7B promoter, we sought to provide direct evidence of TOX4 binding to the promoter region. To do so, we performed luciferase promoter assays and ChIP experiments (Figure 3.21).

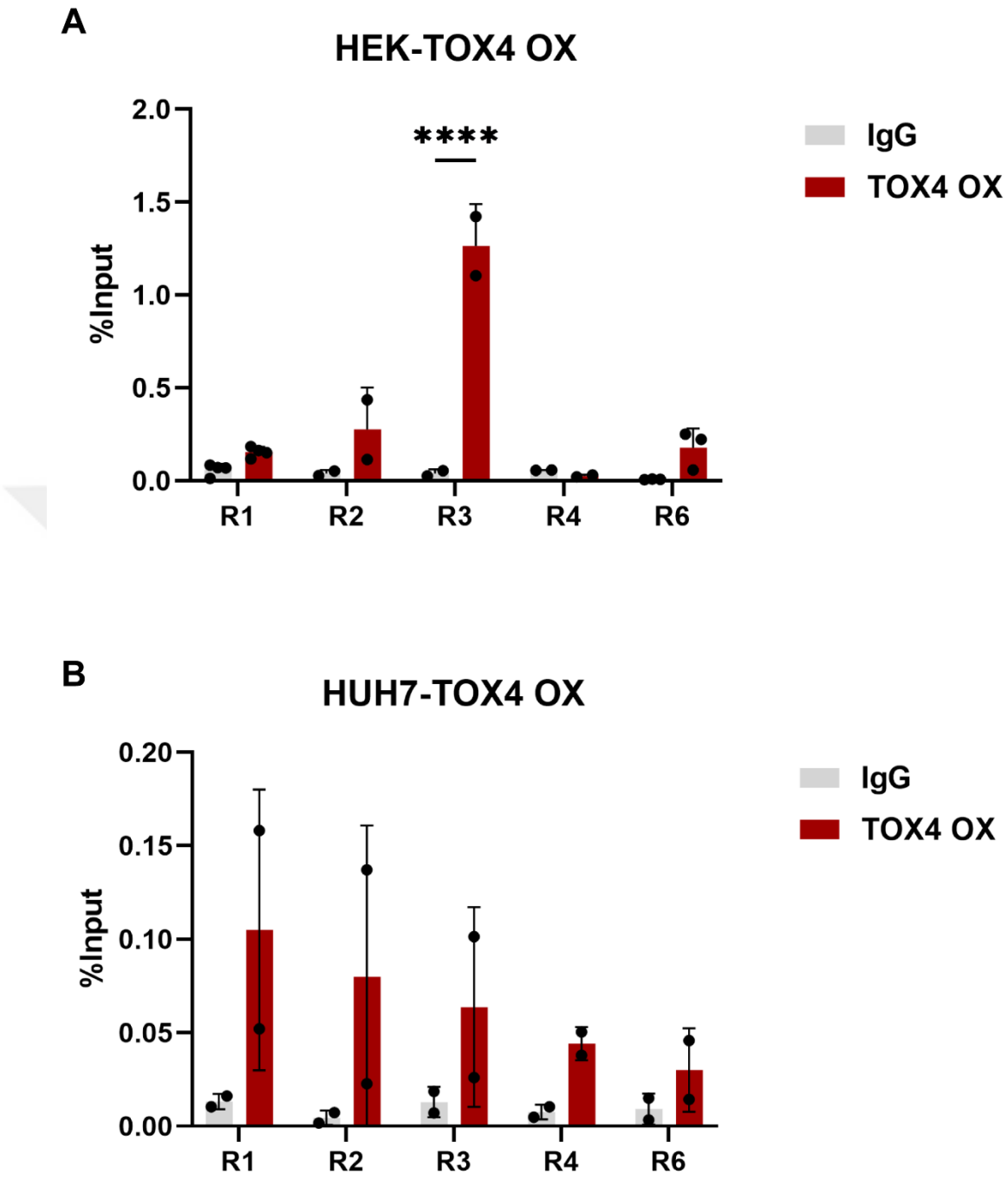

Figure 3.27 TOX4 Binds to the ATP7B Promoter Validated with ChIP-qPCR.

A) TOX4 ChIP-qPCR on HEK-TOX4 Ox Cells: ChIP-qPCR was performed using anti-FLAG antibody to specifically pull down TOX4-bound DNA fragments from chromatin in HEK-TOX4 Ox cells. As a negative control, IgG was used

B) TOX4 ChIP-qPCR on HUH7-TOX4 Ox Cells: Similar to (A), ChIP-qPCR was performed on HUH7-TOX4 Ox cells using anti-FLAG antibody to assess TOX4 binding to the ATP7B promoter.

In the luciferase promoter assay, we observed that Overexpression of TOX4 (TOX4 Ox) led to an increase in luciferase expression specifically on the 1000 bp-Luc construct. This result indicates that TOX4 enhances the activity of the ATP7B promoter, supporting its role as a regulator of ATP7B expression. To further elucidate our findings, we conducted ChIP experiments to directly demonstrate the binding of TOX4 to the ATP7B promoter. Our results confirmed that TOX4 binds to the vicinity of the 1000 bp region of the promoter on HEK293T, providing direct evidence of its interaction with the regulatory elements of ATP7B (Figure 3.27).

Notably, in the HUH7 cell line, the enrichment scores for TOX4 binding were relatively lower, suggesting that the regulatory mechanism of TOX4 on ATP7B expression may vary in different cell lines. Nevertheless, these findings collectively suggest that TOX4 binds to the ATP7B promoter and plays a role in regulating its expression, with potential variations across different cell lines (Figure 3.27).

Furthermore, we conducted viability assays to examine the impact of TOX4 on ATP7B and its relationship with cisplatin treatment. We utilized stable cell lines with TOX4 Ko, specifically HEK-TOX4 Ko-1 and HEK-TOX4 Ko-2 (corresponding to gRNA 1 and gRNA 2) - to assess the response to cisplatin in the absence of TOX4 (Figure 3.28). Interestingly, the TOX4 Ko cells exhibited increased sensitivity to cisplatin, displaying lower viability when exposed to varying doses of the drug compared to the control cells transfected with non-targeting gRNA. The IC50 dose of HEK-TOX4 Ko-2 was found to be 2-fold lower than that of the control. Conversely, in HEK-TOX4 Ox cells, which overexpress TOX4, we observed a significant increase in cell viability, with a 2.5-fold higher viability compared to the control (Figure 3.28).

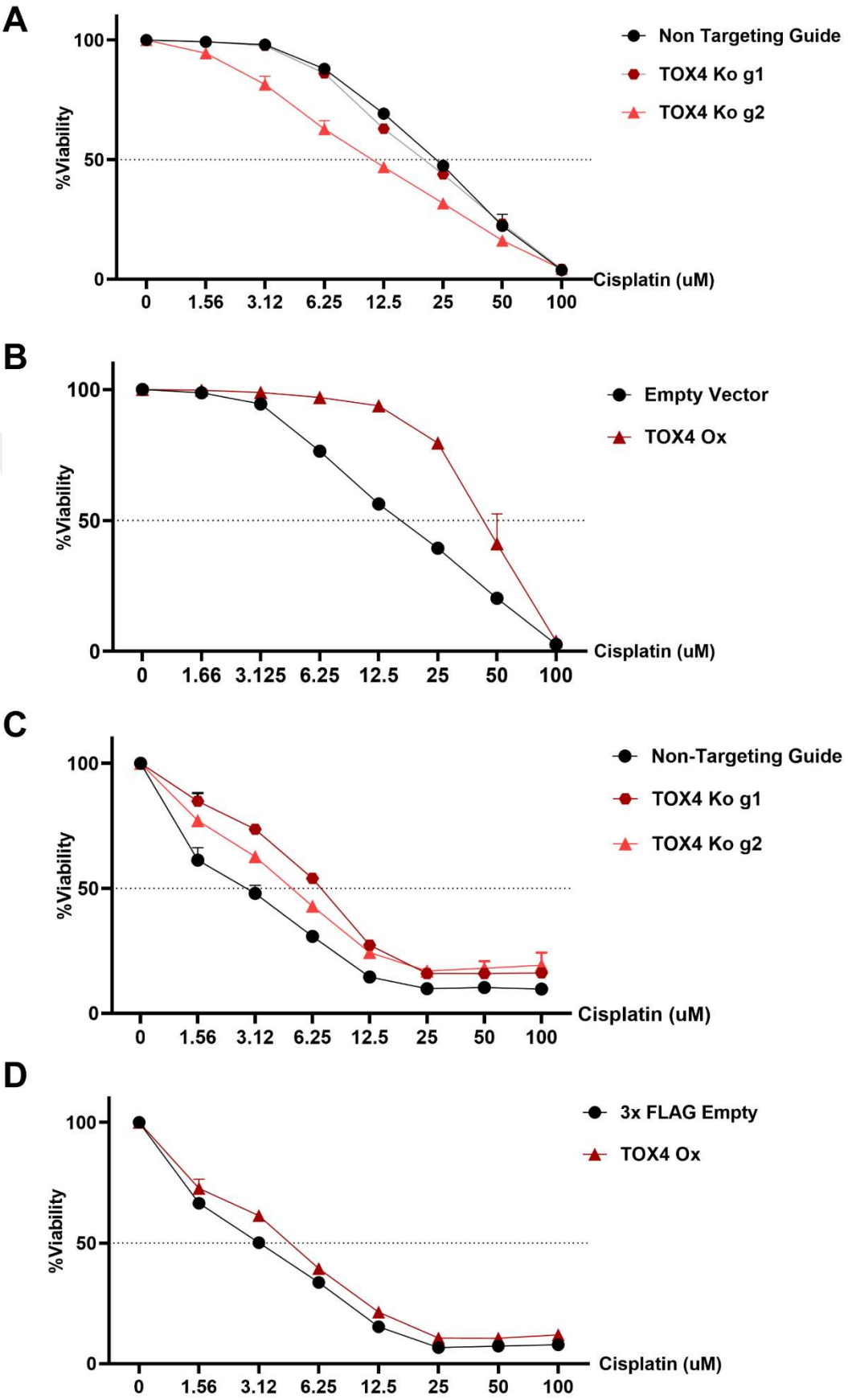
A
100
50
0
%Viability
0 1.56 3.12 6.25 12.5 25 50 100
Cisplatin (uM)
Non Targeting Guide
TOX4 Ko g1
TOX4 Ko g2
B
100
50
0
%Viability
0 1.66 3.125 6.25 12.5 25 50 100
Cisplatin (uM)
Empty Vector
TOX4 Ox
C
100
50
0
%Viability
0 1.56 3.12 6.25 12.5 25 50 100
Cisplatin (uM)
Non-Targeting Guide
TOX4 Ko g1
TOX4 Ko g2
D
100
50
0
%Viability
0 1.56 3.12 6.25 12.5 25 50 100
Cisplatin (uM)
3x FLAG Empty
TOX4 Ox

Figure 3.28 TOX4 Expression Levels Modulate Cisplatin Resistance and Sensitivity.

A) Cisplatin Response of HEK-TOX4 KO Cells: HEK-TOX4 Ko cells were exposed to varying concentrations of cisplatin, and their viability was measured. B) Cisplatin Response of HEK-TOX4 Ox Cells: HEK-TOX4 Ox cells were subjected to cisplatin treatment at different concentrations. C) Cisplatin Response of HUH7-TOX4 KO Cells: HUH7 cells with TOX4 Ko were treated with concentrations of cisplatin in the graph. D) Cisplatin Response of HUH7-TOX4 Ox Cells: Lastly, HUH7 cells overexpressing TOX4 were exposed to different doses of cisplatin.

In contrast to the response observed with cisplatin, the downregulation of TOX4 expression resulted in increased resistance of HEK293T cells to copper, as indicated by higher viability in the presence of the metal. Conversely, Ox of TOX4 in HEK-TOX4 Ox cells restored the sensitivity of cells to copper, leading to reduced viability (Figure 3.29).

On the other hand, in the HUH7 cell line, the downregulation of TOX4 resulted in increased resistance to cisplatin, as evidenced by a 2.5-fold higher IC50 value (Figure 3.28C). This suggests that TOX4 plays a role in modulating the sensitivity of HUH7 cells to cisplatin-induced cytotoxicity. However, upon TOX4 Ox in HUH7 cells, we observed a slight increase in cisplatin resistance. This may indicate that TOX4 has additional targets than ATP7B and effects within the cisplatin pathway, potentially influencing other proteins involved in cisplatin resistance, such as CTR1, ATP7A, MRP2, GSH, ERRCC1, BRCA1/2, and VDAC (Galluzzi et al., 2011).

Interestingly, we found that TOX4 Ko consistently rendered cells sensitive to copper treatments, which is consistent with the role of TOX4 in regulating ATP7B (Figure 3.29). In contrast, TOX4 Ox led to increased sensitivity to copper, suggesting a potential regulatory mechanism between TOX4 and copper-related pathways. These findings highlight the complex and context-dependent role of TOX4 in modulating cellular responses to different treatments and emphasize the need for further investigation to elucidate the underlying mechanisms.

Based on the results highlight the complex and context-dependent role of TOX4 in the response of cells to different treatments, such as cisplatin and copper. The modulation

of TOX4 expression have a significant impact on cell viability and drug resistance, suggesting its involvement in the regulation of cellular responses to these agents.

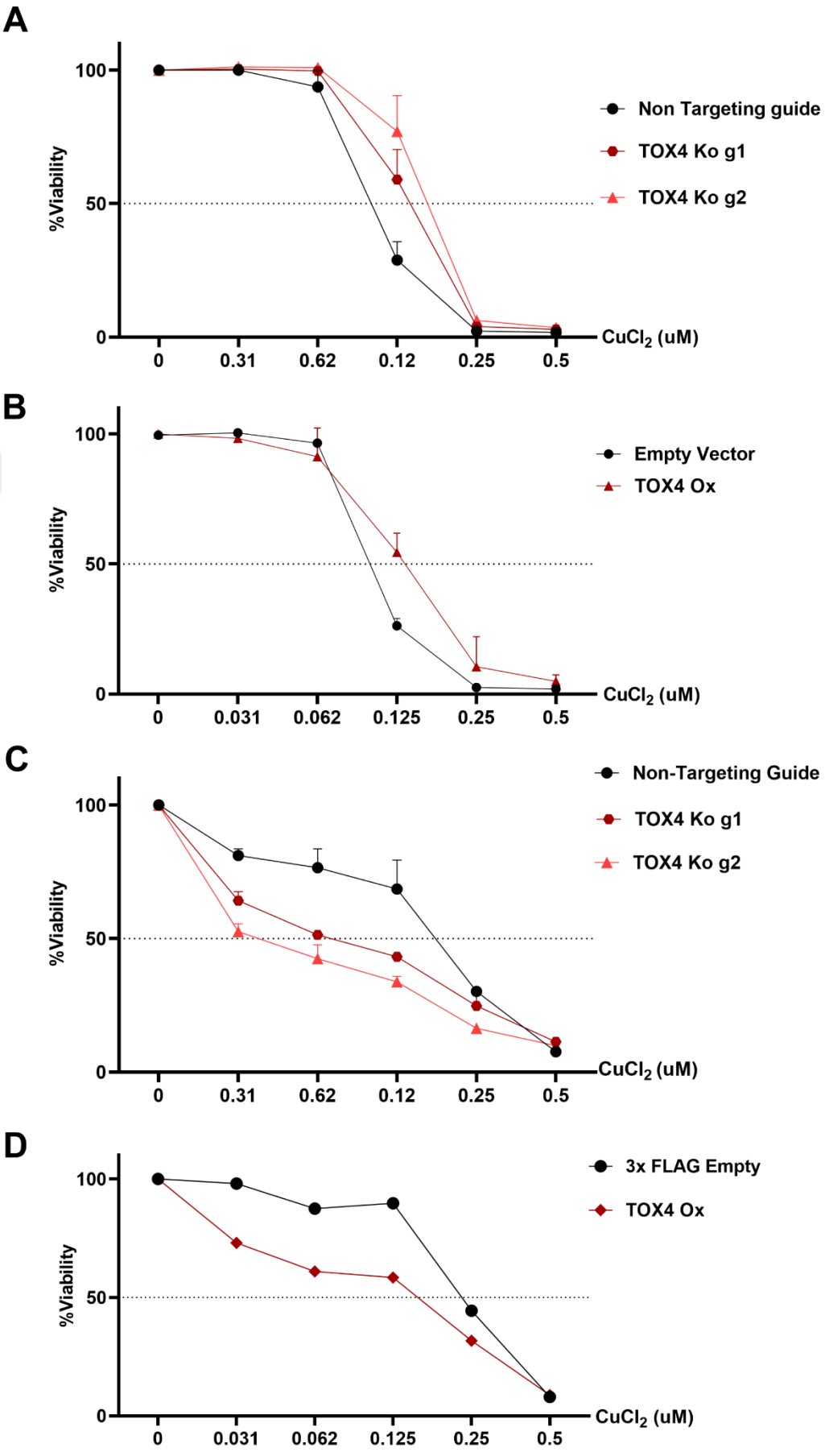
A
100
50
0
%Viability
Non Targeting guide
TOX4 Ko g1
TOX4 Ko g2
0
0.31
0.62
0.12
0.25
0.5
CuCl2 (uM)
B
100
50
0
%Viability
Empty Vector
TOX4 Ox
0
0.031
0.062
0.125
0.25
0.5
CuCl2 (uM)
C
100
50
0
%Viability
Non-Targeting Guide
TOX4 Ko g1
TOX4 Ko g2
0
0.31
0.62
0.12
0.25
0.5
CuCl2 (uM)
D
100
50
0
%Viability
3x FLAG Empty
TOX4 Ox
0
0.031
0.062
0.125
0.25
0.5
CuCl2 (uM)

Figure 3.29 TOX4 Expression Levels Modulate Copper Resistance and Sensitivity.

A) Copper Response of HEK-TOX4 KO Cells: HEK-TOX4 Ko cells were exposed to varying concentrations of copper, and their viability was measured. B) Copper Response of HEK-TOX4 Ox Cells. C) Copper Response of HUH7-TOX4 Ko Cells. D) Copper Response of HUH7-TOX4 Ox Cells.

As we previously confirmed ATP7B Ko verification by qPCR and Western Blotting. TOX4 Ox on these cells protected toxic dose of copper, TOX4 could have additional targets than ATP7B (Figure 3.31).

To investigate the long-term effects of cisplatin exposure and the response in relation to TOX4, we conducted a colony formation assay using different doses of cisplatin (0, 0.5, 1, 2 uM) (Figure 3.30). In the HEK-293T cell line, we observed that TOX4 Ox provided significant protection against cisplatin-induced damage at a dose of 1 uM, while TOX4 Ko (g1 and g2) sensitized the cells to cisplatin. These findings suggest that TOX4 may play a role in modulating the response to cisplatin-induced DNA damage and participate in DNA repair processes, as the absence of TOX4 resulted in increased sensitivity to cisplatin.

Similarly, in the HUH7 cell line, similar results observed, with the cells showing higher sensitivity to cisplatin compared to HEK293T cells. This could be attributed to differences in the expression levels of proteins involved in the cisplatin pathway and ATP7B. Upon TOX4 Ox, HUH7 cells were protected against cisplatin at a dose of 0.5 uM, allowing them to grow more, while the absence of TOX4 resulted in cell death (Figure 3.30B). These findings suggest that TOX4 may play a critical role in modulating the response to cisplatin in HUH7 cells and highlight the importance of TOX4 in regulating cell viability and survival under cisplatin-induced stress.

Indeed, the upregulation of TOX4 led to increased levels of ATP7B in both HEK293T and HUH7 cell lines. However, it is important to consider that TOX4 may have additional targets within the cisplatin pathway that can influence the viability outcomes. These targets include ATP7A, ABCC2, CTR1, ERRC1, and RAD51. In HEK-TOX4 Ox cells, we observed an increase in both ATP7B and ATP7A levels. Interestingly, the levels of ABCC2, which engages in multidrug resistance, were significantly reduced (Figure 3.31A). This suggests that the excretion of cisplatin from the cells may be

compromised. Additionally, while the levels of ERCC1 and CTR1 remained unchanged, the levels of RAD51, involved in DNA damage repair, were significantly increased in response to TOX4 Ox. In HUH7 cells, we observed an increase in both ATP7B and RAD51 levels, while the levels of ATP7A and ABCC2 were decreased (Figure 3.31B). These findings indicate that the Ox of TOX4 affects the cisplatin pathway, but the prediction of viability outcomes may vary between cell lines due to the specific targets of TOX4 and their effects on gene expression levels.

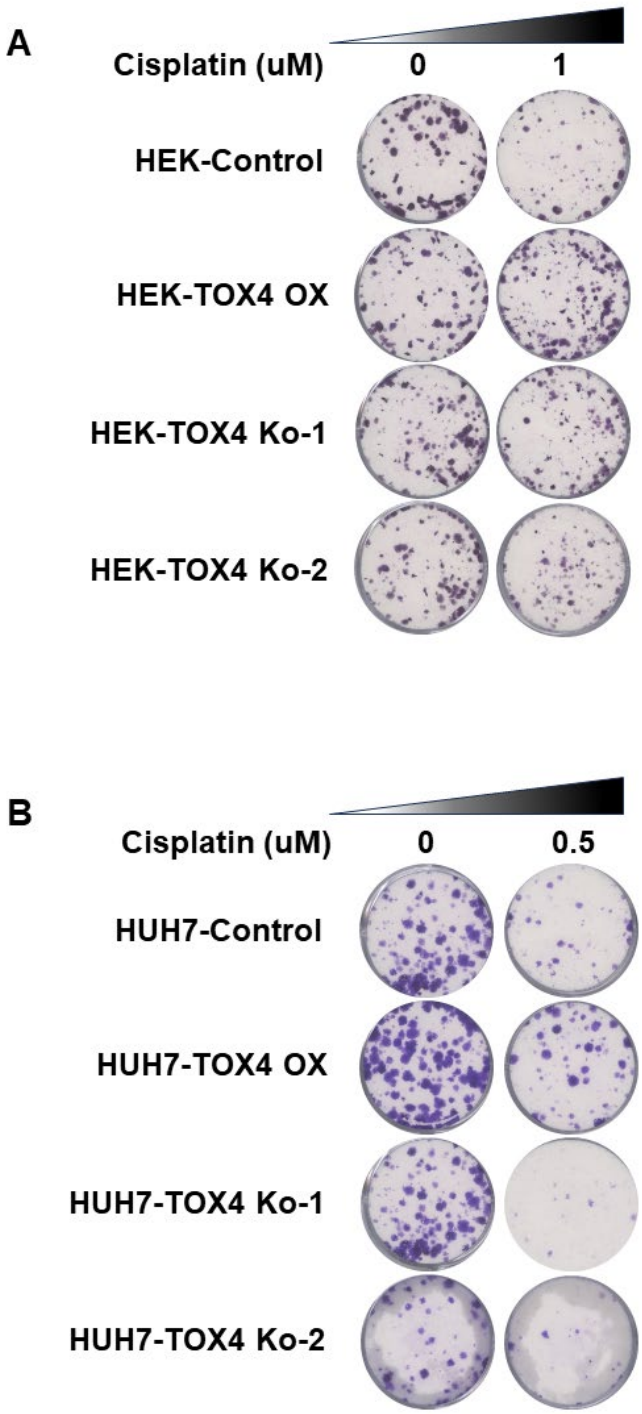

Figure 3.30 TOX4 has Dual Role as Resistance and Sensitization against Cisplatin on 293T and HUH7.

A) Colony formation performed on HEK293T cells with modulated TOX4 Expression (Ox, Kos) and Cisplatin doses (0, 0.5, 1, 2 uM). B) Colony formation

performed on HUH7 cells with modulated TOX4 Expression (Ox, Kos) and Cisplatin doses (0, 0.5, 1, 2 uM).

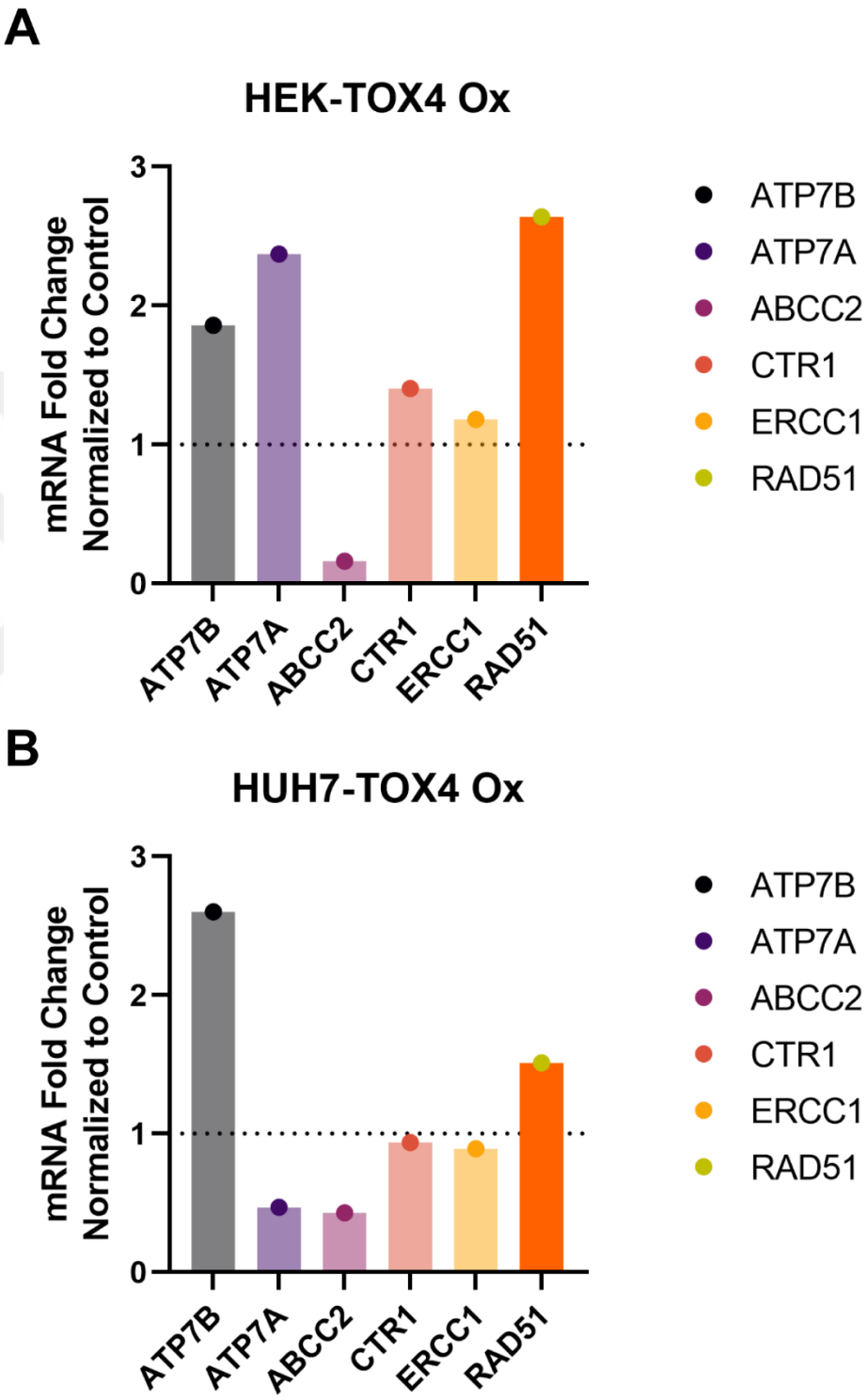

Figure 3.31 Potential Targets of TOX4 on Cisplatin Pathway.

A) Potential Cisplatin pathway associated protein transcriptional levels on HEK-TOX4 Ox. B) Potential Cisplatin pathway associated protein transcriptional levels on HUH7-TOX4 Ox.

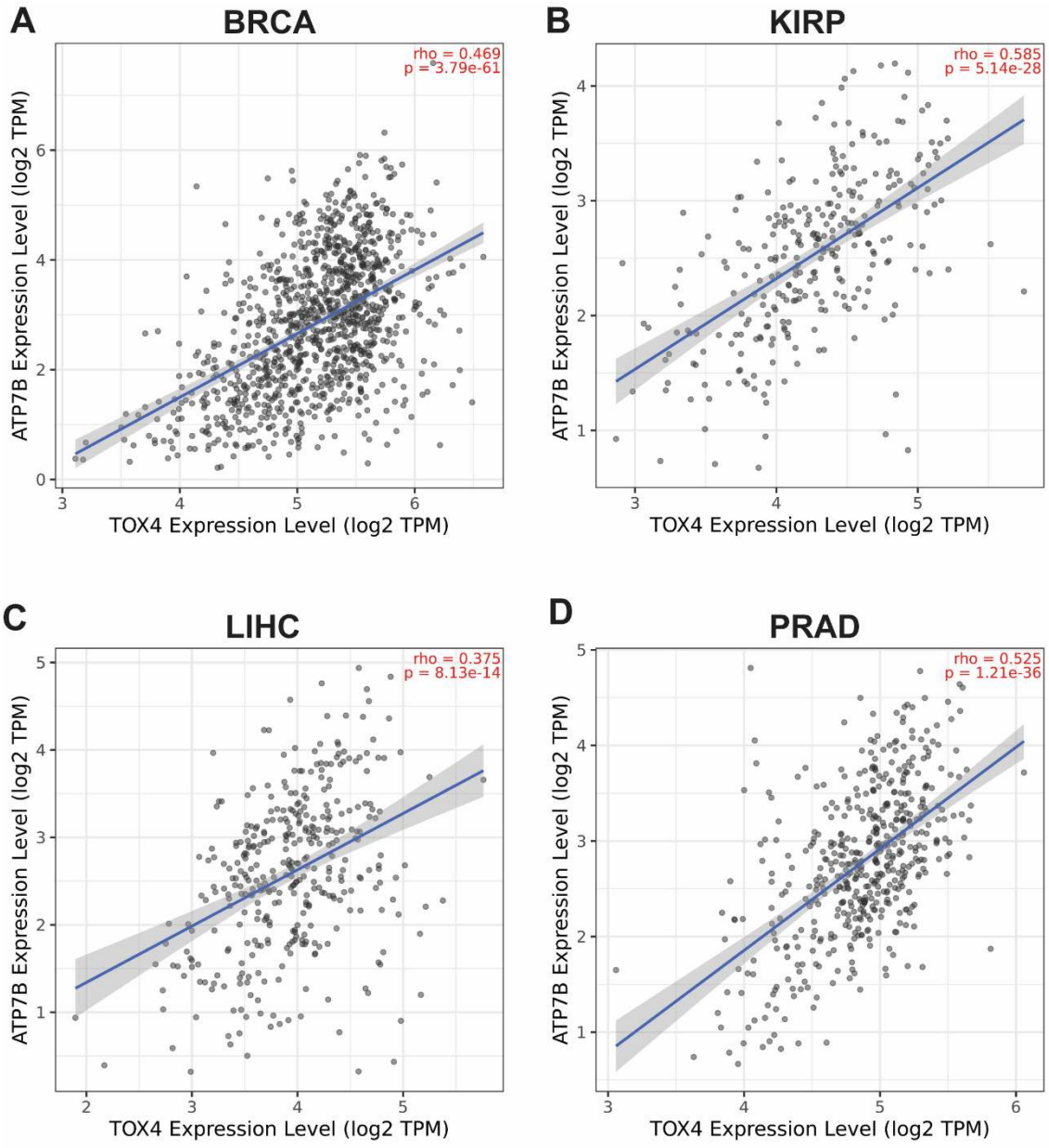

Figure 3.32 Correlation of TOX4 with ATP7B in Breast, Kidney, Liver and Prostate Cancer.

3.6 Epigenetic Regulation of ATP7B

3.6.1 HDAC Inhibitors

Epigenetic changes as acetylation and methylation patterns could lead to ATP7B expression changes and effect its expression to drive cancer cells towards resistance or Wilson's disease phenotypes (Contreras-Sanzón et al., 2022; H. J. Kim & Bae, 2011; Shanmugam et al., 2022). In our laboratory, a Luciferase Knock-in cell line was generated on the HEK-293T cells by Baris Sergi, PhD student. The Luciferase gene was integrated into the transcription start site of the ATP7B promoter. Subsequently, a drug screen was conducted using an epigenetic drug library and inhibitors targeting epigenetic modifiers such as HDACs, BETs, and methylation. From this screen, candidate inhibitors were identified that specifically target the activity of HDAC1 and HDAC3. These inhibitors resulted in a direct increase in Luciferase expression, which is correlated with ATP7B expression.

To assess the functionality of our ATP7B Knock-in system, we generated single colonies from HEK293T cells and measured luciferase expression. Among the generated colonies, HEK-Ki Colony 5, 6, and 8 exhibited relatively high luciferase expression levels, with RLU/ug values around 4-5 (Figure 3.32A).

Next, we aimed to demonstrate the responsiveness of the Knock-in system to exogenous changes. We overexpressed a known, novel regulator of ATP7B, MTF1, using a doxycycline-inducible backbone. The Ox of MTF1 further increased luciferase expression in HEK-Ki #5 and HEK-Ki #6 cells, which harbor the ATP7B promoter (Figure 3.32B).

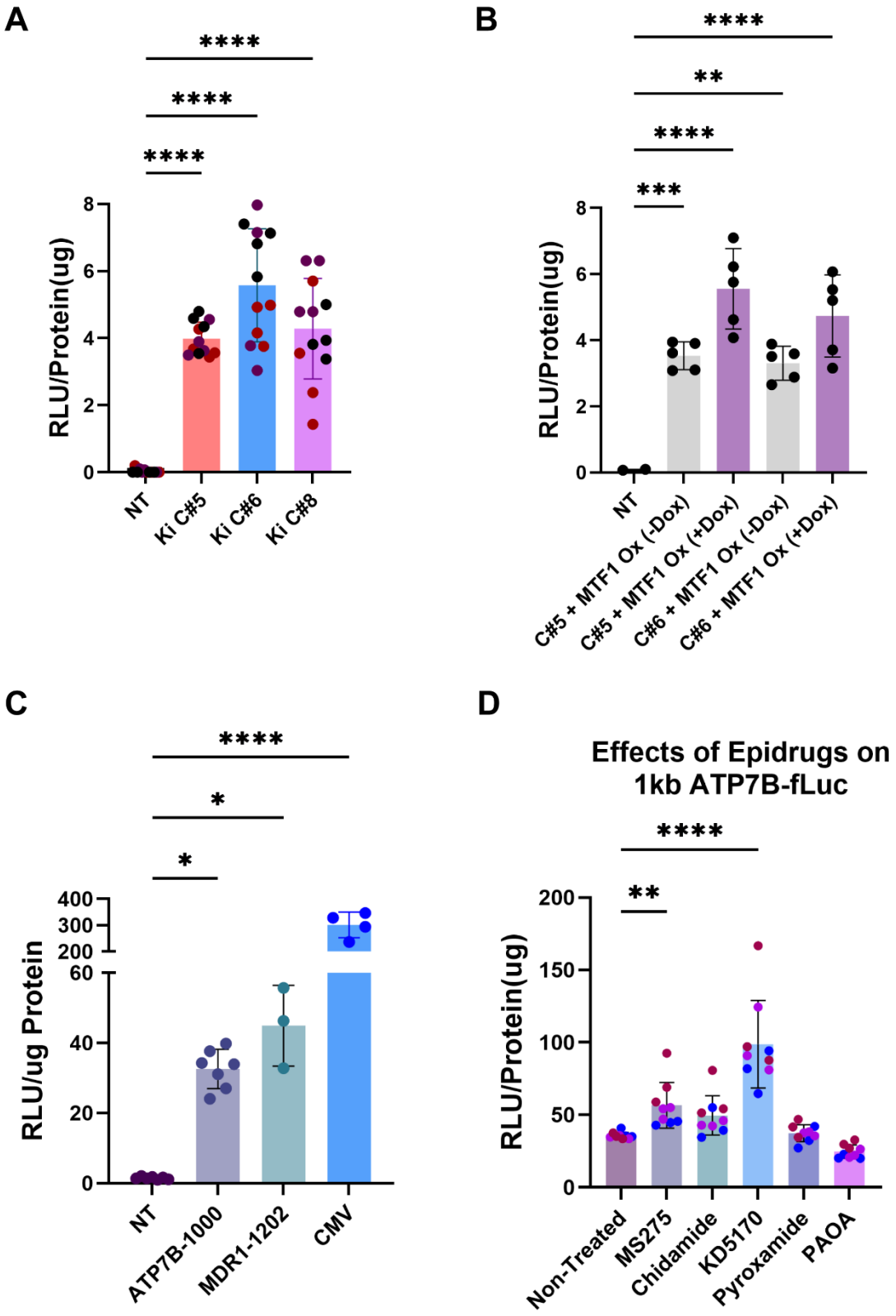

Figure 3.33 Modulation of ATP7B Knock-in (Ki) and Exogenous ATP7B Promoter Activity by HDAC Inhibitors.

A) Knock-in validation with luciferase expression: HEK-Ki colonies (Colony 5, 6, and 8) were subjected to luciferase reporter assay to confirm the successful knock-in of ATP7B. B) MTF1 Ox Activity on HEK-Ki Colonies: The impact of MTF1 Ox on HEK-Ki colonies was assessed. C) Comparison of 1kb ATP7B Promoter Strength with MDR1-1202 and CMV-Luc: D) Effects of HDAC Inhibitors on 1kb ATP7B-fLuc: The effects of HDAC inhibitors on the 1kb ATP7B promoter were evaluated using a fusion luciferase construct (1kb ATP7B-fLuc). HDAC inhibitors were administered to examine their modulatory impact on ATP7B expression.

Additionally, we utilized the 1kb ATP7B promoter-Luc construct, along with other promoter constructs such as MDR1-1202, CMV-Luc, and an empty vector, to evaluate their activity (Figure 3.32C). The 1kb ATP7B promoter exhibited strong promoter activity comparable to the MDR1-1202 promoter, providing further confirmation of the HDAC inhibitors identified through the epigenetic drug screen. These inhibitors target HDAC activity, leading to specific acetylation patterns that influence gene expression*(H. J. Kim & Bae, 2011)*. Moreover, the plasmids used in the experiments interact with histones, potentially influencing their regulatory patterns (Mladenova et al., 2009).

To investigate the expression changes induced by HDAC inhibitors, we transfected HEK293T cells with the 1kb ATP7B-fLuc construct and treated them with five selected HDAC inhibitors (MS275, Chidamide, KD5170, Pyroxamide, and PAOA) at a concentration of 5uM. After 48 hours, we measured luciferase expression and calculated the RLU/Protein ug values. Among the inhibitors, MS275 and KD5170 significantly increased ATP7B promoter expression by 1.53-fold and 2.67-fold, respectively, compared to the control transfection (Figure 3.32D).

Furthermore, the magnitude of the upregulation induced by MS275 and KD5170 invites speculation about the interplay between chromatin remodeling and ATP7B transcriptional control. These HDAC inhibitors likely exert their influence by modulating the acetylation status of histones, thereby altering the chromatin landscape and accessibility of transcriptional machinery to the ATP7B promoter. Elaborate

investigations into the epigenetic modifications induced by MS275 and KD5170, specifically in the context of ATP7B regulation, would shed light on the mechanistic intricacies governing their potent effects.

Importantly, these findings open avenues for potential therapeutic applications. Given the pivotal role of ATP7B in cellular copper homeostasis and its implication in various pathophysiological processes, the capacity to modulate its expression via HDAC inhibitors introduces a novel avenue for therapeutic intervention. Harnessing the distinct properties of MS275 and KD5170 to selectively enhance ATP7B expression could hold promise for addressing disorders associated with aberrant copper metabolism and cancer drug resistance.

Chapter 4:**DISCUSSION**

In this study, we aimed to investigate the transcription factors associated with cisplatin resistance in relation to ATP7B. To achieve this goal, we employed an innovative proximity labeling method to specifically target the ATP7B promoter region from the transcription start site (+1) to 3000 base pairs upstream. Our study aimed to identify transcription factors that are correlated with the expression of ATP7B with CASPEX system(Myers et al., 2018). Using a combination of biotinylation, nuclear protein isolation, and LC-MS LFQ techniques, we identified TOX4 as a transcription factor involved in ATP7B regulation in cancer types.

Initially, we examined the conservation of the ATP7B promoter across eight different species and identified conserved regions within the promoter. Specifically, we focused on the region spanning from -1000 bp to -3000 bp of the ATP7B promoter, which displayed a high degree of conservation. To facilitate our investigations, we implemented various optimization steps. This included the generation of a stable cell line expressing CASPEX in HEK293T cells, which allowed for precise and targeted labeling. To ensure the reliability of our results, we employed sorting techniques and performed single colony selection, ensuring the consistency and accuracy of our experimental model.

Subsequently, we proceeded to validate the efficiency of the selected gRNAs through T7E and ChIP assays, ensuring effective targeting of the ATP7B promoter with the CASPEX system. Our analysis revealed that while gRNA efficiency on the target site is an important factor, it can vary between different cell lines. We encountered challenges with Region-3, requiring us to troubleshoot and test multiple gRNAs before successfully achieving the desired enrichment in the ChIP-qPCR assays.

To investigate the biotinylation potential of the CASPEX system, we performed our initial CASPEX biotinylations using the non-targeting gRNA on Region-7 with eight different stable cell lines, each containing CASPEX and targeting gRNAs specific to different regions of the ATP7B promoter. HEK-CASPEX cells harboring validated gRNAs were induced with doxycycline for 48 hours to initiate APEX2-mediated biotinylation. To confirm the specificity of the biotinylation signal and minimize background noise during subsequent mass spectrometry analysis, cell lysates were divided into cytoplasmic and nuclear fractions, with a focus on isolating nuclear proteins where transcription factors predominantly reside.

To ensure efficient enrichment of biotinylated proteins for subsequent analysis, we compared the use of agarose and streptavidin magnetic beads. Based on our evaluation, we opted to utilize streptavidin magnetic beads for the pulldown experiments due to their superior performance. Following successful CASPEX biotinylation in the eight HEK-CASPEX cell lines containing targeting gRNAs, along with the non-targeting gRNA control, protein samples were meticulously prepared for pulldown experiments and subsequent Label-Free Quantification (LFQ) analysis. Upon examining the raw intensity distributions, we observed striking similarities in the peak patterns of the seven targeting gRNA samples compared to the control sample. To further analyze the enriched proteins, we performed limma and statistical analysis, comparing the samples containing targeting gRNAs to the non-targeting gRNA sample for each of the seven regions within the ATP7B promoter.

Through the utilization of transcription factor databases and comparative analysis, we successfully identified over 150 different transcriptional regulators in our dataset. This comprehensive analysis provided valuable insights and served as a valuable resource for our study. By aligning our data with existing knowledge of transcription factors and regulatory elements, we gained a deeper understanding of the potential transcriptional regulatory network associated with the ATP7B gene.

During the in silico analysis stage of the CASPEX project, we specifically focused on identifying transcription factors involved in the regulation of ATP7B. Through this analysis, we successfully detected several predicted and hypothesized transcription factors, including TP53, ATF3, HOXD13, LEF1, MAZ, PAX6, and YY1. These findings further supported the involvement of these transcription factors in the regulation of ATP7B.

To refine our selection of transcription factors for further investigation, we applied specific criteria. This included factors such as identification of a transcription factor in multiple regions, significance determined by p-value and log-fold change, and correlation between ATP7B expression and the candidate transcription factor. Based on these criteria, we selected ATF3, LEF1, P53, and TOX4 as the most promising transcription factors for further validation through experimental approaches.

In our exploration of various transcription factors, distinctive effects on ATP7B expression were evident. LEF1 Ox led to increased ATP7B transcription but conflicted

with protein abundance. P53 Ox transiently enhanced ATP7B transcription. Interestingly, neither LEF1 nor P53 alterations influenced Cisplatin response in compare to the literature (Chee et al., 2013; Han et al., 1999; Santiago et al., 2017).

Among the factors studied, ATF3 emerged as a compelling candidate. We investigated ATF3's impact on the ATP7B promoter using the CASPEX proteome approach within regions 2 and 3. Luciferase assays and ChIP-qPCR analyses verified ATF3's binding across regions 1, 2, and 3, corresponding to the genomic span 1000 bp to 200 bp upstream of the ATP7B promoter. Notably, ATF3's effects on cisplatin response diverged from its impact on ATP7B expression (Fu et al., 2021). ATF3 Ox heightened ATP7B expression, rendering cells more sensitive to cisplatin. Conversely, ATF3 Kos increased cisplatin resistance compared to the control. In light of the contrasting effects observed in ATF3's influence on ATP7B expression and its impact on cellular response to cisplatin, we decided to exclude ATF3 from further consideration as a primary candidate.

Subsequent studies have highlighted the importance of TOX4 in RNA pol II elongation and its involvement in the development of murine T cells (T. Wang et al., 2023). Moreover, TOX4 has been reported to have a crucial role in maintaining pluripotency in embryonic stem cells. Interestingly, in cancer-related proteomic analyses, TOX4 has been found to exhibit similarities with PNUTS and WDR82, particularly in their localization to platinylated DNA. When platinum-based drugs are employed in chemotherapy, TOX4 and its associated proteins recognize these specific DNA locations and bind to them. This binding may potentially modify the platinum adducts, enabling them to evade cellular death. Furthermore, TOX4 may recruit DNA repair factors and manipulate transcriptional regulators, thereby influencing DNA repair processes and transcriptional activity (M. Lambert et al., 2018; Puch et al., 2011). TOX4 identified as a potential transcriptional regulator of ATP7B, based on its presence in multiple regions of the CASPEX proteome analysis. The significant fold changes in enrichment observed in different regions further support the involvement of TOX4 in the regulation of ATP7B. Specifically, region-1, region-2, region-3, and region-6 exhibited notable changes in enrichment, indicating a potential role for TOX4 in modulating ATP7B expression.

In summary, our study revealed that TOX4 serves as a regulator of ATP7B expression in both HEK293T and HUH7 cell lines. Ko of TOX4 resulted in a reduction in ATP7B expression, while Ox of TOX4 led to an increase in ATP7B transcription,

regardless of the cell line. To adress the regulatory role of TOX4 on ATP7B, we conducted luciferase promoter assays using the ATP7B promoter construct. Our findings suggested that TOX4 may bind to the ATP7B promoter region around 1000 bp, thereby enhancing its expression.

We performed chromatin immunoprecipitation followed by ChIP-qPCR to confirm TOX4 binding to the ATP7B promoter. Interestingly, we observed successful TOX4 binding on Region-3 of the ATP7B promoter in HEK293T cells, located approximately -950 bp from the transcription start site. However, the results obtained from the HUH7 cell line were more complex, with reduced enrichment, indicating potential differences in ATP7B chromatin regulation between the two cell lines. This discrepancy may be attributed to variances in basal ATP7B levels and chromatin accessibility of the promoter between HEK293T and HUH7 cells.

Furthermore, we conducted drug response assays using cisplatin and copper to evaluate the viability of cells in the presence or absence of TOX4, aiming to validate the correlation with ATP7B. In HEK293T cells, Ko of TOX4 sensitized cells to cisplatin, while TOX4 Ox rendered cells more resistant to cisplatin-induced cell death. However, in the case of HUH7 cells, the mechanism was more intricate, as TOX4 Ko resulted in increased viability against cisplatin. Additionally, TOX4 demonstrated variable responses in the presence of copper, depending on the cell line.

These findings indicate that TOX4 may act as a modulator of platinylated DNA from the literature, potentially influencing DNA repair mechanisms and orchestrating the recruitment of transcription factors to protect cells from cisplatin-induced cell death (Puch et al., 2011). Overall, our study sheds light on the intricate regulatory mechanisms involving TOX4 in ATP7B expression and its potential implications in cancer therapy and resistance. Further investigations are needed to elucidate the precise molecular mechanisms by which TOX4 influences ATP7B regulation and to explore its therapeutic potential in overcoming drug resistance in cancer.

Chapter 5:**CONCLUSION**

In conclusion, our findings shed light on the role of TOX4 as a potential regulator of ATP7B expression and its implications in cellular response to cisplatin and copper. Through our investigations on HEK293T and HUH7 cell lines, we observed that TOX4 plays a critical role in modulating ATP7B expression, with its Ko resulting in reduced expression and Ox leading to increased transcription. The ATP7B promoter luciferase assay further supported our hypothesis by demonstrating that TOX4 binds to the ATP7B promoter, particularly around the -1000 bp region, thereby enhancing its expression. Furthermore, our ChIP-qPCR analysis revealed TOX4 binding on Region-3 of the ATP7B promoter in HEK293T cells, while the complexities observed in HUH7 cells suggest differential regulation. These findings highlight the importance of TOX4 in the regulation of ATP7B and provide insight into the potential mechanisms underlying cisplatin resistance. The observed effects of TOX4 on the response to cisplatin and copper further suggest its involvement in DNA repair processes and its ability to modulate the cellular fate in response to these agents. Moving forward, future studies should aim to elucidate the precise molecular mechanisms by which TOX4 regulates ATP7B expression and investigate its potential as a therapeutic target for enhancing the efficacy of cisplatin-based chemotherapy and understanding copper-related disorders.

BIBLIOGRAPHY

Ariöz, C., Li, Y., & Wittung-Stafshede, P. (2017). The six metal binding domains in human copper transporter, ATP7B: molecular biophysics and disease-causing mutations. *Biometals*, *30*(6), 823. https://doi.org/10.1007/S10534-017-0058-2

Bartee, M. Y., & Lutsenko, S. (2007). Hepatic copper-transporting ATPase ATP7B: Function and inactivation at the molecular and cellular level. *BioMetals*, *20*(3–4), 627–637. https://doi.org/10.1007/S10534-006-9074-3/FIGURES/3

Belluti, S., Rigillo, G., & Imbriano, C. (2020). Transcription Factors in Cancer: When Alternative Splicing Determines Opposite Cell Fates. *Cells 2020, Vol. 9, Page 760*, *9*(3), 760. https://doi.org/10.3390/CELLS9030760

Bentires-Alj, M., Barbu, V., Fillet, M., Chariot, A., Relic, B., Jacobs, N., Gielen, J., Merville, M. P., & Bours, V. (2003). NF-κB transcription factor induces drug resistance through MDR1 expression in cancer cells. *Oncogene 2003 22:1*, *22*(1), 90–97. https://doi.org/10.1038/sj.onc.1206056

Bitter, R. M., Oh, S. C., Deng, Z., Rahman, S., Hite, R. K., & Yuan, P. (2022). Structure of the Wilson disease copper transporter ATP7B. *Science Advances*, *8*(9). https://doi.org/10.1126/SCIADV.ABL5508

Brayer, K. J., & Segal, D. J. (2008). Keep your fingers off my DNA: Protein-protein interactions mediated by C2H2 zinc finger domains. *Cell Biochemistry and Biophysics*, *50*(3), 111–131. https://doi.org/10.1007/S12013-008-9008-5/TABLES/5

Chee, J. L. Y., Saidin, S., Lane, D. P., Leong, S. M., Noll, J. E., Neilsen, P. M., Phua, Y. T., Gabra, H., & Lim, T. M. (2013). Wild-type and mutant p53 mediate cisplatin resistance through interaction and inhibition of active caspase-9. *Cell Cycle*, *12*(2), 278. https://doi.org/10.4161/CC.23054

Chen, A., & Koehler, A. N. (2020). Transcription Factor Inhibition: Lessons Learned and Emerging Targets. *Trends in Molecular Medicine*, *26*(5), 508. https://doi.org/10.1016/J.MOLMED.2020.01.004

Chen, H. I., Jagadeesh, K. A., Birgmeier, J., Wenger, A. M., Guturu, H., Schelley, S., Bernstein, J. A., & Bejerano, G. (2018). An MTF1 binding site disrupted by a homozygous variant in the promoter of ATP7B likely causes Wilson Disease.

European Journal of Human Genetics 2018 26:12, *26*(12), 1810–1818. https://doi.org/10.1038/s41431-018-0221-4

Cho, K. F., Branon, T. C., Udeshi, N. D., Myers, S. A., Carr, S. A., & Ting, A. Y. (2020). Proximity labeling in mammalian cells with TurboID and split-TurboID. *Nature Protocols 2020 15:12*, *15*(12), 3971–3999. https://doi.org/10.1038/s41596-020-0399-0

Cohen-Solal, K. A., Kaufman, H. L., & Lasfar, A. (2018). Transcription factors as critical players in melanoma invasiveness, drug resistance, and opportunities for therapeutic drug development. *Pigment Cell & Melanoma Research*, *31*(2), 241–252. https://doi.org/10.1111/PCMR.12666

Contreras-Sanzón, E., Prado-Garcia, H., Romero-Garcia, S., Nuñez-Corona, D., Ortiz-Quintero, B., Luna-Rivero, C., Martínez-Cruz, V., & Carlos-Reyes, Á. (2022). Histone deacetylases modulate resistance to the therapy in lung cancer. *Frontiers in Genetics*, *13*, 960263. https://doi.org/10.3389/FGENE.2022.960263/BIBTEX

Di Pietro, A., Koster, R., Boersma-van Eck, W., Dam, W. A., Mulder, N. H., Gietema, J. A., De Vries, E. G. E., & De Jong, S. (2012). Pro- and anti-apoptotic effects of p53 in cisplatin-treated human testicular cancer are cell context-dependent. *Cell Cycle*, *11*(24), 4552. https://doi.org/10.4161/CC.22803

Farré, D., Roset, R., Huerta, M., Adsuara, J. E., Roselló, L., Albà, M. M., & Messeguer, X. (2003). Identification of patterns in biological sequences at the ALGGEN server: PROMO and MALGEN. *Nucleic Acids Research*, *31*(13), 3651. https://doi.org/10.1093/NAR/GKG605

Fu, D., Wang, C., Yu, L., & Yu, R. (2021). Induction of ferroptosis by ATF3 elevation alleviates cisplatin resistance in gastric cancer by restraining Nrf2/Keap1/xCT signaling. *Cellular and Molecular Biology Letters*, *26*(1), 1–14. https://doi.org/10.1186/S11658-021-00271-Y/FIGURES/6

Galluzzi, L., Senovilla, L., Vitale, I., Michels, J., Martins, I., Kepp, O., Castedo, M., & Kroemer, G. (2011). Molecular mechanisms of cisplatin resistance. *Oncogene 2012 31:15*, *31*(15), 1869–1883. https://doi.org/10.1038/onc.2011.384

Gao, X. D., Tu, L. C., Mir, A., Rodriguez, T., Ding, Y., Leszyk, J., Dekker, J., Shaffer, S. A., Zhu, L. J., Wolfe, S. A., & Sontheimer, E. J. (2018). C-BERST: defining subnuclear proteomic landscapes at genomic elements with dCas9–APEX2. *Nature Methods 2018 15:6*, *15*(6), 433–436. https://doi.org/10.1038/s41592-018-0006-2

Godwin, P., Baird, A. M., Heavey, S., Barr, M. P., O'Byrne, K. J., & Gately, K. (2013). Targeting nuclear factor-kappa B to overcome resistance to chemotherapy. *Frontiers in Oncology*, *3 MAY*, 47567. https://doi.org/10.3389/FONC.2013.00120/BIBTEX

Günther, V., Lindert, U., & Schaffner, W. (2012). The taste of heavy metals: Gene regulation by MTF-1. *Biochimica et Biophysica Acta (BBA) - Molecular Cell Research*, *1823*(9), 1416–1425. https://doi.org/10.1016/J.BBAMCR.2012.01.005

Han, J. Y., Chung, Y. J., Park, S. W., Kim, J. S., Rhyu, M. G., Kim, H. K., & Lee, K. S. (1999). The relationship between cisplatin-induced apoptosis and p53, bcl-2 and bax expression in human lung cancer cells. *The Korean Journal of Internal Medicine*, *14*(1), 42. https://doi.org/10.3904/KJIM.1999.14.1.42

He, Q., Bardet, A. F., Patton, B., Purvis, J., Johnston, J., Paulson, A., Gogol, M., Stark, A., & Zeitlinger, J. (2011). High conservation of transcription factor binding and evidence for combinatorial regulation across six Drosophila species. *Nature Genetics 2011 43:5*, *43*(5), 414–420. https://doi.org/10.1038/ng.808

Höflich, C., Brieger, A., Zeuzem, S., & Plotz, G. (2021). Investigation of the Wilson gene ATP7B transcriptional start site and the effect of core promoter alterations. *Scientific Reports 2021 11:1*, *11*(1), 1–10. https://doi.org/10.1038/s41598-021-87000-9

Hsu, P. D., Scott, D. A., Weinstein, J. A., Ran, F. A., Konermann, S., Agarwala, V., Li, Y., Fine, E. J., Wu, X., Shalem, O., Cradick, T. J., Marraffini, L. A., Bao, G., & Zhang, F. (2013). DNA targeting specificity of RNA-guided Cas9 nucleases. *Nature Biotechnology 2013 31:9*, *31*(9), 827–832. https://doi.org/10.1038/nbt.2647

Huo, S., Wang, Q., Shi, W., Peng, L., Jiang, Y., Zhu, M., Guo, J., Peng, D., Wang, M., Men, L., Huang, B., Lv, J., & Lin, L. (2023). ATF3/SPI1/SLC31A1 Signaling Promotes Cuproptosis Induced by Advanced Glycosylation End Products in Diabetic Myocardial Injury. *International Journal of Molecular Sciences*, *24*(2), 1667. https://doi.org/10.3390/IJMS24021667/S1

Inoue, Y., Matsumoto, H., Yamada, S., Kawai, K., Suemizu, H., Gika, M., Takanami, I., Nakamura, M., & Iwazaki, M. (2010). ATP7B expression is associated with in vitro sensitivity to cisplatin in non-small cell lung cancer. *Oncology Letters*, *1*(2), 279. https://doi.org/10.3892/OL_00000049

Islam, Z., Ali, A. M., Naik, A., Eldaw, M., Decock, J., & Kolatkar, P. R. (2021). Transcription Factors: The Fulcrum Between Cell Development and Carcinogenesis. *Frontiers in Oncology*, *11*, 681377. https://doi.org/10.3389/FONC.2021.681377/BIBTEX

Janardhanan, P., Somasundaran, A. K., Balakrishnan, A. J., & Pilankatta, R. (2022). Sensitization of cancer cells towards Cisplatin and Carboplatin by protein kinase D inhibitors through modulation of ATP7A/B (copper transport ATPases). *Cancer Treatment and Research Communications*, *32*, 100613. https://doi.org/10.1016/J.CTARC.2022.100613

Joung, J., Ma, S., Tay, T., Geiger-Schuller, K. R., Kirchgatterer, P. C., Verdine, V. K., Guo, B., Arias-Garcia, M. A., Allen, W. E., Singh, A., Kuksenko, O., Abudayyeh, O. O., Gootenberg, J. S., Fu, Z., Macrae, R. K., Buenrostro, J. D., Regev, A., & Zhang, F. (2023). A transcription factor atlas of directed differentiation. *Cell*, *186*(1), 209-229.e26. https://doi.org/10.1016/J.CELL.2022.11.026

Kardos, J., Héja, L., Simon, Á., Jablonkai, I., Kovács, R., & Jemnitz, K. (2018). Copper signalling: Causes and consequences 06 Biological Sciences 0601 Biochemistry and Cell Biology. *Cell Communication and Signaling*, *16*(1), 1–22. https://doi.org/10.1186/S12964-018-0277-3/FIGURES/4

Katzman, S., Kern, A. D., Bejerano, G., Fewell, G., Fulton, L., Wilson, R. K., Salama, S. R., & Haussler, D. (2007). Human genome ultraconserved elements are ultraselected. *Science*, *317*(5840), 915. https://doi.org/10.1126/SCIENCE.1142430/SUPPL_FILE/KATZMAN.SOM.PDF

Kim, B. R., Coyaud, E., Laurent, E. M. N., St-Germain, J., Van De Laar, E., Tsao, M. S., Raught, B., & Moghal, N. (2017). Identification of the SOX2 Interactome by BioID Reveals EP300 as a Mediator of SOX2-dependent Squamous Differentiation and Lung Squamous Cell Carcinoma Growth. *Molecular & Cellular Proteomics : MCP*, *16*(10), 1864. https://doi.org/10.1074/MCP.M116.064451

Kim, H. J., & Bae, S. C. (2011). Histone deacetylase inhibitors: molecular mechanisms of action and clinical trials as anti-cancer drugs. *American Journal of Translational Research*, *3*(2), 166. /pmc/articles/PMC3056563/

Ku, H. C., & Cheng, C. F. (2020). Master Regulator Activating Transcription Factor 3 (ATF3) in Metabolic Homeostasis and Cancer. *Frontiers in Endocrinology*, *11*, 552603. https://doi.org/10.3389/FENDO.2020.00556/BIBTEX

Kurtenbach, S., Reddy, R., & Harbour, J. W. (2019). ChIPprimersDB: a public repository of verified qPCR primers for chromatin immunoprecipitation (ChIP). *Nucleic Acids Research*, *47*(Database issue), D46. https://doi.org/10.1093/NAR/GKY813

Lam, S. S., Martell, J. D., Kamer, K. J., Deerinck, T. J., Ellisman, M. H., Mootha, V. K., & Ting, A. Y. (2014). Directed evolution of APEX2 for electron microscopy and proximity labeling. *Nature Methods 2014 12:1*, *12*(1), 51–54. https://doi.org/10.1038/nmeth.3179

Lambert, S. A., Jolma, A., Campitelli, L. F., Das, P. K., Yin, Y., Albu, M., Chen, X., Taipale, J., Hughes, T. R., & Weirauch, M. T. (2018a). The Human Transcription Factors. *Cell*, *172*(4), 650–665. https://doi.org/10.1016/J.CELL.2018.01.029

Lambert, S. A., Jolma, A., Campitelli, L. F., Das, P. K., Yin, Y., Albu, M., Chen, X., Taipale, J., Hughes, T. R., & Weirauch, M. T. (2018b). The Human Transcription Factors. *Cell*, *172*(4), 650–665. https://doi.org/10.1016/J.CELL.2018.01.029

Lee, T. I., & Young, R. A. (2013). Transcriptional Regulation and Its Misregulation in Disease. *Cell*, *152*(6), 1237–1251. https://doi.org/10.1016/J.CELL.2013.02.014

Leonhardt, K., Gebhardt, R., Mössner, J., Lutsenko, S., & Huster, D. (2009a). Functional Interactions of Cu-ATPase ATP7B with Cisplatin and the Role of ATP7B in the Resistance of Cells to the Drug. *Journal of Biological Chemistry*, *284*(12), 7793–7802. https://doi.org/10.1074/JBC.M805145200

Leonhardt, K., Gebhardt, R., Mössner, J., Lutsenko, S., & Huster, D. (2009b). Functional Interactions of Cu-ATPase ATP7B with Cisplatin and the Role of ATP7B in the Resistance of Cells to the Drug. *The Journal of Biological Chemistry*, *284*(12), 7793. https://doi.org/10.1074/JBC.M805145200

Li, T., Fu, J., Zeng, Z., Cohen, D., Li, J., Chen, Q., Li, B., & Liu, X. S. (2020). TIMER2.0 for analysis of tumor-infiltrating immune cells. *Nucleic Acids Research*, *48*(W1), W509–W514. https://doi.org/10.1093/NAR/GKAA407

Li, X., Wang, F., Xu, X., Zhang, J., & Xu, G. (2021). The Dual Role of STAT1 in Ovarian Cancer: Insight Into Molecular Mechanisms and Application Potentials. *Frontiers in Cell and Developmental Biology*, *9*, 636595. https://doi.org/10.3389/FCELL.2021.636595/BIBTEX

Liu, Z., Chen, O., Wall, J. B. J., Zheng, M., Zhou, Y., Wang, L., Ruth Vaseghi, H., Qian, L., & Liu, J. (2017). Systematic comparison of 2A peptides for cloning

multi-genes in a polycistronic vector. *Scientific Reports 2017 7:1*, *7*(1), 1–9. https://doi.org/10.1038/s41598-017-02460-2

Lukanović, D., Herzog, M., Kobal, B., & Černe, K. (2020). The contribution of copper efflux transporters ATP7A and ATP7B to chemoresistance and personalized medicine in ovarian cancer. *Biomedicine & Pharmacotherapy*, *129*, 110401. https://doi.org/10.1016/J.BIOPHA.2020.110401

Ma, J. (2011). Transcriptional activators and activation mechanisms. *Protein & Cell*, *2*(11), 879. https://doi.org/10.1007/S13238-011-1101-7

Martínez Corrales, G., & Alic, N. (2020). Evolutionary Conservation of Transcription Factors Affecting Longevity. *Trends in Genetics*, *36*(5), 373–382. https://doi.org/10.1016/J.TIG.2020.02.003

Martinez-Balibrea, E., & Ciribilli, Y. (2021). Editorial: Transcriptional Regulation as a Key Player in Cancer Cells Drug Resistance. *Frontiers in Oncology*, *11*, 764506. https://doi.org/10.3389/FONC.2021.764506/BIBTEX

Matys, V., Kel-Margoulis, O. V., Fricke, E., Liebich, I., Land, S., Barre-Dirrie, A., Reuter, I., Chekmenev, D., Krull, M., Hornischer, K., Voss, N., Stegmaier, P., Lewicki-Potapov, B., Saxel, H., Kel, A. E., & Wingender, E. (2006). TRANSFAC® and its module TRANSCompel®: transcriptional gene regulation in eukaryotes. *Nucleic Acids Research*, *34*(suppl_1), D108–D110. https://doi.org/10.1093/NAR/GKJ143

Mitra, P. (2020). Targeting transcription factors in cancer drug discovery. *Exploration of Targeted Anti-Tumor Therapy*, *1*(6), 401–412. https://doi.org/10.37349/ETAT.2020.00025

Miyashita, H., Nitta, Y., Mori, S., Kanzaki, A., Nakayama, K., Terada, K., Sugiyama, T., Kawamura, H., Sato, A., Morikawa, H., Motegi, K., & Takebayashi, Y. (2003). Expression of copper-transporting P-type adenosine triphosphatase (ATP7B) as a chemoresistance marker in human oral squamous cell carcinoma treated with cisplatin. *Oral Oncology*, *39*(2), 157–162. https://doi.org/10.1016/S1368-8375(02)00038-6

Mladenova, V., Mladenov, E., & Russev, G. (2009). Biotechnology & Biotechnological Equipment Organization of Plasmid DNA into Nucleosome-Like Structures after Transfection in Eukaryotic Cells. *Biotechnology & Biotechnological Equipment*, *23*(1). https://doi.org/10.1080/13102818.2009.10817609

Mu, F., Huang, J., Xing, T., Jing, Y., Cui, T., Guo, Y., Yan, X., Li, H., & Wang, N. (2019). The Wnt/β-catenin/Lef1 pathway promotes cell proliferation at least in part through direct upregulation of miR-17-92 cluster. *Frontiers in Genetics*, *10*(MAY), 452515. https://doi.org/10.3389/FGENE.2019.00525/BIBTEX

Myers, S. A., Wright, J., Peckner, R., Kalish, B. T., Zhang, F., & Carr, S. A. (2018). Discovery of proteins associated with a predefined genomic locus via dCas9–APEX-mediated proximity labeling. *Nature Methods 2018 15:6*, *15*(6), 437–439. https://doi.org/10.1038/s41592-018-0007-1

Nakayama, K., Kanzaki, A., Terada, K., Mutoh, M., Ogawa, K., Sugiyama, T., Takenoshita, S., Itoh, K., Yaegashi, N., Miyazaki, K., Neamati, N., & Takebayashi, Y. (2004). Prognostic Value of the Cu-Transporting ATPase in Ovarian Carcinoma Patients Receiving Cisplatin-Based Chemotherapy. *Clinical Cancer Research*, *10*(8), 2804–2811. https://doi.org/10.1158/1078-0432.CCR-03-0454

Nguyen, T. M. T., Kim, J., Doan, T. T., Lee, M. W., & Lee, M. (2020). APEX Proximity Labeling as a Versatile Tool for Biological Research. *Biochemistry*, *59*(3), 260–269. https://doi.org/10.1021/ACS.BIOCHEM.9B00791/ASSET/IMAGES/MEDIUM/BI9B00791_0001.GIF

Nitta, K. R., Jolma, A., Yin, Y., Morgunova, E., Kivioja, T., Akhtar, J., Hens, K., Toivonen, J., Deplancke, B., Furlong, E. E. M., & Taipale, J. (2015). Conservation of transcription factor binding specificities across 600 million years of bilateria evolution. *ELife*, *2015*(4). https://doi.org/10.7554/ELIFE.04837

Olivier, M., Hollstein, M., & Hainaut, P. (2010). TP53 Mutations in Human Cancers: Origins, Consequences, and Clinical Use. *Cold Spring Harbor Perspectives in Biology*, *2*(1). https://doi.org/10.1101/CSHPERSPECT.A001008

Petruzzelli, R., Mariniello, M., De Cegli, R., Catalano, F., Guida, F., Di Schiavi, E., & Polishchuk, R. S. (2022). TFEB Regulates ATP7B Expression to Promote Platinum Chemoresistance in Human Ovarian Cancer Cells. *Cells 2022, Vol. 11, Page 219*, *11*(2), 219. https://doi.org/10.3390/CELLS11020219

Petruzzelli, R., & Polishchuk, R. S. (2019). Activity and Trafficking of Copper-Transporting ATPases in Tumor Development and Defense against Platinum-Based Drugs. *Cells 2019, Vol. 8, Page 1080*, *8*(9), 1080. https://doi.org/10.3390/CELLS8091080

Puch, C. B. M. Du, Barbier, E., Kraut, A., Couté, Y., Fuchs, J., Buhot, A., Livache, T., Sève, M., Favier, A., Douki, T., Gasparutto, D., Sauvaigo, S., & Breton, J. (2011). TOX4 and its binding partners recognize DNA adducts generated by platinum anticancer drugs. *Archives of Biochemistry and Biophysics*, *507*(2), 296–303. https://doi.org/10.1016/J.ABB.2010.12.021

Qin, W., Cho, K. F., Cavanagh, P. E., & Ting, A. Y. (2021). Deciphering molecular interactions by proximity labeling. *Nature Methods 2021 18:2*, *18*(2), 133–143. https://doi.org/10.1038/s41592-020-01010-5

Qiu, W., Xu, Z., Zhang, M., Zhang, D., Fan, H., Li, T., Wang, Q., Liu, P., Zhu, Z., Du, D., Tan, M., Wen, B., & Liu, Y. (2019). Determination of local chromatin interactions using a combined CRISPR and peroxidase APEX2 system. *Nucleic Acids Research*, *47*(9), e52–e52. https://doi.org/10.1093/NAR/GKZ134

Randolph, L. N., Bao, X., Zhou, C., & Lian, X. (2017). An all-in-one, Tet-On 3G inducible PiggyBac system for human pluripotent stem cells and derivatives. *Scientific Reports*, *7*(1). https://doi.org/10.1038/S41598-017-01684-6

Redell, M. S., & Tweardy, D. J. (2006a). Targeting transcription factors in cancer: Challenges and evolving strategies. *Drug Discovery Today: Technologies*, *3*(3), 261–267. https://doi.org/10.1016/J.DDTEC.2006.09.010

Redell, M. S., & Tweardy, D. J. (2006b). Targeting transcription factors in cancer: Challenges and evolving strategies. *Drug Discovery Today: Technologies*, *3*(3), 261–267. https://doi.org/10.1016/J.DDTEC.2006.09.010

Roy, S., McCann, C. J., Ralle, M., Ray, K., Ray, J., Lutsenko, S., & Jayakanthan, S. (2020). Analysis of Wilson disease mutations revealed that interactions between different ATP7B mutants modify their properties. *Scientific Reports 2020 10:1*, *10*(1), 1–15. https://doi.org/10.1038/s41598-020-70366-7

Ruiz, L. M., Libedinsky, A., & Elorza, A. A. (2021). Role of Copper on Mitochondrial Function and Metabolism. *Frontiers in Molecular Biosciences*, *8*, 691. https://doi.org/10.3389/FMOLB.2021.711227/BIBTEX

Safaei, R., Holzer, A. K., Katano, K., Samimi, G., & Howell, S. B. (2004). The role of copper transporters in the development of resistance to Pt drugs. *Journal of Inorganic Biochemistry*, *98*(10), 1607–1613. https://doi.org/10.1016/J.JINORGBIO.2004.05.006

Santiago, L., Daniels, G., Wang, D., Deng, F. M., & Lee, P. (2017a). Wnt signaling pathway protein LEF1 in cancer, as a biomarker for prognosis and a target for treatment. *American Journal of Cancer Research*, *7*(6), 1389. /pmc/articles/PMC5489786/

Santiago, L., Daniels, G., Wang, D., Deng, F. M., & Lee, P. (2017b). Wnt signaling pathway protein LEF1 in cancer, as a biomarker for prognosis and a target for treatment. *American Journal of Cancer Research*, *7*(6), 1389. /pmc/articles/PMC5489786/

Sentmanat, M. F., Peters, S. T., Florian, C. P., Connelly, J. P., & Pruett-Miller, S. M. (2018). A Survey of Validation Strategies for CRISPR-Cas9 Editing. *Scientific Reports 2018 8:1*, *8*(1), 1–8. https://doi.org/10.1038/s41598-018-19441-8

Shanmugam, G., Rakshit, S., & Sarkar, K. (2022). HDAC inhibitors: Targets for tumor therapy, immune modulation and lung diseases. *Translational Oncology*, *16*, 101312. https://doi.org/10.1016/J.TRANON.2021.101312

Shen, D. W., Pouliot, L. M., Hall, M. D., & Gottesman, M. M. (2012). Cisplatin Resistance: A Cellular Self-Defense Mechanism Resulting from Multiple Epigenetic and Genetic Changes. *Pharmacological Reviews*, *64*(3), 706. https://doi.org/10.1124/PR.111.005637

Shen, J., Lin, H., Li, G., Jin, R.-A., Shi, L., Chen, M., Chang, C., Cai, X., Shen, J., Lin, H., Li, G., Jin, R.-A., Shi, L., Chen, M., Chang, C., & Cai, X. (2016). TR4 nuclear receptor enhances the cisplatin chemo-sensitivity via altering the ATF3 expression to better suppress HCC cell growth. *Oncotarget*, *7*(22), 32088–32099. https://doi.org/10.18632/ONCOTARGET.8525

Shkel, O., Kharkivska, Y., Kim, Y. K., & Lee, J. S. (2022). Proximity Labeling Techniques: A Multi-Omics Toolbox. *Chemistry – An Asian Journal*, *17*(2), e202101240. https://doi.org/10.1002/ASIA.202101240

Spitz, F., & Furlong, E. E. M. (2012). Transcription factors: from enhancer binding to developmental control. *Nature Reviews Genetics 2012 13:9*, *13*(9), 613–626. https://doi.org/10.1038/nrg3207

St. Germain, C., Niknejad, N., Ma, L., Garbui, K., Hai, T., & Dimitroulakos, J. (2010). Cisplatin Induces Cytotoxicity through the Mitogen-Activated Protein Kinase Pathways and Activating Transcription Factor 3. *Neoplasia (New York, N.Y.)*, *12*(7), 527. https://doi.org/10.1593/NEO.92048

Stalke, A., Pfister, E. D., Baumann, U., Illig, T., Reischl, E., Sandbothe, M., Vajen, B., Huge, N., Schlegelberger, B., von Neuhoff, N., & Skawran, B. (2020a). MTF1 binds to metal-responsive element e within the ATP7B promoter and is a strong candidate in regulating the ATP7B expression. *Annals of Human Genetics*, *84*(2), 195–200. https://doi.org/10.1111/AHG.12355

Stalke, A., Pfister, E. D., Baumann, U., Illig, T., Reischl, E., Sandbothe, M., Vajen, B., Huge, N., Schlegelberger, B., von Neuhoff, N., & Skawran, B. (2020b). MTF1 binds to metal-responsive element e within the ATP7B promoter and is a strong candidate in regulating the ATP7B expression. *Annals of Human Genetics*, *84*(2), 195–200. https://doi.org/10.1111/AHG.12355

Tyanova, S., Temu, T., & Cox, J. (2016). The MaxQuant computational platform for mass spectrometry-based shotgun proteomics. *Nature Protocols 2016 11:12*, *11*(12), 2301–2319. https://doi.org/10.1038/nprot.2016.136

Ummethum, H., & Hamperl, S. (2020). Proximity Labeling Techniques to Study Chromatin. *Frontiers in Genetics*, *11*, 450. https://doi.org/10.3389/FGENE.2020.00450/BIBTEX

Varnavides, G., Madern, M., Anrather, D., Hartl, N., Reiter, W., & Hartl, M. (2022). In Search of a Universal Method: A Comparative Survey of Bottom-Up Proteomics Sample Preparation Methods. *Journal of Proteome Research*, *21*(10), 2397–2411. https://doi.org/10.1021/ACS.JPROTEOME.2C00265/SUPPL_FILE/PR2C00265_SI_005.ZIP

Vishnoi, K., Viswakarma, N., Rana, A., & Rana, B. (2020a). Transcription Factors in Cancer Development and Therapy. *Cancers*, *12*(8), 1–32. https://doi.org/10.3390/CANCERS12082296

Vishnoi, K., Viswakarma, N., Rana, A., & Rana, B. (2020b). Transcription Factors in Cancer Development and Therapy. *Cancers 2020, Vol. 12, Page 2296*, *12*(8), 2296. https://doi.org/10.3390/CANCERS12082296

Wang, L., Zhao, X., Fu, J., Xu, W., & Yuan, J. (2021). The Role of Tumour Metabolism in Cisplatin Resistance. *Frontiers in Molecular Biosciences*, *8*, 691795. https://doi.org/10.3389/FMOLB.2021.691795/BIBTEX

Wang, T., Zhao, R., Zhi, J., Liu, Z., Wu, A., Yang, Z., Wang, W., Ni, T., Jing, L., & Yu, M. (2023). Tox4 regulates transcriptional elongation and reinitiation during murine

T cell development. *Communications Biology 2023 6:1*, *6*(1), 1–17. https://doi.org/10.1038/s42003-023-04992-y

Wingender, E., Schoeps, T., & Dönitz, J. (2013). TFClass: an expandable hierarchical classification of human transcription factors. *Nucleic Acids Research*, *41*(D1), D165–D170. https://doi.org/10.1093/NAR/GKS1123

Wingender, E., Schoeps, T., Haubrock, M., & Dönitz, J. (2015). TFClass: a classification of human transcription factors and their rodent orthologs. *Nucleic Acids Research*, *43*(Database issue), D97. https://doi.org/10.1093/NAR/GKU1064

Wu, F., Wang, J., Pu, C., Qiao, L., & Jiang, C. (2015). Wilson's Disease: A Comprehensive Review of the Molecular Mechanisms. *International Journal of Molecular Sciences 2015, Vol. 16, Pages 6419-6431*, *16*(3), 6419–6431. https://doi.org/10.3390/IJMS16036419

Xiang, X., Corsi, G. I., Anthon, C., Qu, K., Pan, X., Liang, X., Han, P., Dong, Z., Liu, L., Zhong, J., Ma, T., Wang, J., Zhang, X., Jiang, H., Xu, F., Liu, X., Xu, X., Wang, J., Yang, H., … Luo, Y. (2021). Enhancing CRISPR-Cas9 gRNA efficiency prediction by data integration and deep learning. *Nature Communications 2021 12:1*, *12*(1), 1–9. https://doi.org/10.1038/s41467-021-23576-0

Yan, C., & Boyd, D. D. (2006). ATF3 Regulates the Stability of p53: A Link to Cancer. *Http://Dx.Doi.Org/10.4161/Cc.5.9.2714*, *5*(9), 926–929. https://doi.org/10.4161/CC.5.9.2714

Yang, Q., Lang, C., Wu, Z., Dai, Y., He, S., Guo, W., Huang, S., Du, H., Ren, D., & Peng, X. (2019). MAZ promotes prostate cancer bone metastasis through transcriptionally activating the KRas-dependent RalGEFs pathway. *Journal of Experimental and Clinical Cancer Research*, *38*(1), 1–17. https://doi.org/10.1186/S13046-019-1374-X/FIGURES/7

Zhao, Y., Zhu, J., Shi, B., Wang, X., Lu, Q., Li, C., & Chen, H. (2019). The transcription factor LEF1 promotes tumorigenicity and activates the TGF-β signaling pathway in esophageal squamous cell carcinoma. *Journal of Experimental and Clinical Cancer Research*, *38*(1), 1–16. https://doi.org/10.1186/S13046-019-1296-7/FIGURES/7